UNIVERSITY OF CALIFORNIA,
IRVINE

CXCR2 signaling regulates neuroinflammation in models of viral and autoimmune-induced neurodegenerative disease

DISSERTATION

submitted in partial satisfaction of the requirements
for the degree of

DOCTOR OF PHILOSOPHY

in Biological Sciences

by

Brett Steven Marro

Dissertation Committee:
Professor Thomas E. Lane, Chair
Professor Charles G. Glabe
Professor Irene M. Pedersen
Professor Manuela Raffatellu
Professor Craig M. Walsh

2015

DEDICATION

To my parents, George and Linda Marro

Sister Erica Bell,

and

my friends and family

I thank you for your love and support

TABLE OF CONTENTS

LIST OF FIGURES

Chapter Three

Chapter Four

LIST OF ABBREVIATIONS

7-AAD	7-actinomycin D
APC	antigen presenting cell
BBB	blood-brain-barrier
CFA	complete freund's adjuvant
CMV	cytomegalovirus
CNS	central nervous system
DAPI	4',6-diamidino-2-phenylindole
DMA	disease modifying agent
DNA	deoxyribonucleic acid
EAE	autoimmune encephalomyelitis
ELR	glutamic acid-leucine-arginine
ER	endoplasmic reticulum
FADDdd	dominantly interfering form of FADD
G-CSF	granulocyte-colony stimulating factor
GFAP	glial fibrillary acidic protein
H&E	hematoxylin and eosin
i.c.	intracranial
i.p.	intraperitoneal
IBV	infectious bronchitis virus
IFNAR	interferon alpha receptor
IFN-γ	interferon gamma

IL	interleukin
JHMV	John Howard Mueller virus
LCMV	lymphocytic choriomeningitis virus
LFB	luxol fast blue
MHV	mouse hepatitis virus
MMP	matrix metalloproteinase
MOG	myelin oligodendrocyte protein
MS	multiple sclerosis
NK	natural killer
NOS2	nitric oxide synthase 2
NPC	neural progenitor cell
OPC	oligodendrocyte precursor cell
ORF	open reading frame
OVA	ovalbumin
PLP	proteolipid protein
PMN	polymorphonuclear neutrophil
RICD	restimulation-induced cell death
RIPK	receptor-interacting protein kinase
RNA	ribonucleic acid
RRMS	relapse-remitting multiple sclerosis
RTC	replication/transcription complex
rtTA	reverse tetracycline transactivator protein
SPMS	secondary progressive multiple sclerosis

tetO	tetracycline operator
tetR	tetracycline repressor
TMEV	Theiler's murine encephalomyelitis virus
TNF	tumor necrosis factor
TRE	tetracycline-responsive promoter element
WNV	west nile virus

ACKNOWLEDGMENTS

First and foremost, I owe a debt of gratitude to my mentor and friend, Professor Thomas E. Lane, who has been instrumental in my development as a scientist. His unwavering support, encouragement and intellectual guidance throughout my graduate career allowed me to stay focused and productive. It has been an honor to work in his laboratory and I am truly thankful.

I would like to thank my committee members, Professor Craig M. Walsh, Professor Charles G. Glabe, Professor Irene M. Pedersen and Professor Manuela Raffatellu for their insight and support throughout my graduate career.

I thank former members of the Lane Laboratory including Dr. Jason Weinger, Dr. Kathy Held, Dr. Lucia Whitman, Dr. Martin Hosking, Dr. Kevin Carbajal, Dr. Lu Chen, Dr. Emanuele Tirotta, Dr. Caroline Blanc, Warren Plaisted, Michelle Tsukamoto, Edna Hingco, Patrick Duncker and Leslie Kirby, as well as new members including Dr. Laura Dickey, Jonathan Grist and Colleen Worne.

I thank Elsevier, Informa Plc, Future Medicine Ltd. and the National Academy of Sciences to include previously published work in my dissertation. Financial support was provided by the University of California, Irvine, NIH T32 Grant 5T32AI007319 and NIH Grants RO1 NS041249 and RO1 NS074987.

CURRICULUM VITAE

Brett Steven Marro

EDUCATION

2006 Bachelor's of Science, Biochemistry
University of California, Los Angeles
Los Angeles, CA

2010 Master's of Science in Biotechnology
University of California, Irvine
Irvine, CA
Mentor: Prof. Thomas E. Lane, PhD.

2015 Doctorate of Philosophy in Biological Sciences
University of California, Irvine
Irvine, CA
Mentor: Prof. Thomas E. Lane, PhD.

RESEARCH EXPERIENCE

2009-2010 *Master's Student*
Laboratory of Prof. Thomas E. Lane, PhD.
University of California, Irvine
Exploring molecular and cellular mechanisms associated with impaired host-defense responses to viral infections following spinal cord injury

2010-2015 *Graduate Student*
Laboratory of Prof. Thomas E. Lane, PhD.
University of California, Irvine
Evaluating how genetic manipulation of ELR-chemokine signaling pathways regulates viral and autoimmune-induced neurodegenerative disease

AWARDS

2011-2013 NIH T32 Virology Training Grant 5T32AI007319

PUBLICATIONS

Marro BS and Lane TE. Inducible expression of CXCL1 from astrocytes amplifies demyelination that is associated with increased neutrophil infiltration into the CNS following CNS viral infection. **(Manuscript in preparation)**

Marro BS, Grist J, Doty DJ, Ransohoff RM, Fujinami RS, Lane TE. Inducible ablation of CXCR2 on oligodendroglia attenuates autoimmune, but not viral, mediated neuroinflammation and demyelination. **(Manuscript in preparation)**

Marro BS*, Blanc CA*, Loring JF, Cahalan MD, Lane TE. Promoting remyelination: utilizing a viral model of demyelination to assess cell-based therapies. *Expert Review of Neurotherapeutics*. 2014; 14(10): 1169-79

Weinger JG*****, **Marro BS***, Hosking MP, Lane TE. The chemokine receptor CXCR2 and coronavirus-induced neurologic disease. *Virology*. 2013 Jan 5; 435(1): 110-7.

Marro BS, Hosking MP, Lane TE. CXCR2 signaling and host defense following coronavirus-induced encephalomyelitis. *Future Virol*. 2012 Apr; 7(4): 349-359.

Lu JV, Weist BM, van Raam BJ, **Marro BS**, Nguyen LV, Srinivas P, Bell BD, Luhrs KA, Lane TE, Salvesen GS, Walsh CM. Complementary roles of Fas-associated death domain (FADD) and receptor interacting protein kinase-3 (RIPK3) in T-cell homeostasis and antiviral immunity. *Proc Natl Acad Sci U S A*. 2011 Sep 13; 108(37): 15312-7

***** Indicates co-first authorship

ABSTRACT OF THE DISSERTATION

CXCR2 signaling regulates neuroinflammation in models of viral and autoimmune-induced neurodegenerative disease

By

Brett Steven Marro

Doctor of Philosophy in Biological Sciences

University of California, Irvine, 2015

Professor Thomas Edward Lane, Chair

Chemokines and their cognant receptors have been identified as an essential immune component in attracting activated immune cells into the central nervous system (CNS) following experimental infection with the neurotropic JHM strain of mouse hepatitis (JHMV) as well as within the experimental autoimmune encephalomyelitis (EAE) model of Multiple Sclerosis (MS). The primary focus of this dissertation is to investigate how ELR-chemokine signaling within the CNS regulates neuroinflammation and neurologic disease. To this end, we have generated a doxycycline (Dox) inducible CXCL1 overexpressing mouse line to assess how overproduction of this chemokine from astrocytes impacts host-defense responses and the demyelinated disease that results following JHMV infection. Overexpression of CXCL1 enhanced the accumulation of CXCR2-expressing neutrophils in the CNS without impacting BBB permeability or the infiltration of inflammatory leukocytes. Neutrophils were found to accumulate within the parenchyma during the persistent phase of disease and this was associated with severe white matter demyelination. These data

suggest that chronic CXCL1 expression from the CNS can amplify JHMV-induced neurologic disease that is neutrophil dependent.

We next investigated if loss of CXCR2 signaling in oligodendroglia lineage cells results in altered immunopathogenesis within the JHMV and EAE models of demyelination. Using a tamoxifen-inducible Cre-ER^{T2} transgenic mouse system, we induced ablation of *Cxcr2* in oligodendrocytes and subsequently infected mice with JHMV or immunized with a peptide derived from myelin oligodendrocyte glycoprotein (MOG) to induce EAE disease. Interestingly, EAE-induced *Cxcr2* $^{fl/fl}$ mice treated with tamoxifen displayed dampened disease severity and this was associated with reduced expression of inflammatory cytokines and chemokines in the CNS, as well as a significant reduction in the infiltration of neutrophils, macrophages and IFN-γ-secreting CD4+ T cells. These data implicates CXCR2-signaling in oligodendrocytes as an amplifier of neuroinflammation and demyelination within the context of the autoimmune EAE model of demyelination. Conversely, tamoxifen-treated *Cxcr2* $^{fl/fl}$ mice infected with JHMV resulted in a similar host-defense response as well as disease progression compared to control animals, suggesting that CXCR2 signaling in oligodendrocytes within the context of JHMV infection of the CNS does not have a prominent role in promoting chronic JHMV-induced demyelinating disease.

CHAPTER ONE

Utilizing mouse hepatitis virus and experimental autoimmune encephalomyelitis as surrogate mouse models to study neuroinflammation and immune-mediated demyelination

1.1 Introduction to Mouse Hepatitis Virus (MHV)

The Coronaviridae family is composed of large (26-32kb) enveloped single-stranded RNA viruses in the Order Nidovirales [1] that are classified into three groups based on shared sequencing homologies and serologic cross-reactivity [1,2]. Their naming dates to the 1960s when Tyrrell and McIntosh isolated infectious bronchitis virus (IBV)-like virions from the upper respiratory tracts of patients with common colds [3]. When electron micrographs of avian IBV and the newly isolated human strains were compared, the "club- or pear-shaped" projections on their viral coats showed strikingly similar characteristics. In 1968, Tyrrell, McIntosh and six other scientists grouped these viruses together and proposed the coronavirus family name based on the Latin root "corona" for their crown-like appearance [4].

Mouse Hepatitis Virus (MHV) is the prototype Group II coronavirus and arguably the most extensively studied of the three groups. Like other coronaviruses, MHV utilizes a unique transcription strategy to produce mature virions. Following viral uncoating and transport of the viral genome to the endoplasmic reticulum (ER) of infected cells, proteins comprising the replicase-transcriptase machinery are generated through direct translation of MHV genomic RNA. This includes open-reading frame 1a (ORF1a) that generates the large polyprotein, pp1a and ORF1b that generates pp1ab following a ribosomal frame shift during translation of ORF1a [5]. Through proteolytic auto-processing by virus-encoded proteinases, 11 non-structural proteins (nsp1-nsp11) are generated from pp1a while nsp12 to nsp16 are found within pp1b [5]. Nsps and host cell proteins jointly accumulate at perinuclear foci located on cellular membranes leading to the formation replication/transcription complexes (RTCs) [6,7]. To generate mRNAs encoding for the

structural components, discontinuous negative strand synthesis occurs at the 3' end of the genome to generate negative sense RNAs of variable length. RTCs engage these RNAs and direct plus-strand synthesis while releasing the minus-strand templates upon completion. This results in a nested set of sub-genomic mRNAs that encode for the proteins that confer the structure of a mature MHV virus [5].

MHV includes a variety of strains that can induce wide-ranging pathologies dependent on the age and strain of the mouse as well as the route of infection. Enterotropic MHV strains such as MHV-Y can cause severe enteritis and are highly contagious, leading to devastating natural outbreaks of housed mouse laboratory colonies [8]. The hepatotropic MHV-2 strain results in fulminant hepatitis following intraperitoneal (i.p.) injection, but is weakly neurotropic, causing only mild acute meningitis following intracranial (i.c.) inoculation [9]. In contrast, i.c. infection of susceptible mice with the dual neurotropic and hepatotropic A59 strain results in infection of neurons and glial cells within the CNS, leading to mild encephalomyelitis and limited demyelination, while i.p. inoculation results in hepatitis [10,11].

1.2 DM-MHV and necroptotic signaling in T cells

DM-MHV, a plaque-purified isolate derived from suckling mouse brains, is a moderately neurovirulent MHV variant [12]. Moreover, when i.p. injected into susceptible mice, this strain can be an effective tool for interrogating mechanisms associated with host-defense to viral infections within the periphery, as a robust CD4+ and CD8+ antiviral T cell response is generated. In collaboration with Dr. Craig Walsh (University of California, Irvine), we have recently utilized an *in vivo* DM-MHV infection model for studying necroptotic signaling within effector T cells [13]. Necroptosis is a programmed cell death pathway that occurs when pro-apoptotic caspases are inhibited [14]. Indeed, mice lacking pro-apoptotic caspase-8 or expressing a dominantly interfering form of FADD (FADDdd), a key protein involved in activating the caspase-dependent apoptotic pathway, displayed blunted T cell responses and a disruption of overall T cell homeostasis [15-17]. This is likely attributed to the activation of the alternative necroptotic death pathway, mediated by RIP1 and RIP3 kinases, as a fail-safe mechanism to induce cell death [18,19]. Within this study [13], RAG1-deficient mice that received FADDdd T cells following adoptive transfer are unable to properly mount an immune response to DM-MHV due to a defective anti-viral response by T cells. However, mice that received FADDdd T cells that also had *Ripk3* genetically deleted resulted in a restoration of T cell function and clearance of virus, highlighting the importance of RIPK3 in necroptosis. Detailed results from this study are presented in **Chapter 2**.

1.3 JHMV-Induced Acute Encephalomyelitis

The neuroattenuated J2.2v-1 variant of the John Howard Mueller (JHM) strain of mouse hepatitis virus (JHMV), a well-characterized laboratory strain derived from a mAb escape mutant from the highly lethal JHM-DL virus, can cause severe encephalomyelitis and demyelination in adult mice [20,21]. Infection of susceptible mice with JHMV have proven to be effective mouse models for i) viral-induced encephalomyelitis, ii) defining molecular mechanisms governing neuroinflammation, iii) characterizing mechanisms associated with viral-induced immune-mediated demyelination, and iv) developing novel approaches to promote remyelination within the context of persistent viral infection of the CNS.

Following a sublethal i.c infection with JHMV, virus infects and replicates within ependymal cells lining the lateral ventricles [22]. Within 24-hours, JHMV rapidly spreads and penetrates further into the parenchyma where astrocytes, oligodendrocytes, and microglia are targets of infection [20,22]. Virus also disseminates to the spinal cord through cerebrospinal fluid targeting ependymal cells prior to spreading to glial cells of the white matter tracts [22]. Viral titers within the brain peak between days 5-7 post-infection (p.i.) and decline below levels of detection by plaque assay (~100 PFU/g tissue) between 10-14 days post-infection (p.i.) [23]. However, sterilizing immunity is incomplete since viral antigen and RNA is capable of persisting within the CNS [24], and this is associated with chronic neuroinflammation leading to an immune-mediated demyelinating disease with clinical and histologic similarities to the human demyelinating disease multiple sclerosis (MS).

An innate antiviral response is triggered following JHMV infection, characterized by increased expression of pro-inflammatory cytokines and chemokines along with matrix-

metalloproteinases (MMPs) [25,26]. A cytokine milieu consisting of IL-1α, IL-1β, IL-6, IL-12 and TNF-α is detected within CNS during the first 48 hours following JHMV infection [27,28]. Type I IFN-α and IFN-β are also detected early in response to JHMV infection suggesting an important role in host defense. Elegant studies by Bergmann and colleagues [29] showed an increase in viral spread and mortality in JHMV infected *IfnaR -/-* mice, while exogenous treatment of mice with either type I interferon limits viral replication and dissemination [30,31]. In addition to directly inhibiting viral replication, type I interferons are believed to enhance antigen presentation via increased MHC class I expression, helping link innate and adaptive immune responses [32].

Cellular components of the innate immune response consist of neutrophils, natural killer (NK) cells and monocyte/macrophages that rapidly migrate to the CNS in response to JHMV infection. Although these cells were initially not considered important in host defense, this opinion has been revised based upon recent studies that have more carefully examined their functional contributions. Both neutrophils and monocyte/macrophages are now thought to contribute to the permeabilization of the blood-brain-barrier (BBB) through secretion of MMPs, and this is critical for allowing access of virus-specific T cells into the CNS [33-37]. With regards to NK cells, Trifilo et al. [38] provide a proof-of-principle that NK cells can contribute to control of viral replication following infection of immunodeficient mice with a recombinant JHMV engineered to express the chemokine CXCL10. However, a more relevant study evaluating the functional contributions of NK cells in host defense in response to JHMV infection was provided by Zuo et al., [39] in which IL-15-deficient mice that lack NK cells were shown to control JHMV replication within the

CNS as efficiently as wildtype mice and effectively argue that NK cells are dispensable with regards to effectively controlling JHMV replication during acute disease.

JHMV specific CD4+ and CD8+ T cells expand to viral antigens presented within draining cervical lymph nodes [40] and traffic into the CNS through a permeable BBB in response to chemotactic signals including the chemokines CXCL9, CXCL10 and CCL5 [40-45]. Evidence for this is supported by chemokine neutralization studies where administration of anti-CXCL10 or anti-CCL5 blocking antibodies during acute JHM infection abrogates early CD4+ and CD8+ T cell infiltration to the CNS [41-44]. Administration of blocking antibodies specific for CXCL10 to JHMV-infected mice during acute disease impaired CD4+ and CD8+ T cell access to the CNS and inability to control viral replication [42]. Similarly, JHMV infection of CXCL10-deficient mice limited entry of CD4+ and CD8+ T cells into the CNS [46]. In contrast, treatment with anti-CXCL10 antisera in mice persistently infected with virus in which demyelination is established selectively inhibited virus-specific CD4+ T cells, but not virus-specific CD8+ T cell trafficking into the CNS resulting in a dramatic improvement in motor skills [47,48]. Additionally, blocking CXCR3, the receptor for CXCL10, also negatively impacts CD4+ T cell recruitment to the CNS while trafficking of CD8+ T cells is not significantly impacted [41]. Follow up studies further support the role of CXCL10 in promoting T cell migration following JHMV infection but not in enhancing T cell antiviral effector functions [49]. These findings argue for differential roles for CXCL10 in mediating trafficking of CXCR3-bearing T cells into the CNS in response to JHMV infection and this is dictated, in part, by the stage of disease (i.e., acute versus chronic). One potential explanation to these findings may lie in different trafficking patterns of T cells during chronic disease as well as evidence indicating that virus-specific

CD8+ T cells are retained within the CNS during persistence [50]. Importantly, other chemokines may promote the chemotaxis of T cells, macrophages, as well as other inflammatory cells following JHMV infection. Indeed, adoptive transfer studies indicate that CCR5-deficient CD4+ T cells (i.e., those that do not respond to the chemokine CCL5), transferred into JHMV-infected *Rag1* -/- mice display muted ability to traffic to the CNS [51]. However, adoptive transfer of *Ccr5* -/- CD8+ T cells can infiltrate into the CNS in infected RAG1-deficient mice, demonstrating that differential signaling cues control CD4+ and CD8+ T cell migration during acute JHMV infection [52]. Genetic ablation of *Ccr2*, but not its signaling ligand CCL2, results in increased mortality associated with impaired ability to control JHMV replication within the brain and this correlated with limited infiltration of virus-specific T cells into the CNS [53]. CCR2 has been shown to critical in regulating BBB permeability by signaling through the receptor expressed on endothelial cells in other neuroinflammatory disease models suggesting that CCR2 signaling influences leukocyte access to the CNS by controlling BBB integrity in response to JHMV infection [54]. However, both CCL2 and CCR2 promote macrophage accumulation within the CNS of infected mice [53]. Follow up studies confirmed the importance of CCL2 in mediating monocyte/macrophage recruitment to the CNS of JHMV-infected mice [35,55].

Antiviral effector mechanisms associated with viral clearance within the CNS include the elevated expression of MHC class I and MHC class II on antigen presenting cells (APCs) following secretion of IFN-γ by both CD4+ and CD8+ T cells as well as perforin-mediated cytolysis of astrocytes and microglia by virus-specific CD8+ T cells [23,56,57]. Upon JHMV infection of the CNS, CD4+ T cells promote CD8+ T cell expansion within the periphery and aid in enhancing antiviral effector functions [58]. Depletion of CD4+ T cells

diminishes CD8+ T cell-mediated control of viral replication within the CNS that is associated with reduced expression of IFN-γ and granzyme B and elevated CD8+ T cell apoptosis [58]. These results support and extend earlier studies [12,59] that CD4+ T cells play a central role in both enhancing peripheral activation of CD8+ T cells and prolonging their antiviral function within the CNS and further suggest that IL-21 may be a critical factor in mediating these effects [58]. Infected oligodendrocytes appear to be resistant to the cytolytic effector functions of CD8+ T cells, but rather control JHMV replication through IFN-γ signaling generated from virus-specific T cells [56,57,60,61]. The potent anti-viral response reduces viral replication to below detectable levels (as defined by plaque assay) between days 10-14 p.i., but sterile immunity does not occur; viral RNA and antigens persist and are sequestered primarily within white matter tracts, and this is accompanied by the presence of activated glial cells and retention of virus-specific CD4+ and CD8+ T cells [23,24,62]. Neutralizing JHMV-specific antibody is detected during chronic disease and is critical in preventing viral recrudescence [63-65].

More recently, Perlman and colleagues have provided important insight into the functional role of regulatory T cells (Tregs) during acute JHMV-induced CNS disease [66,67]. Tregs are detected within the CNS at the same time as effector CD4+ T cells indicating the emergence and accumulation of both populations of cells is on a similar timeline following viral infection. Further, virus-specific Tregs express both IFN-γ and IL-10 suggesting immune regulatory capacities mediated through cytokines secreted following antigen stimulation. Indeed, virus-specific Tregs dampen proliferation of virus-specific effector CD4+ T cells and depletion of Tregs increases mortality [66,67]. These data suggest that within the context of acute JHMV-induced neurologic disease, Tregs limit

immunopathological CNS disease without negatively impacting viral clearance [66]. The early immunological events within the CNS following infection with JHMV are highlighted in **Figure 1.1.**

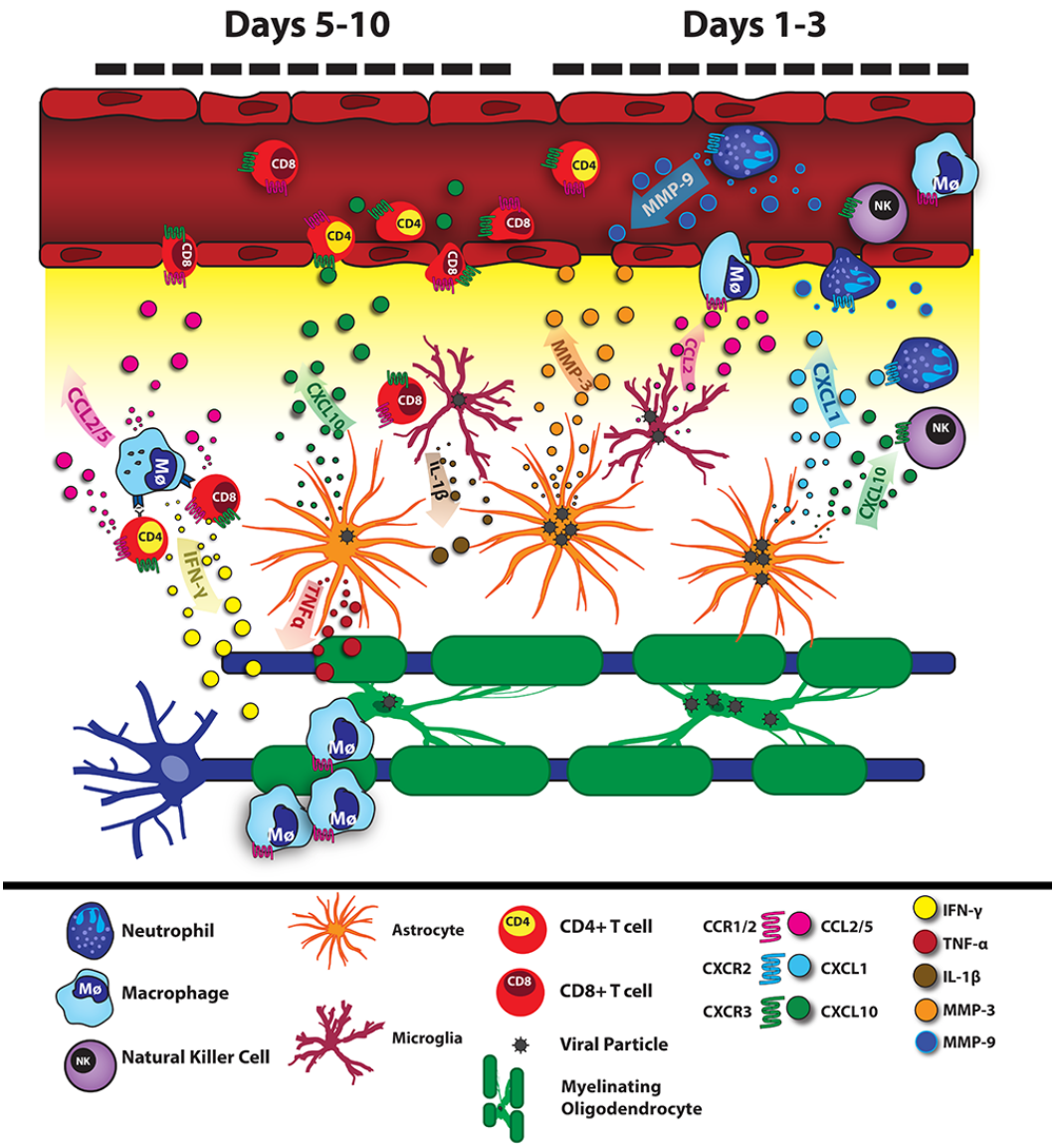

Figure 1.1 Pathogenesis of the JHM-strain of mouse hepatitis virus. Intracranial inoculation of C57BL/6 mice with the JHMV variant of mouse hepatitis virus (MHV) results in viral replication within astrocytes and oligodendrocytes. In response to viral replication within the CNS, several chemokines (e.g., CCL2, CXCL1 and CXCL2) are produced by reactive glia that act to recruit neutrophils and macrophages to the CNS. Here, these cells can degrade components of the blood-brain-barrier through the release of matrix metalloproteinases (MMP), including MMP9. Permeabilization of the blood-brain-barrier (BBB) facilitates the entry of virus-specific T cells into the parenchyma via a CXCL10 gradient where they act to clear infected cells through perforin-mediated cytolysis as well as IFN-γ secretion. However, sterile immunity is not achieved as viral RNA persists within oligodendroglia, resulting in an immune-mediated demyelinating disease that is characterized by myelin loss and oligodendrocyte dysregulation.

1.4 Neutrophils, BBB breakdown and CXCR2 Signaling During Acute JHMV-Induced Disease

Polymorphonuclear (PMN) neutrophils can infiltrate into the CNS within 24-hours p.i. following i.c. inoculation with JHMV where are thought to carry out critical effector functions in host defense including the release of matrix metalloproteinase-9 (MMP9) from stored granules [37,68]. Their rapid migration to the luminal side of the perivascular space correlates with degradation of the basal lamina and extracellular matrix of the blood-brain-barrier (BBB), thus enhancing inflammation by facilitating the extravasation of monocytes and leukocytes into the parenchyma [34,36,69-71]. The importance of neutrophils in host-defense following JHMV infection was initially highlighted by Stohlman and colleagues [37] demonstrating that there is an increase in viral burden and mortality of neutropenic mice infected with the DM-MHV lethal variant of JHMV. This correlated with a lack of detectable MMP9 within CNS extracts and only minor disruption of the BBB, indicating a protective role for neutrophils during the early stages of DM-MHV infection [37].

The ELR-positive chemokines CXCL1 and CXCL2 in mice (the ortholog being CXCL8 in humans), delineated by a glutamic acid-leucine-arginine (ELR) amino acid sequence preceding a group of conserved cysteine residues (CXC) at the amino termini of the molecules, are potent chemoattractants for neutrophils which express the cognate chemokine receptor CXCR2. Indeed, CXCL1 overexpression from oligodendrocytes within the CNS of naive transgenic mice results in rapid neutrophil accumulation into the perivascular, meningeal and parenchymal areas of the brain [72]. CXCL1 and CXCL2 are up-regulated early within the brain and spinal cord of JHMV-infected mice with CXCL1 protein expression appearing to co-localize with reactive astrocytes [34,71]. Similar to the results

of neutropenic mice infected with the DM-MHV variant, blocking neutrophil recruitment to the CNS through antibody mediated neutralization of the ligand domain of CXCR2 during sublethal JHMV-infection leads to a significant increase in mortality and the inability to control virus replication [34]. This is associated with over a 50% reduction in leukocytes infiltrating into the CNS that correlated with an intact BBB and demonstrates a critical role of ELR-positive chemokines in shaping the adaptive immune response to JHMV [34].

Curiously, host-defense to JHMV infection in CXCR2-deficient mice contradicts the CXCR2 neutralization studies as CXCR2-deficient mice infected with JHMV have no deficits in survival, viral clearance or BBB degradation [34]. Although reduced in numbers, neutrophils were still detected within the CNS of JHMV infected *Cxcr2* -/- mice indicating that their migration may be the result of induction of compensatory receptors that may promote their chemotaxis, such as CXCR1 [34,73]. Furthermore, recent evidence has shown that MMP secretion from neutrophils is not essential for promoting inflammation since JHMV-infected *Mmp9 -/-* mice show similar BBB permeability and subsequent leukocyte infiltration compared to infected *Mmp9 +/+* controls, indicating that MMP9 is dispensable for BBB disruption and compensatory mechanisms to promote BBB permeability exist, such as enhanced MMP-3 secretion from resident glia [74]. In addition to MMP9 secretion by neutrophils, it is also feasible that these cells can also influence MMP production by resident cells of the CNS. Finally, Bergmann and colleagues [35] have shown that by impairing monocyte recruitment to the CNS through genetic ablation of *CCR2* there is the retention of leukocytes within the perivascular space of the CNS, corresponding to a reduction in neuroinflammation. This occurs regardless of neutrophil activity at the BBB,

and further illustrates the complexity of early events leading to breakdown of the BBB following JHMV infection [35].

Neutrophil effector activity has also been shown to have critical roles in other CNS-based viral infections. Depletion of PMNs following infection of susceptible mice with West Nile Virus (WNV) leads to higher viremia and reduced survival arguing for a protective role for these cells [75]. Indeed, Bai et al. [75] demonstrated that infection of CXCR2-deficient mice with WNV results in higher viremia at D5 p.i. However, one caveat to this study is that neutrophils may be a viral reservoir for WNV, and the lack of neutrophil accumulation within the brains of *Cxcr2* -/- results in lower viremia at early time points post-inoculation with WNV. Nonetheless, neutrophils were shown to be important in host-defense to WNV. Conversely, McGavern and colleagues [76] showed a detrimental effect of neutrophil activity following infection with the mouse adapted Armstrong strain of lymphocytic choriomeningitis virus (LCMV), where it was demonstrated that cytotoxic CD8+ T cells promote neutrophil accumulation at the BBB, leading to a loss of vascular integrity that results in fatal encephalitis. Moreover, silencing of CXCR2 through antibody blockade or genetic ablation has been shown to dampen inflammation and tissue injury in models in which neutrophil infiltration correlates with disease initiation such as inflammatory mediated injury to the lung [77-79] and during experimental bacterial infections within the brain [80].

Emerging evidence also suggests that CXCR2 bearing neutrophils are necessary to promote CNS-based autoimmune disorders in mice [81,82]. Willenborg and colleagues [83] first demonstrated that antibody depletion of PMNs could dampen clinical severity of early effector phases of experimental autoimmune encephalomyelitis (EAE) following

immunization with defined encephalitogenic myelin peptides. Neutrophils are rapidly mobilized from the bone marrow within 48 hours following MOG_{35-55} immunization, and granulocyte-colony stimulating factor (G-CSF) and CXCL1 appear to be critical in this process [84]. Furthermore, CXCL1 and CXCL2 are up-regulated within the CNS during chronic EAE disease and genetic ablation or antibody blockade of CXCR2 within mice resulted in the failure to develop EAE, while adoptive transfer of CXCR2 expressing PMNs into *Cxcr2 -/-* mice reestablished EAE disease, although with slightly less severity [81,82]. The functions of neutrophils following EAE immunization appear to be within the preclinical phase of the disease as they likely contribute to both BBB breakdown as well and maturating local APC's within the perivascular space spinal cord[85]. Finally, using a cuprizone-induced demyelinating disease model, Liu et al. [86] discovered that neutrophils are necessary to induce demyelination following cuprizone treatment, but *CXCR2*-deficient mice were resistant to demyelination even though these cells accumulated within the CNS, implicating abherrant effector functions in *Cxcr2 -/-* neutrophils. Together, these findings highlight a role of ELR+ chemokines in initiating and amplifying inflammation within the CNS in response to infection with a neurotropic virus and sensitization to encephalitogenic myelin peptides by enhancing migration, accumulation and effector functions of neutrophils.

To expand our understanding of how ELR-positive chemokines influence host defense and disease progression following JHMV infection of the CNS, we have generated transgenic mice that utilize the tetracycline-controlled transcriptional activation system to induce ELR-positive chemokine expression from the CNS **(Figure 1.2)** [87-89]. Within this binary transgenic system, expression of CXCL1 from astrocytes is dependent on the activity

of the doxycycline-inducible reverse tetracycline transactivator protein (rtTA). This transactivator is a fusion protein containing a mutated Tet repressor DNA binding protein (TetR) from the Tc resistance operon of E. coli transposon Tn10 that is fused to the transactivating domain of VP16 from Herpes simplex virus. It can recognize the tetracycline-responsive promoter element (TRE) that is comprised of a Tet operator (tetO) linked to a minimal cytomegalovirus (CMV) immediate early promoter [90]. In a "tet-on" system, the rtTA fusion protein is capable of binding to tetO only if bound and activated by a tetracycline. A more optimized version of the rtTA protein, named rtTA2s-M2, was recently developed to increase the sensitivity of binding doxycycline (Dox), leading to improved binding to the TRE element [91]. The successful generation of the Dox-inducible CXCL1 overexpressing mouse line has allowed us to selectively increase CXCL1 within the CNS and evaluate its impact on neuroinflammation, viral spread and demyelination following infection with JHMV. The results from this study are covered in **Chapter 3**.

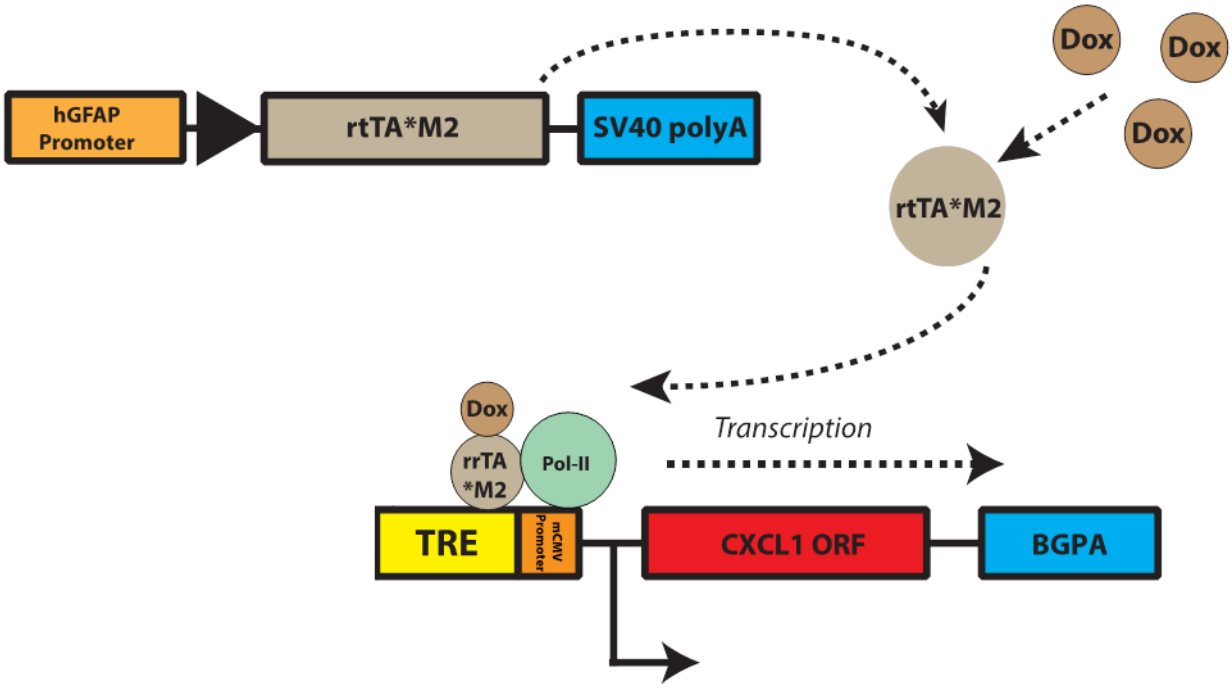

Figure 1.2 A TET-On binary transgenic system to control CXCL1 expression from astrocytes. An optimized form of the doxycycline-inducible reverse tetracycline transactivator protein (rtTA2s-M2) was placed downstream of the human version of the GFAP promoter (hGFAP) that has been previously shown to be active within mature astrocytes derived from mice. When bound to doxycycline, the rtTA2s-M2 protein can recognize a tetracycline-responsive element (TRE) upstream of a mCMV promoter as well as the open reading frame of CXCL1. Successful generation of the TET-On system has allowed us to selectively increase CXCL1 within the CNS upon doxycycline administration to mice containing both elements.

1.5 Chronic JHMV-induced neurologic disease as a model for Multiple Sclerosis

Multiple Sclerosis (MS) is a complex disease of the central nervous system (CNS) that is characterized by heterogenous pathologies composed of both inflammatory and neurodegenerative components [92]. Although the identification of an etiological trigger of MS remains elusive, disease induction is thought to result from several features including both genetic predispositions and environmental factors (e.g., microbial infections) [93-98]. The most common histopathologic feature at early stages of the disease includes intermittent episodes of acute inflammation within patches of white matter, resulting in demyelination [99]. Myelin is critical for maintaining efficient axonal conduction and oligodendrocytes, the myelin producer and maintainer of axonal health within the CNS, are damaged or destroyed by the misguided attack by T cells that target proteins comprising the myelin sheath. The role of leukocytes in disease initiation are highlighted through the use of disease modifying agents (DMA) that block the infiltration of inflammatory T cells into the CNS, resulting in extended periods of remission for MS patients with the relapsing-remitting forms of the disease. For a majority of those with MS, focal attacks are generally episodic, varying from 24 hours to several weeks in length and are usually followed by near complete recovery of clinical symptoms, a disease course collectively referred to as relapse-remitting MS (RRMS) [100]. Spontaneous remission can be associated with waning inflammation and partial restoration of axonal conductivity due to remyelination [101,102]. Endogenous oligodendrocyte precursor cells (OPCs) are found to be universally dispersed within the human CNS and are enriched within high density within some subacute lesions during early stages of MS [103]. Within a subacute demyelinating lesion, perivascular infiltrates composed of activated CD4+ and CD8+ T cells as well as

macrophages are thought to act in concert with reactive microglia to release a milieu of pro-inflammatory factors that lead to oligodendrocyte dysregulation [99,104]. Additionally, clonally expanded MHC class-I restricted CD8+ T cells are found in close proximity to demyelinated axons and potentially target myelin epitopes [105]. Remyelination following OPC maturation leads to the formation of shadow plaques, in which patches of remyelinated white matter are composed of disproportionally thin myelin sheaths surrounding axons [103,106-111].

Although RRMS can last throughout the individual's lifespan, approximately 80% of patients with RRMS will develop a progressive disease within two decades following diagnosis, whereas 15% of individuals diagnosed with MS are classified as progressive patients [112]. In general, progressive MS is the latest stage of the disease, characterized by a gradual worsening of symptoms without remission. Severe neurological impairments dramatically reduce the quality of life for the individual, and this is mainly attributed to expanding cortical lesions impacting motor function. Pathologically, there is widespread axonal degeneration and grey matter neuropathy without a significant presence of the adaptive arm of immunity contributing to the immunopathology [113-116]. Rather, diffuse white and gray matter inflammation has been reported that correlated, in part, to global microglial activation as well as the presence of T cells, B cells and myelin-laden macrophages, which are restricted to the borders of preexisting lesions [104,117]. Furthermore, there is an overall failure of OPCs to efficiently remyelinate damaged white and gray matter areas, dramatically reducing the possibility for recovery [102,118].

The JHMV model of demyelination is a relevant MS model that differs from autoimmune mediated demyelination including experimental autoimmune

encephalomyelitis (EAE) as well as glial toxin models (e.g., cuprizone, lysolecithin, and ethidium bromide) [1,119-121]. Mice infected with neurotropic variants of MHV mice undergo chronic demyelination that is promoted through effector activity of virus-specific and non-specific T cells [122,123]. Given the possibility of viral infection in initiating demyelination in humans as well as the fact that numerous neurotropic viruses exist that are capable of persisting within the CNS, JHMV provides an exceptional surrogate mouse model of MS for studying chronic neuroinflammation and demyelination. A hallmark feature of JHMV infection of the CNS occurs following the acute stage of disease in which virus has spread into the spinal cord where it infects astrocytes and oligodendroglia. As a result, virus persists as non-infectious RNA and animals develop demyelinating lesions within the brain and spinal cord that are associated with clinical manifestations including awkward gait and hindlimb paralysis.

An effective way to visualize and quantify demyelination on a macroscopic scale is via luxol fast blue (LFB) staining. LFB contains a copper phthalocyanine dye that readily binds to lipoproteins found on myelin sheaths, resulting in a blue staining of myelin-rich regions and a lack of staining within demyelinating lesions. LFB analysis of spinal cord sections during persistent JHMV-infection reveals new lesion formation within the anterior funiculus of the spinal cord as early as day 7 p.i. [22]. As the severity neuroinflammation increases, new lesions are often observed within the lateral funiculus and posterior funiculus [22]. Additionally, axonopathy within the white matter tracts of the spinal cord is present as observed with the use of the SMI-32 stain or the Bielschowsky's silver impregnation stain and initial observations suggested that this occurred concomitantly

with demyelination, whereas axonal degeneration has been argued to precede oligodendrocyte dysregulation in MS [124,125].

Current evidence suggests that demyelination in JHMV-infected mice is not the result of induction of an autoimmune response against neuroantigens as has recently been reported to occur during Theiler's virus-induced demyelination [126-128]. However, adoptive transfer of T cells from JHMV-infected rats to naïve recipients results in demyelination [129]. Whether a similar response occurs in JHMV-infected mice and what the contributions are to demyelination are unknown at this time. A recent report has suggested that infection with mouse hepatitis virus strain A59 promotes activation of autoreactive T cells specific to myelin basic protein although the contributions of these cells to demyelination are defined [130].

Oligodendrocytes are an important viral reservoir during chronic JHMV-induced disease [20,22]. However viral-induced lysis of oligodendrocytes is not considered a primary mechanism contributing to demyelination, as JHMV-infection of immunodeficient mice, *e.g,* those lacking thymically-educated T and B lymphocytes, results in wide-spread viral replication within oligodendrocytes with very limited demyelination [131]. Moreover, adoptive transfer of splenocytes from JHMV-immunized immunocompetent mice into JHMV infected immunodeficient mice results in robust demyelination, implicating T cells as mediators of white matter damage [131-133]. Additionally, JHMV infected *Cd4 -/-* or *Cd8 -/-* mice develop demyelination demonstrating the importance of both T cell subsets in contributing to neuropathology, although JHMV-infected *Cd4 -/-* mice exhibited a diminished severity of myelin loss in the white matter tracts of the spinal cord compared to infected *Cd8 -/-* mice, suggesting an important role for CD4+ T cells in amplifying disease

progression [44]. One possible mechanism by which CD4+ T cells accelerate demyelination is through secretion of the chemokine CCL5, a potent chemoattractant for inflammatory macrophages [44]. Macrophages have been shown to be important in development of demyelinating lesions within spinal cord white matter during chronic JHMV-infection [131,134]. Furthermore, CCL5 neutralization or genetic ablation of *Ccr5* is associated with reduced macrophage infiltration correlating to a reduction in demyelination [135,136].

Early studies also implicated the release of nitric oxide (NO) from activated inflammatory macrophages and resident microglia as a factor involved in inducing demyelination [137]. Treatment of JHMV-infected mice with aminoguanidine (AG), a selective inhibitor of nitric oxide synthase 2 (NOS2), diminished clinical disease severity and this was associated with reduced neuroinflammation and demyelination arguing for a potential role of NOS2-derived NO in regulating proinflammatory gene expression within the CNS of infected mice [137]. However, genetic ablation of *Nos2* did not dampen demyelination in response to JHMV infection when compared to wildtype control mice indicating that NO does not contribute to myelin damage [138,139]. Differences may relate to off-target effects of AG that, in addition to muting NOS2 activity, also alter gene expression of specific chemokine genes within resident glial cells.

An alternate view is the CD8+ T cells also enhance demyelination through release of IFN-γ and this promotes migration and accumulation of activated macrophages/microglia within white matter tracts of JHMV-infected mice [140]. Other studies argue for a more protective role for CD4+ T cells through IFN-γ-mediated control of viral replication and/or additional undefined mechanisms [141,142]. Bystander CD4+ T cells, such as those activated yet not specific for viral antigens, are also thought to not be involved in white

matter damage in JHMV-infected mice [143]. Adding additional insight into how T cells contribute to either disease or defense are studies from Trandem et al. [144] showing that adoptive transfer of Tregs to JHMV-infected mice attenuates clinical disease severity and this is associated with dampened neuroinflammation and demyelination. Clearly, T cell infiltration into the CNS of mice persistently infected with JHMV is important in the pathogenesis of disease although a unifying mechanism(s) attributed to how these cells contribute to disease progression as wells protection remains elusive and, most likely, reflects different model systems used to evaluate functional roles for T cell subsets.

Although infectious virus is cleared by day 12 p.i., IFN-γ secretion from activated T-lymphocytes can be detected within the brain for up to four weeks p.i. and likely contributes to the deleterious effects on oligodendrocytes during the chronic stage of the disease [27]. Early studies have shown adoptive transfer of enriched CD8+ T cells obtained from JHMV-sensitized IFN-γ-deficient mice into JHMV-infected *Rag1 -/-* mice exhibited less severe demyelination compared to recipients of IFN-γ-expressing CD8+ T cells, implicating CD8+ T cell-derived IFN-γ as an important contributor to demyelination via destruction/damage to oligodendroglia [140]. Numerous groups have demonstrated increased sensitivity of oligodendrocyte progenitor cells (OPCs) to IFN-γ–induced apoptosis when compared to mature oligodendrocytes illustrating that susceptibility to IFN-γ-induced death is controlled, in part, by the maturation state of the cell [145-150]. Interestingly, demyelination is observed within JHMV-infected mice in which the IFN-γ receptor is selectively ablated in oligodendrocyte lineage cells suggesting that demyelination is multifaceted and additional mechanisms, including the local release of chemokines such as CXCL10 from activated resident glia, may directly contribute to

dysregulation of oligodendrocyte function and/or death [60,137,151]. It is also possible that IFN-γ secretion by CD8+ T cells promotes the migration and accumulation of activated macrophages/microglia within white matter tracts of JHMV-infected mice, leading to demyelination [131,140]. Indeed, ultrastructural and immunofluorescence analysis of JHMV-induced demyelinating lesions features macrophages/microglia engulfing myelin near demyelinated axons [134,152,153]. However, discriminating between these cells types by immunophenotyping and light microscopy remains a challenge to determine the exact role each play in contributing to pathology during chronic neurologic disease. More recently, Ransohoff and colleagues [154] have used electron microscopy to show a more pathogenic role for macrophages compared to microglia in EAE model of MS. All together, these findings suggest that demyelination is multifaceted and numerous factors could contribute to pathology.

1.6 Remyelination during JHMV infection

Numerous experimental models of CNS-injury have demonstrated that endogenous OPCs can respond to ongoing demyelination through proliferation and maturation, restoring depleted pools of mature oligodendrocytes and actively participating in CNS remyelination [155-160]. Following JHMV-infection, PDGFRα-positive OPCs found within the spinal cord increase six-fold between days 6 and 14 p.i., suggesting that OPCs become mitotically active following the onset of demyelination [161]. Additionally, a rebound in the total frequency of mature oligodendrocytes to pre-infection levels by 7 weeks p.i is also observed, presumably due to the maturation of the expanding OPC population [161]. Nevertheless, OPC differentiation does not lead to substantial clinical recovery and full remyelination within persistently infected mice, as exposed axons are still detected months later following infection [161].

Several studies have identified a plethora of cytokines, chemokines and growth factors that can impact OPC proliferation and maturation *in vivo* [159,161-163]. For example, signaling through the CXCR2 chemokine receptor has been shown to enhance OPC proliferation and aid in the directional migration of OPCs within the developing mouse spinal cord, while its inhibition resulted in reduced proliferation and increased maturation in an autoimmune model of demyelination [162-164]. Using the A59 variant of MHV, Armstrong and colleagues [163] demonstrated that PDGF and FGF2 can regulate OPC biology by stimulating proliferation and limiting maturation through activation of the notch signaling pathway. Within the context of JHMV-induced neurologic disease, the CXCR4/CXCL12 signaling axis may also play a crucial role in aiding OPC maturation. Indeed, blocking CXCL12's ability to bind to CXCR4 using the small molecule AMD3100

leads to an increase in PDGFRa-positive OPCs and a decrease in mature oligodendrocytes within the spinal cord, suggesting that CXCR4 signaling promotes OPC differentiation [161]. These results are supported and extended by Klein and colleagues [165] showing that activation of the CXCL12 scavenger receptor CXCR7 as well as CXCR4, results in OPC maturating during cuprizone-induced demyelination.

1.7 Experimental autoimmune encephalomyelitis (EAE): A model of autoimmune inflammatory demyelination.

Experimental autoimmune encephalomyelitis (EAE) is another widely used mouse model of MS for studying immune-mediated demyelination. Within this model, the type of antigenic immunization, age, sex and genetic strain of the mouse dictates the disease course, resulting in heterogeneous pathologies that share similarities to the wide spectrum of disease states that exist in MS [166]. In the prototypic induction regime, mice are immunized by subcutaneous injection with defined encephalitogenic peptides that are emulsified in innate adjuvants including Complete Freund's Adjuvant (CFA), as well as intravenous injection of pertussis toxin (PTx) [167]. CFA is composed of killed mycobacteria dissolved in mineral oil and functions by promoting the proliferation of autoreactive T cells as a result of the bacterium-derived antigens and toll-like receptor agonists [166]. Although the exact function of PTx is still under investigation, evidence suggests that it can promote breakdown of the BBB by increasing the expression of cytokines and chemokines that act to attract myeloid cells to endothelial membranes, resulting in their adhesion to the BBB and release of proteases that can degrade components of the BBB [168,169].

Immunization of SJL mice with a proteolipid protein (PLP) neuroantigen cocktail results in a relapse-remitting disease course, with the acute induction phase resulting in ascending hind limb paralysis due to white matter demyelination. This is followed by a remission phase for which mice show clinical recovery for at least 2 days after peak score of acute phase [167]. Conversely, injecting C57BL/6 mice with a peptide cocktail derived from myelin oligodendrocyte protein (MOG) spanning amino acid residues 35-55 (MOG_{35-}

$_{55}$) results in a progressive chronic demyelinating disease that shares many similarities to the pathology associated with JHMV-infection as well as the later stages of MS [167]. Compared to the relapsing form of EAE, mice with chronic EAE disease develop increased lesion burden and more expansive axonal loss. Immunologically, chronic-EAE generates a wider and more robust cytokine and chemokine expression profile and an increased predominance of cytotoxic CD8+ T cells in CNS exhibiting MOG specificity [170]. An alternative approach to induce EAE is through the passive induction model [171]. Within this protocol, naïve mice are immunized with MOG_{35-55} peptide in CFA. After 10-14 days post-immunization, draining lymph nodes are isolated and T cells are cultured *ex vivo* in the presence MOG_{35-55} peptide and polarizing cytokines that promote Th1 or Th17 CD4+ T cell proliferation. The CD4+ T cells are purified and subsequently adoptively transferred in naïve recipient mice, resulting in a neuroinflammatory disease with histologic similarities to the active MOG_{35-55} immunization model [172]. The benefits to this method include the ability to partition the contribution of Th1 and Th17 cells to pathogenesis of EAE. Furthermore, mice receiving the polarized T cells are not administered CFA or PTx, thus bypassing any immunomodulatory effects these factors induce following EAE immunization.

The initial immune response generated following MOG_{35-55} peptide immunization is primarily driven by proliferation and infiltration of pathogenic Th17 CD4+ T cells and neutrophils into the CNS [173,174]. As disease progresses, IFN-γ-expressing CD4+ and CD8+ T cells, as well as inflammatory macrophages, predominate the cellular composition and can induce damage within the parenchyma [175]. Although IL-17A expressing Th17 cells are found at lower frequencies at later stages of the disease, evidence indicates that

these cells can express an array of pro-inflammatory cytokines, such as GM-CSF, IL-2, IL-9, IL-17A and IL-21, which can impact glial survival [173]. Within the context of MS, IL-17 mRNA and protein levels have been found to be elevated within cells found in the CSF of MS patients during relapses [176,177]. In addition, IL-17 has been detected in both CD4 and CD8 T cells via immunohistochemical analysis of active MS lesions, although a majority of acute lesions during RRMS display a Th1 type immune profile [178].

1.8 *ELR+ Chemokine Signaling During Chronic JHMV-Induced Disease and EAE*

CXCR2 signaling may serve beneficial roles that extend beyond its influence on promoting chemotaxis towards ELR-positive chemokine gradients. CXCR2 is expressed on a variety of CNS cell subsets including neurons [179,180], astrocytes [181], microglia [182], and cells of the oligodendrocyte lineage [71,151,183]. Human CXCL8, a ligand for CXCR2, provides a neurotrophic effect on cultured hippocampal and cerebellar granule neurons during *in vitro* viability assays [184,185], and also blocks Fas-mediated apoptosis of cultured astrocytes [186]. Furthermore, cultured mouse OPCs proliferate in response to CXCL1 secreted from spinal cord astrocytes [187], while the CXCL1/CXCR2 signaling system is associated with the proliferation of human fetal OPCs [188] and OPC positioning and proliferation within the developing mouse spinal cord [189]. Transgenic mice devoid of CXCR2 have misalignments and an overall paucity of OPCs that remains into adulthood and this results in reduced myelin within the spinal cord white matter (Padovani-Claudio 2006). In addition, OPCs derived from *Cxcr2 -/-* mice have reduced numbers of mature oligodendrocytes when maturated in culture, demonstrating an essential role for CXCR2 in OPC differentiation.

More recently, a study by Liu and colleagues [158] used bone marrow chimeric mice to partition the contribution of CXCR2 expression on hematopoietic cells and CNS cells. Following adoptive transfer of bone marrow derived CXCR2-expressing cells from WT mice into *Cxcr2 −/−* mice, OPCs divided more rapidly associated with greater oligodendrocyte differentiation within demyelinated areas in both EAE and cuprizone models of demyelination [158]. This study indicates that CXCR2 expression on cells of the CNS is inhibitory for myelin repair following demyelination and therefore contributes to chronic

disease. Other studies using CXCR2 antagonists in EAE and spinal cord injury showed that blocking CXCR2 induced oligodendrocyte differentiation and promoted recovery, further suggesting a pathologic role for CXCR2 under defined experimental conditions [190,191]. However, CXCR2 antagonist treatments result in a global reduction of CXCR2 and some of the benefits observed in these studies were likely due to decreased inflammatory cell infiltration into the CNS. Nevertheless, while CXCR2 is necessary for OPC proliferation during development it appears to be deleterious under some pathologic conditions.

Cell specific manipulation of proteins involved in ELR-signaling within the CNS during EAE has recently been addressed by Kang and colleagues [192] where OPC specific ablation of Act1, the intralleculllar adaptor protein for IL-17 signaling, lead to dramatic reduction in the expression levels of CXCL1 and CXCL2 in the CNS and correlated with dampened severity of clinical disease. The Th17 cytokine pathway is a strong inducer of ELR-positive chemokine signaling and this study suggests that oligodendrocyte progenitors can enhance inflammation following IL-17R activation. Act1 ablation within neurons and mature oligodendrocytes lead to no reduction in inflammation while ablation in GFAP-positive astrocytes resulted in a modest reduction in inflammation. Conversely, Omari et al. [193] have described a potential protective effect of CXCL1 overexpression during EAE. Using a doxcycline-inducible transgenic mouse system, the authors revealed that astrocyte-specific CXCL1 overexpression following the induction of EAE reduces clinical severity and is associated with diminished demyelination and enhanced remyelination [193]. However, the results of this study remain enigmatic due to the difficulty in defining the exact mechanism by which CXCL1 leads to the observed effects as overexpression of CXCL1 could

desensitize CXCR2 signaling on neutrophils and negatively impact their migration to the CNS [194].

With regards to a protective role for CXCR2 in preventing cells from an oligodendrocyte lineage from death during JHMV infection, we have recently demonstrated that administration of a blocking antibody specific for CXCR2 to JHMV-infected mice increases clinical disease severity, and this correlates with a significant increase in oligodendrocyte apoptosis and demyelination [71]. Furthermore, JHMV infection of cultured OPCs derived from mouse neural progenitor cells (NPCs) results in apoptosis and this is blocked following inclusion of the CXCL1 [71]. The protective effect of CXCR2 signaling also extends to IFN-γ - induced apoptosis of cultured OPCs as addition of CXCL1 to IFN-γ - treated cultures restricts cell death [151]. Our findings suggest that one mechanism by which IFN-γ induces OPC death is through induction of CXCL10 that subsequently signals through CXCR3 [151]. Highlighting the importance of CXCL10 in enhancing IFN-γ - mediated cell death is the demonstration of reduced apoptosis in IFN- γ - treated OPC cultures derived from *Cxcr3 -/-* mice [151]. This observation supports and extends other studies demonstrating CXCL10 promotes neuronal apoptosis during simian immunodeficiency virus-induced encephalitis [195] and WNV-induced encephalitis [196-198]. Furthermore, the significance of CXCR2 signaling to OPC protection from IFN-γ and CXCL10-mediated cell death is further underscored by the finding that CXCR2-deficient OPCs are resistant to the tonic effects of CXCL1 in response to treatment with either IFN-γ or CXCL10. Mechanisms associated with CXCR2-mediated protection in these findings [151] include reduced activation of the pro-apoptotic caspase 3 and increased expression of the anti-apoptotic Bcl2 in CXCL1-treated cultures. Collectively, findings derived from *in*

vivo models ranging from development, as well as disease models such as EAE and JHMV-induced demyelination, to *in vitro* studies examining how cytokine/chemokine signaling affects oligodendroglia biology advocate that CXCR2 signaling is involved in many of these processes. However, all of these experiments have employed either germline-deficient mice deleted of *Cxcr2* or treatment with blocking antibodies and small molecule antagonists to assess how CXCR2 signaling controls these events. Therefore, accurate interpretation of how CXCR2 signaling modulates oligodendroglia biology is confounded by the fact that microglia, astrocytes, and neurons may express CXCR2, leading to potential of off-target effects of CXCR2-targeted therapies. To circumvent this issue, we have generated mice in which *Cxcr2* is inducibly ablated in oligodendroglia in adult mice in order to evaluate how signaling through this receptor affects disease progression in EAE and JHMV-induced neurologic disease (**Figure 1.3**). These findings are detailed in **Chapter 4**.

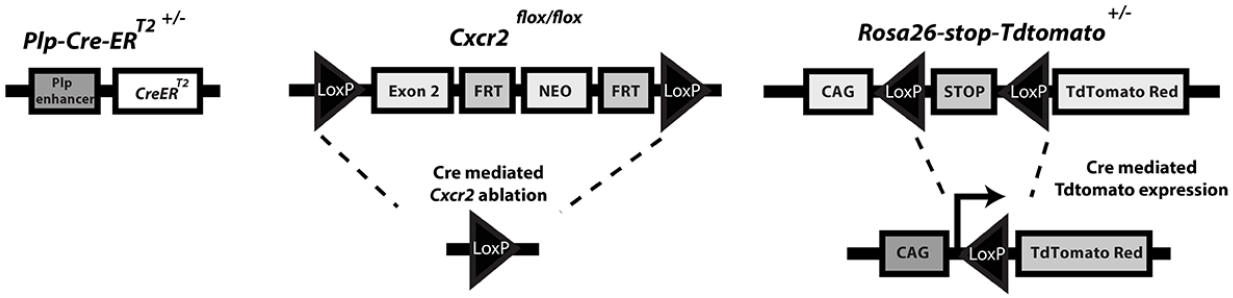

Figure 1.3 A tamoxifen-inducible transgenic mouse line to ablate *Cxcr2* in oligodendroglia lineage cells. To ablate *Cxcr2* in oligodendrocyte-lineage cells, a tamoxifen-inducible *Cre-ER* ^{T2} mouse line was generated in which an enhancer element derived from the *Plp* gene promotes expression of a tamoxifen-inducible form of Cre recombinase (*CreER*^{T2}), generating *Plp-Cre-ER*$^{T2\ +/+}$ *; Cxcr2* $^{fl/fl}$ mice . These mice were then crossed to a Cre-inducible reporter strain to generate *Plp-Cre-ER* $^{T2\ +/+}$ *:: Cxcr2* $^{fl/fl}$ *:: R26-stop-Td* $^{+/-}$ mice.

1.9 Summary

JHMV infection of susceptible mice reveals important clues about how the ELR-chemokines CXCL1 and CXCL2 and their cognant receptor CXCR2 orchestrate leukocyte infiltration into the CNS to combat viral infection. Moreover, the biphasic pathogenesis of JHMV that ultimately results in chronic demyelination shares several histologic features with human demyelinating disease MS, making it a useful model to study ELR-chemokine signaling on oligodendroglia within context of chronic neurologic disease. To expand our understanding on how CXCR2 signaling within the CNS signaling impacts neuroinflammation, we have also utilized the EAE model of MS that features distinct immunopathological features when compared to the JHMV model.

Chapter 2 describes a role for RIPK3 in facilitating an alternative death pathway within T cells lacking a functional form on the proapoptotic FADD protein. *In vitro*, homeostatic proliferation and survival of CD8+ T cells derived from FADDdd mice was restored when CD8+ T cells also lacked RIPK3. Following intraperitoneal inoculation of with the DM strain of MHV, mice that were reconstituted with FADDdd T cells were unable to mount a proper immune response to the virus, leading to uncontrolled viral titers as a result of a paucity of virus-specific effector T cells. These data suggest that the principle defect in these mice is the survival and protraction of MHV-specific T cells. Alternatively, T-cell-intrinsic loss of RIPK3 within FADDdd mice led to a restoration of anti-viral activity and efficient viral clearance, indicating that FADDdd and RIPK3 have antagonistic roles in T cell homeostasis and that RIPK3 is an essential component of TCR-induced necroptosis in T cells lacking FADD.

Chapter 3 examines how ELR-positive chemokines influence host-defense and progression of JHMV-induced neurologic disease. Within this study, transgenic mice were engineered in which CXCL1 is under control of a doxycycline-responsive element specifically in astrocytes. Elevated CXCL1 protein levels within the brain and spinal cord of transgenic mice resulted in significant accumulation of neutrophils within the CNS, leading to augmented clinical disease severity. However, no differences were observed in BBB integrity or in the recruitment of other immune cells into the CNS, suggesting that increased accumulation of neutrophils following infection with JHMV does not enhance leukocyte entry into the parenchyma. To determine if neutrophils contributed to the increase in white matter pathology, neutrophils were depleted with an anti-Ly-6g antibody. Treatment resulted in a modest decrease in clinical disease that reach significance at day 12 post-infection and reduced demyelination, suggesting that neutrophils were associated with white matter damage.

Chapter 4 reveals disparate roles for CXCR2 signaling on oligodendroglia within the JHMV and MOG_{33-55} EAE mouse model of neuroinflammation. Tamoxifen-inducible *PLP-Cre-ER^{T2}; Cxcr2 fl/fl* transgenic mice were utilized to ablate *Cxcr2* in oligodendrocytes. Following MOG_{33-55} EAE immunization, tamoxifen treated mice mice displayed delayed onset of disease and markedly reduced disease severity that correlated with a reduction in immune cell infiltration and damped expression of proinflammatory factors within the CNS, indicating an immunomodulatory role for CXCR2 signaling on resident oligodendroglia. In contrast, CNS infection of tamoxifen-treated *PLP-Cre-ER^{T2} ; Cxcr2 $^{fl/fl}$* mice with JHMV, which results in a Th1/IFN-γ-mediated demyelinating disease, did not affect either neuroinflammation or demyelination and proinflammatory gene expression

between tamoxifen-treated and control mice remained similar. These findings highlight differential roles between the immunological events that take place within these two models.

Collectively, these findings reveal important insights into mechanisms that govern neuroinflammation within the context of viral infections within the CNS as well as EAE autoimmune model of demyelination. By using novel approaches to manipulate cell-specific chemokine and chemokine receptor expression, we have demonstrated that CXCL1 overexpression augments JHMV-induced clinical disease as a result of chronic neutrophil accumulation within the CNS. Furthermore, inducible ablation of *Cxcr2* in oligodendrocytes reveals a novel immunomodulatory role the CXCR2 signaling axis on oligodendroglia within MOG_{33-55} immunized mice. Continuing to understand how chemokine signaling events regulate immune cell tracking into the CNS and their functions on endogenous glia may reveal novel targets for therapeutic intervention.

1.10 References

1. Bergmann CC, Lane TE, Stohlman SA. Coronavirus infection of the central nervous system: host-virus stand-off. *Nat Rev Microbiol*, 4(2), 121-132 (2006).
2. Gorbalenya AE, Enjuanes L, Ziebuhr J, Snijder EJ. Nidovirales: evolving the largest RNA virus genome. *Virus Res*, 117(1), 17-37 (2006).
3. McIntosh K, Dees JH, Becker WB, Kapikian AZ, Chanock RM. Recovery in tracheal organ cultures of novel viruses from patients with respiratory disease. *Proc Natl Acad Sci U S A*, 57(4), 933-940 (1967).
4. J.D. Almeida DMB, C.H. Cunningham, D. Hamre, M.S. Hofstad, L. Mallucci, K. McIntosh, D.A.J. Tyrrell. Coronaviruses. *Nature (Lond.)*, 220, p. 650 (1968).
5. Sawicki SG, Sawicki DL, Siddell SG. A contemporary view of coronavirus transcription. *J Virol*, 81(1), 20-29 (2007).
6. Brockway SM, Clay CT, Lu XT, Denison MR. Characterization of the expression, intracellular localization, and replication complex association of the putative mouse hepatitis virus RNA-dependent RNA polymerase. *J Virol*, 77(19), 10515-10527 (2003).
7. Snijder EJ, van der Meer Y, Zevenhoven-Dobbe J *et al.* Ultrastructure and origin of membrane vesicles associated with the severe acute respiratory syndrome coronavirus replication complex. *J Virol*, 80(12), 5927-5940 (2006).
8. Barthold SW, Beck DS, Smith AL. Enterotropic coronavirus (mouse hepatitis virus) in mice: influence of host age and strain on infection and disease. *Lab Anim Sci*, 43(4), 276-284 (1993).
9. Das Sarma J, Fu L, Hingley ST, Lavi E. Mouse hepatitis virus type-2 infection in mice: an experimental model system of acute meningitis and hepatitis. *Exp Mol Pathol*, 71(1), 1-12 (2001).
10. Lavi E, Gilden DH, Wroblewska Z, Rorke LB, Weiss SR. Experimental demyelination produced by the A59 strain of mouse hepatitis virus. *Neurology*, 34(5), 597-603 (1984).
11. Lavi E, Gilden DH, Highkin MK, Weiss SR. The organ tropism of mouse hepatitis virus A59 in mice is dependent on dose and route of inoculation. *Lab Anim Sci*, 36(2), 130-135 (1986).
12. Stohlman SA, Bergmann CC, Lin MT, Cua DJ, Hinton DR. CTL effector function within the central nervous system requires CD4+ T cells. *J Immunol*, 160(6), 2896-2904 (1998).
13. Lu JV, Weist BM, van Raam BJ *et al.* Complementary roles of Fas-associated death domain (FADD) and receptor interacting protein kinase-3 (RIPK3) in T-cell homeostasis and antiviral immunity. *Proc Natl Acad Sci U S A*, 108(37), 15312-15317 (2011).
14. Walsh CM. Grand challenges in cell death and survival: apoptosis vs. necroptosis. *Frontiers in cell and developmental biology*, 2, 3 (2014).
15. Newton K, Harris AW, Bath ML, Smith KG, Strasser A. A dominant interfering mutant of FADD/MORT1 enhances deletion of autoreactive thymocytes and inhibits proliferation of mature T lymphocytes. *EMBO J*, 17(3), 706-718 (1998).
16. Walsh CM, Wen BG, Chinnaiyan AM, O'Rourke K, Dixit VM, Hedrick SM. A role for FADD in T cell activation and development. *Immunity*, 8(4), 439-449 (1998).

17. Bell BD, Leverrier S, Weist BM *et al.* FADD and caspase-8 control the outcome of autophagic signaling in proliferating T cells. *Proc Natl Acad Sci U S A*, 105(43), 16677-16682 (2008).
18. Zhang DW, Shao J, Lin J *et al.* RIP3, an Energy Metabolism Regulator That Switches TNF-Induced Cell Death from Apoptosis to Necrosis. *Science*, 325(5938), 332-336 (2009).
19. Declercq W, Vanden Berghe T, Vandenabeele P. RIP kinases at the crossroads of cell death and survival. *Cell*, 138(2), 229-232 (2009).
20. Fleming JO, Trousdale MD, Elzaatari FAK, Stohlman SA, Weiner LP. Pathogenicity of antigenic variants of murine coronavirus JHM selected with monoclonal-antibodies. *Journal of Virology*, 58(3), 869-875 (1986).
21. Cheever FS, Daniels JB, et al. A murine virus (JHM) causing disseminated encephalomyelitis with extensive destruction of myelin. *J Exp Med*, 90(3), 181-210 (1949).
22. Wang FI, Hinton DR, Gilmore W, Trousdale MD, Fleming JO. Sequential infection of glial cells by the murine hepatitis virus JHM strain (MHV-4) leads to a characteristic distribution of demyelination. *Lab Invest*, 66(6), 744-754 (1992).
23. Ramakrishna C, Stohlman SA, Atkinson RA, Hinton DR, Bergmann CC. Differential regulation of primary and secondary CD8(+) T cells in the central nervous system. *Journal of Immunology*, 173(10), 6265-6273 (2004).
24. Marten NW, Stohlman SA, Bergmann CC. Role of viral persistence in retaining CD8(+) T cells within the central nervous system. *Journal of Virology*, 74(17), 7903-7910 (2000).
25. Hosking MP, Lane TE. The Role of Chemokines during Viral Infection of the CNS. *PLoS Pathog.*, 6(7), 4).
26. Bender SJ, Weiss SR. Pathogenesis of murine coronavirus in the central nervous system. *J Neuroimmune Pharmacol*, 5(3), 336-354 (2010).
27. Parra B, Hinton DR, Lin MT, Cua DJ, Stohlman SA. Kinetics of cytokine mRNA expression in the central nervous system following lethal and nonlethal coronavirus-induced acute encephalomyelitis. *Virology*, 233(2), 260-270 (1997).
28. Pearce BD, Hobbs MV, McGraw TS, Buchmeier MJ. Cytokine induction during T-cell-mediated clearance of mouse hepatitis virus from neurons in vivo. *J Virol*, 68(9), 5483-5495 (1994).
29. Ireland DD, Stohlman SA, Hinton DR, Atkinson R, Bergmann CC. Type I interferons are essential in controlling neurotropic coronavirus infection irrespective of functional CD8 T cells. *J Virol*, 82(1), 300-310 (2008).
30. Smith AL, Barthold SW, Beck DS. Intranasally administered alpha/beta interferon prevents extension of mouse hepatitis virus, strain JHM, into the brains of BALB/cByJ mice. *Antiviral Res*, 8(5-6), 239-245 (1987).
31. Minagawa H, Takenaka A, Mohri S, Mori R. Protective effect of recombinant murine interferon beta against mouse hepatitis virus infection. *Antiviral Res*, 8(2), 85-95 (1987).
32. Akwa Y, Hassett DE, Eloranta ML *et al.* Transgenic expression of IFN-alpha in the central nervous system of mice protects against lethal neurotropic viral infection but induces inflammation and neurodegeneration. *J Immunol*, 161(9), 5016-5026 (1998).

33. Yong VW, Zabad RK, Agrawal S, DaSilva AG, Metz LM. Elevation of matrix metalloproteinases (MMPs) in multiple sclerosis and impact of immunomodulators. *J. Neurol. Sci.*, 259(1-2), 79-84 (2007).
34. Hosking MP, Liu L, Ransohoff RM, Lane TE. A protective role for ELR+ chemokines during acute viral encephalomyelitis. *PLoS Pathog*, 5(11), e1000648 (2009).
35. Savarin C, Stohlman SA, Atkinson R, Ransohoff RM, Bergmann CC. Monocytes regulate T cell migration through the glia limitans during acute viral encephalitis. *J Virol*, 84(10), 4878-4888 (2010).
36. Zhou J, Stohlman SA, Atkinson R, Hinton DR, Marten NW. Matrix metalloproteinase expression correlates with virulence following neurotropic mouse hepatitis virus infection. *J Virol*, 76(15), 7374-7384 (2002).
37. Zhou J, Stohlman SA, Hinton DR, Marten NW. Neutrophils promote mononuclear cell infiltration during viral-induced encephalitis. *J Immunol*, 170(6), 3331-3336 (2003).
38. Trifilo MJ, Montalto-Morrison C, Stiles LN *et al.* CXC chemokine ligand 10 controls viral infection in the central nervous system: evidence for a role in innate immune response through recruitment and activation of natural killer cells. *J Virol*, 78(2), 585-594 (2004).
39. Zuo J, Stohlman SA, Hoskin JB, Hinton DR, Atkinson R, Bergmann CC. Mouse hepatitis virus pathogenesis in the central nervous system is independent of IL-15 and natural killer cells. *Virology*, 350(1), 206-215 (2006).
40. Marten NW, Stohlman SA, Zhou J, Bergmann CC. Kinetics of virus-specific CD8+ -T-cell expansion and trafficking following central nervous system infection. *J Virol*, 77(4), 2775-2778 (2003).
41. Stiles LN, Hosking MP, Edwards RA, Strieter RM, Lane TE. Differential roles for CXCR3 in CD4+ and CD8+ T cell trafficking following viral infection of the CNS. *Eur J Immunol*, 36(3), 613-622 (2006).
42. Liu MT, Chen BP, Oertel P *et al.* The T cell chemoattractant IFN-inducible protein 10 is essential in host defense against viral-induced neurologic disease. *J Immunol*, 165(5), 2327-2330 (2000).
43. Liu MT, Armstrong D, Hamilton TA, Lane TE. Expression of Mig (monokine induced by interferon-gamma) is important in T lymphocyte recruitment and host defense following viral infection of the central nervous system. *J Immunol*, 166(3), 1790-1795 (2001).
44. Lane TE, Liu MT, Chen BP *et al.* A central role for CD4(+) T cells and RANTES in virus-induced central nervous system inflammation and demyelination. *J Virol*, 74(3), 1415-1424 (2000).
45. Trifilo MJ, Lane TE. The CC chemokine ligand 3 regulates CD11c+CD11b+CD8alpha-dendritic cell maturation and activation following viral infection of the central nervous system: implications for a role in T cell activation. *Virology*, 327(1), 8-15 (2004).
46. Dufour JH, Dziejman M, Liu MT, Leung JH, Lane TE, Luster AD. IFN-gamma-inducible protein 10 (IP-10; CXCL10)-deficient mice reveal a role for IP-10 in effector T cell generation and trafficking. *J Immunol*, 168(7), 3195-3204 (2002).
47. Liu MT, Keirstead HS, Lane TE. Neutralization of the chemokine CXCL10 reduces inflammatory cell invasion and demyelination and improves neurological function

in a viral model of multiple sclerosis. *Journal of Immunology*, 167(7), 4091-4097 (2001).
48. Stiles LN, Liu MT, Kane JA, Lane TE. CXCL10 and trafficking of virus-specific T cells during coronavirus-induced demyelination. *Autoimmunity*, 42(6), 484-491 (2009).
49. Stiles LN, Hardison JL, Schaumburg CS, Whitman LM, Lane TE. T cell antiviral effector function is not dependent on CXCL10 following murine coronavirus infection. *J Immunol*, 177(12), 8372-8380 (2006).
50. Bergmann CC, Altman JD, Hinton D, Stohlman SA. Inverted immunodominance and impaired cytolytic function of CD8(+) T cells during viral persistence in the central nervous system. *Journal of Immunology*, 163(6), 3379-3387 (1999).
51. Glass WG, Lane TE. Functional expression of chemokine receptor CCR5 on CD4(+) T cells during virus-induced central nervous system disease. *J Virol*, 77(1), 191-198 (2003).
52. Glass WG, Lane TE. Functional analysis of the CC chemokine receptor 5 (CCR5) on virus-specific CD8+ T cells following coronavirus infection of the central nervous system. *Virology*, 312(2), 407-414 (2003).
53. Held KS, Chen BP, Kuziel WA, Rollins BJ, Lane TE. Differential roles of CCL2 and CCR2 in host defense to coronavirus infection. *Virology*, 329(2), 251-260 (2004).
54. Dimitrijevic OB, Stamatovic SM, Keep RF, Andjelkovic AV. Absence of the chemokine receptor CCR2 protects against cerebral ischemia/reperfusion injury in mice. *Stroke*, 38(4), 1345-1353 (2007).
55. Kim TS, Perlman S. Viral expression of CCL2 is sufficient to induce demyelination in RAG1-/- mice infected with a neurotropic coronavirus. *J Virol*, 79(11), 7113-7120 (2005).
56. Parra B, Hinton DR, Marten NW *et al.* IFN-gamma is required for viral clearance from central nervous system oligodendroglial. *Journal of Immunology*, 162(3), 1641-1647 (1999).
57. Lin MT, Stohlman SA, Hinton DR. Mouse hepatitis virus is cleared from the central nervous systems of mice lacking perforin-mediated cytolysis. *J Virol*, 71(1), 383-391 (1997).
58. Phares TW, Stohlman SA, Hwang M, Min B, Hinton DR, Bergmann CC. CD4 T Cells Promote CD8 T Cell Immunity at the Priming and Effector Site during Viral Encephalitis. *J Virol*, 86(5), 2416-2427 (2012).
59. Zhou J, Hinton DR, Stohlman SA, Liu CP, Zhong L, Marten NW. Maintenance of CD8+ T cells during acute viral infection of the central nervous system requires CD4+ T cells but not interleukin-2. *Viral Immunol*, 18(1), 162-169 (2005).
60. Gonzalez JM, Bergmann CC, Ramakrishna C *et al.* Inhibition of interferon-gamma signaling in oligodendroglia delays coronavirus clearance without altering demyelination. *Am J Pathol*, 168(3), 796-804 (2006).
61. Malone KE, Stohlman SA, Ramakrishna C, Macklin W, Bergmann CC. Induction of class I antigen processing components in oligodendroglia and microglia during viral encephalomyelitis. *Glia*, 56(4), 426-435 (2008).
62. Marten NW, Stohlman SA, Atkinson RD, Hinton DR, Fleming JO, Bergmann CC. Contributions of CD8+ T cells and viral spread to demyelinating disease. *J Immunol*, 164(8), 4080-4088 (2000).

63. Lin MT, Hinton DR, Marten NW, Bergmann CC, Stohlman SA. Antibody prevents virus reactivation within the central nervous system. *J Immunol*, 162(12), 7358-7368 (1999).
64. Ramakrishna C, Bergmann CC, Atkinson R, Stohlman SA. Control of central nervous system viral persistence by neutralizing antibody. *J Virol*, 77(8), 4670-4678 (2003).
65. Ramakrishna C, Stohlman SA, Atkinson RD, Shlomchik MJ, Bergmann CC. Mechanisms of central nervous system viral persistence: the critical role of antibody and B cells. *J Immunol*, 168(3), 1204-1211 (2002).
66. Anghelina D, Zhao J, Trandem K, Perlman S. Role of regulatory T cells in coronavirus-induced acute encephalitis. *Virology*, 385(2), 358-367 (2009).
67. Zhao J, Fett C, Trandem K, Fleming E, Perlman S. IFN-gamma- and IL-10-expressing virus epitope-specific Foxp3(+) T reg cells in the central nervous system during encephalomyelitis. *J Exp Med*, 208(8), 1571-1577 (2011).
68. Mantovani A, Cassatella MA, Costantini C, Jaillon S. Neutrophils in the activation and regulation of innate and adaptive immunity. *Nature Reviews Immunology*, 11(8), 519-531 (2011).
69. Scott EP, Branigan PJ, Del Vecchio AM, Weiss SR. Chemokine expression during mouse-hepatitis-virus-induced encephalitis: contributions of the spike and background genes. *J Neurovirol*, 14(1), 5-16 (2008).
70. Lane TE, Asensio VC, Yu N, Paoletti AD, Campbell IL, Buchmeier MJ. Dynamic regulation of alpha- and beta-chemokine expression in the central nervous system during mouse hepatitis virus-induced demyelinating disease. *J Immunol*, 160(2), 970-978 (1998).
71. Hosking MP, Tirotta E, Ransohoff RM, Lane TE. CXCR2 Signaling Protects Oligodendrocytes and Restricts Demyelination in a Mouse Model of Viral-Induced Demyelination. *PLoS One*, 5(6), 12 (2010).
72. Tani M, Fuentes ME, Peterson JW *et al.* Neutrophil infiltration, glial reaction, and neurological disease in transgenic mice expressing the chemokine N51/KC in oligodendrocytes. *J Clin Invest*, 98(2), 529-539 (1996).
73. Fan X, Patera AC, Pong-Kennedy A *et al.* Murine CXCR1 is a functional receptor for GCP-2/CXCL6 and interleukin-8/CXCL8. *J Biol Chem*, 282(16), 11658-11666 (2007).
74. Savarin C, Stohlman SA, Rietsch AM, Butchi N, Ransohoff RM, Bergmann CC. MMP9 deficiency does not decrease blood–brain barrier disruption, but increases astrocyte MMP3 expression during viral encephalomyelitis. *Glia*, 59(11), 1770-1781 (2011).
75. Bai F, Kong KF, Dai J *et al.* A paradoxical role for neutrophils in the pathogenesis of West Nile virus. *J Infect Dis*, 202(12), 1804-1812 (2010).
76. Kim JV, Kang SS, Dustin ML, McGavern DB. Myelomonocytic cell recruitment causes fatal CNS vascular injury during acute viral meningitis. *Nature*, 457(7226), 191-195 (2009).
77. Belperio JA, Keane MP, Burdick MD *et al.* CXCR2/CXCR2 ligand biology during lung transplant ischemia-reperfusion injury. *J Immunol*, 175(10), 6931-6939 (2005).
78. Strieter RM, Keane MP, Burdick MD, Sakkour A, Murray LA, Belperio JA. The role of CXCR2/CXCR2 ligands in acute lung injury. *Current Drug Targets - Inflammation and Allergy*, 4(3), 299-303 (2005).

79. Wareing MD, Shea AL, Inglis CA, Dias PB, Sarawar SR. CXCR2 is required for neutrophil recruitment to the lung during influenza virus infection, but is not essential for viral clearance. *Viral Immunol.*, 20(3), 369-377 (2007).
80. Kielian T, Barry B, Hickey WF. CXC chemokine receptor-2 ligands are required for neutrophil-mediated host defense in experimental brain abscesses. *Journal of Immunology*, 166(7), 4634-4643 (2001).
81. Carlson T, Kroenke M, Rao P, Lane TE, Segal B. The Th17-ELR+ CXC chemokine pathway is essential for the development of central nervous system autoimmune disease. *J Exp Med*, 205(4), 811-823 (2008).
82. Glabinski AR, Tani M, Strieter RM, Tuohy VK, Ransohoff RM. Synchronous synthesis of alpha- and beta-chemokines by cells of diverse lineage in the central nervous system of mice with relapses of chronic experimental autoimmune encephalomyelitis. *Am J Pathol*, 150(2), 617-630 (1997).
83. McColl SR, Staykova MA, Wozniak A, Fordham S, Bruce J, Willenborg DO. Treatment with anti-granulocyte antibodies inhibits the effector phase of experimental autoimmune encephalomyelitis. *J Immunol*, 161(11), 6421-6426 (1998).
84. Rumble JM, Huber AK, Krishnamoorthy G *et al.* Neutrophil-related factors as biomarkers in EAE and MS. *J Exp Med*, 212(1), 23-35 (2015).
85. Steinbach K, Piedavent M, Bauer S, Neumann JT, Friese MA. Neutrophils amplify autoimmune central nervous system infiltrates by maturing local APCs. *J Immunol*, 191(9), 4531-4539 (2013).
86. Liu L, Belkadi A, Darnall L *et al.* CXCR2-positive neutrophils are essential for cuprizone-induced demyelination: relevance to multiple sclerosis. *Nat Neurosci*, 13(3), 319-326 (2010).
87. Furth PA, St Onge L, Boger H *et al.* Temporal control of gene expression in transgenic mice by a tetracycline-responsive promoter. *Proc Natl Acad Sci U S A*, 91(20), 9302-9306 (1994).
88. Gossen M, Bujard H. Tight control of gene expression in mammalian cells by tetracycline-responsive promoters. *Proc Natl Acad Sci U S A*, 89(12), 5547-5551 (1992).
89. Kistner A, Gossen M, Zimmermann F *et al.* Doxycycline-mediated quantitative and tissue-specific control of gene expression in transgenic mice. *Proc Natl Acad Sci U S A*, 93(20), 10933-10938 (1996).
90. Schonig K, Bujard H. Generating conditional mouse mutants via tetracycline-controlled gene expression. *Methods Mol Biol*, 209, 69-104 (2003).
91. Urlinger S, Baron U, Thellmann M, Hasan MT, Bujard H, Hillen W. Exploring the sequence space for tetracycline-dependent transcriptional activators: novel mutations yield expanded range and sensitivity. *Proc Natl Acad Sci U S A*, 97(14), 7963-7968 (2000).
92. Steinman L. Immunology of relapse and remission in multiple sclerosis. *Annu Rev Immunol*, 32, 257-281 (2014).
93. International Multiple Sclerosis Genetics C. Network-based multiple sclerosis pathway analysis with GWAS data from 15,000 cases and 30,000 controls. *American journal of human genetics*, 92(6), 854-865 (2013).

94. International Multiple Sclerosis Genetics C, Wellcome Trust Case Control C, Sawcer S *et al.* Genetic risk and a primary role for cell-mediated immune mechanisms in multiple sclerosis. *Nature*, 476(7359), 214-219 (2011).
95. Ascherio A, Munger KL. Environmental risk factors for multiple sclerosis. Part I: the role of infection. *Ann Neurol*, 61(4), 288-299 (2007).
96. Ascherio A, Munger KL. Environmental risk factors for multiple sclerosis. Part II: Noninfectious factors. *Ann Neurol*, 61(6), 504-513 (2007).
97. Haines JL, Terwedow HA, Burgess K *et al.* Linkage of the MHC to familial multiple sclerosis suggests genetic heterogeneity. The Multiple Sclerosis Genetics Group. *Human molecular genetics*, 7(8), 1229-1234 (1998).
98. Barcellos LF, Sawcer S, Ramsay PP *et al.* Heterogeneity at the HLA-DRB1 locus and risk for multiple sclerosis. *Human molecular genetics*, 15(18), 2813-2824 (2006).
99. Lassmann H, Bruck W, Lucchinetti CF. The immunopathology of multiple sclerosis: an overview. *Brain Pathol*, 17(2), 210-218 (2007).
100. Compston A, Coles A. Multiple sclerosis. *Lancet*, 359(9313), 1221-1231 (2002).
101. Kornek B, Storch MK, Weissert R *et al.* Multiple sclerosis and chronic autoimmune encephalomyelitis: a comparative quantitative study of axonal injury in active, inactive, and remyelinated lesions. *Am J Pathol*, 157(1), 267-276 (2000).
102. Chang A, Tourtellotte WW, Rudick R, Trapp BD. Premyelinating oligodendrocytes in chronic lesions of multiple sclerosis. *N Engl J Med*, 346(3), 165-173 (2002).
103. Chang A, Nishiyama A, Peterson J, Prineas J, Trapp BD. NG2-positive oligodendrocyte progenitor cells in adult human brain and multiple sclerosis lesions. *J Neurosci*, 20(17), 6404-6412 (2000).
104. Traugott U, Reinherz EL, Raine CS. Multiple sclerosis: distribution of T cell subsets within active chronic lesions. *Science*, 219(4582), 308-310 (1983).
105. Neumann H, Medana IM, Bauer J, Lassmann H. Cytotoxic T lymphocytes in autoimmune and degenerative CNS diseases. *Trends Neurosci*, 25(6), 313-319 (2002).
106. Prineas JW, Kwon EE, Goldenberg PZ *et al.* Multiple sclerosis. Oligodendrocyte proliferation and differentiation in fresh lesions. *Lab Invest*, 61(5), 489-503 (1989).
107. Lucchinetti C, Bruck W, Parisi J, Scheithauer B, Rodriguez M, Lassmann H. A quantitative analysis of oligodendrocytes in multiple sclerosis lesions. A study of 113 cases. *Brain*, 122 (Pt 12), 2279-2295 (1999).
108. Roy NS, Wang S, Harrison-Restelli C *et al.* Identification, isolation, and promoter-defined separation of mitotic oligodendrocyte progenitor cells from the adult human subcortical white matter. *J Neurosci*, 19(22), 9986-9995 (1999).
109. Lassmann H. Comparative neuropathology of chronic experimental allergic encephalomyelitis and multiple sclerosis. *Schriftenreihe Neurologie*, 25, 1-135 (1983).
110. Schlesinger H. Zur Frage der akuten multiplen Sklerose und der encephalomyelitis disseminata im Kindesalter. *Arb Neurol Inst [Wien]*, 17, 410-432 (1909).
111. Halfpenny C, Benn T, Scolding N. Cell transplantation, myelin repair, and multiple sclerosis. *Lancet neurology*, 1(1), 31-40 (2002).
112. Kremenchutzky M, Rice GP, Baskerville J, Wingerchuk DM, Ebers GC. The natural history of multiple sclerosis: a geographically based study 9: observations on the progressive phase of the disease. *Brain*, 129(Pt 3), 584-594 (2006).

113. Antel J, Antel S, Caramanos Z, Arnold DL, Kuhlmann T. Primary progressive multiple sclerosis: part of the MS disease spectrum or separate disease entity? *Acta Neuropathol*, 123(5), 627-638 (2012).
114. Trapp BD, Peterson J, Ransohoff RM, Rudick R, Mork S, Bo L. Axonal transection in the lesions of multiple sclerosis. *N Engl J Med*, 338(5), 278-285 (1998).
115. Peterson JW, Bo L, Mork S, Chang A, Trapp BD. Transected neurites, apoptotic neurons, and reduced inflammation in cortical multiple sclerosis lesions. *Ann Neurol*, 50(3), 389-400 (2001).
116. Bjartmar C, Wujek JR, Trapp BD. Axonal loss in the pathology of MS: consequences for understanding the progressive phase of the disease. *J Neurol Sci*, 206(2), 165-171 (2003).
117. Prineas JW, Wright RG. Macrophages, lymphocytes, and plasma cells in the perivascular compartment in chronic multiple sclerosis. *Lab Invest*, 38(4), 409-421 (1978).
118. Wolswijk G. Chronic stage multiple sclerosis lesions contain a relatively quiescent population of oligodendrocyte precursor cells. *J Neurosci*, 18(2), 601-609 (1998).
119. Yajima K, Suzuki K. Demyelination and remyelination in the rat central nervous system following ethidium bromide injection. *Lab Invest*, 41(5), 385-392 (1979).
120. Hall SM. The effect of injections of lysophosphatidyl choline into white matter of the adult mouse spinal cord. *J Cell Sci*, 10(2), 535-546 (1972).
121. Matsushima GK, Morell P. The neurotoxicant, cuprizone, as a model to study demyelination and remyelination in the central nervous system. *Brain Pathol*, 11(1), 107-116 (2001).
122. Lane TE, Buchmeier MJ. Murine coronavirus infection: a paradigm for virus-induced demyelinating disease. *Trends Microbiol*, 5(1), 9-14 (1997).
123. Templeton SP, Perlman S. Pathogenesis of acute and chronic central nervous system infection with variants of mouse hepatitis virus, strain JHM. *Immunol Res*, 39(1-3), 160-172 (2007).
124. Dandekar AA, Wu GF, Pewe L, Perlman S. Axonal damage is T cell mediated and occurs concomitantly with demyelination in mice infected with a neurotropic coronavirus. *J Virol*, 75(13), 6115-6120 (2001).
125. Das Sarma J, Kenyon LC, Hingley ST, Shindler KS. Mechanisms of primary axonal damage in a viral model of multiple sclerosis. *J Neurosci*, 29(33), 10272-10280 (2009).
126. Lehmann PV, Forsthuber T, Miller A, Sercarz EE. Spreading of T-cell autoimmunity to cryptic determinants of an autoantigen. *Nature*, 358(6382), 155-157 (1992).
127. McMahon EJ, Bailey SL, Castenada CV, Waldner H, Miller SD. Epitope spreading initiates in the CNS in two mouse models of multiple sclerosis. *Nat. Med.*, 11(3), 335-339 (2005).
128. Miller SD, Vanderlugt CL, Begolka WS *et al.* Persistent infection with Theiler's virus leads to CNS autoimmunity via epitope spreading. *Nat. Med.*, 3(10), 1133-1136 (1997).
129. Watanabe R, Wege H, ter Meulen V. Adoptive transfer of EAE-like lesions from rats with coronavirus-induced demyelinating encephalomyelitis. *Nature*, 305(5930), 150-153 (1983).

130. Gruslin E, Moisan S, St-Pierre Y, Desforges M, Talbot PJ. Transcriptome profile within the mouse central nervous system and activation of myelin-reactive T cells following murine coronavirus infection. *J Neuroimmunol*, 162(1-2), 60-70 (2005).
131. Wu GF, Perlman S. Macrophage infiltration, but not apoptosis, is correlated with immune-mediated demyelination following murine infection with a neurotropic coronavirus. *J Virol*, 73(10), 8771-8780 (1999).
132. Wang FI, Stohlman SA, Fleming JO. Demyelination induced by murine hepatitis virus JHM strain (MHV-4) is immunologically mediated. *J Neuroimmunol*, 30(1), 31-41 (1990).
133. Houtman JJ, Fleming JO. Dissociation of demyelination and viral clearance in congenitally immunodeficient mice infected with murine coronavirus JHM. *J Neurovirol*, 2(2), 101-110 (1996).
134. Fleury HJA, Sheppard RD, Bornstein MB, Raine CS. Further ultrastructural observations of virus morphogenesis and myelin pathology in JHM virus encephalomyelitis. *Neuropathol. Appl. Neurobiol.*, 6(3), 165-179 (1980).
135. Glass WG, Hickey MJ, Hardison JL, Liu MT, Manning JE, Lane TE. Antibody targeting of the CC chemokine ligand 5 results in diminished leukocyte infiltration into the central nervous system and reduced neurologic disease in a viral model of multiple sclerosis. *J Immunol*, 172(7), 4018-4025 (2004).
136. Glass WG, Liu MT, Kuziel WA, Lane TE. Reduced macrophage infiltration and demyelination in mice lacking the chemokine receptor CCR5 following infection with a neurotropic coronavirus. *Virology*, 288(1), 8-17 (2001).
137. Lane TE, Fox HS, Buchmeier MJ. Inhibition of nitric oxide synthase-2 reduces the severity of mouse hepatitis virus-induced demyelination: implications for NOS2/NO regulation of chemokine expression and inflammation. *J Neurovirol*, 5(1), 48-54 (1999).
138. Chen BP, Lane TE. Lack of nitric oxide synthase type 2 (NOS2) results in reduced neuronal apoptosis and mortality following mouse hepatitis virus infection of the central nervous system. *J Neurovirol*, 8(1), 58-63 (2002).
139. Wu GF, Pewe L, Perlman S. Coronavirus-induced demyelination occurs in the absence of inducible nitric oxide synthase. *J Virol*, 74(16), 7683-7686 (2000).
140. Pewe L, Perlman S. Cutting edge: CD8 T cell-mediated demyelination is IFN-gamma dependent in mice infected with a neurotropic coronavirus. *J Immunol*, 168(4), 1547-1551 (2002).
141. Pewe L, Haring J, Perlman S. CD4 T-cell-mediated demyelination is increased in the absence of gamma interferon in mice infected with mouse hepatitis virus. *J Virol*, 76(14), 7329-7333 (2002).
142. Stohlman SA, Hinton DR, Parra B, Atkinson R, Bergmann CC. CD4 T cells contribute to virus control and pathology following central nervous system infection with neurotropic mouse hepatitis virus. *J Virol*, 82(5), 2130-2139 (2008).
143. Haring JS, Perlman S. Bystander CD4 T cells do not mediate demyelination in mice infected with a neurotropic coronavirus. *Journal of Neuroimmunology*, 137(1-2), 42-50 (2003).
144. Trandem K, Anghelina D, Zhao J, Perlman S. Regulatory T cells inhibit T cell proliferation and decrease demyelination in mice chronically infected with a coronavirus. *J Immunol*, 184(8), 4391-4400 (2010).

145. Lin WS, Kunkler PE, Harding HP, Ron D, Kraig RP, Popko B. Enhanced Integrated Stress Response Promotes Myelinating Oligodendrocyte Survival in Response to Interferon-gamma. *Am. J. Pathol.*, 173(5), 1508-1517 (2008).
146. Horiuchi M, Itoh A, Pleasure D, Itoh T. MEK-ERK signaling is involved in interferon-gamma-induced death of oligodendroglial progenitor cells. *J Biol Chem*, 281(29), 20095-20106 (2006).
147. Chew LJ, King WC, Kennedy A, Gallo V. Interferon-gamma inhibits cell cycle exit in differentiating oligodendrocyte progenitor cells. *Glia*, 52(2), 127-143 (2005).
148. Balabanov R, Strand K, Kemper A, Lee JY, Popko B. Suppressor of cytokine signaling 1 expression protects oligodendrocytes from the deleterious effects of interferon-gamma. *Journal of Neuroscience*, 26(19), 5143-5152 (2006).
149. Baerwald KD, Popko B. Developing and mature oligodendrocytes respond differently to the immune cytokine interferon-gamma. *J. Neurosci. Res.*, 52(2), 230-239 (1998).
150. Wang Y, Ren Z, Tao D, Tilwalli S, Goswami R, Balabanov R. STAT1/IRF-1 signaling pathway mediates the injurious effect of interferon-gamma on oligodendrocyte progenitor cells. *Glia*, 58(2), 195-208 (2010).
151. Tirotta E, Ransohoff RM, Lane TE. CXCR2 signaling protects oligodendrocyte progenitor cells from IFN-gamma/CXCL10-mediated apoptosis. *Glia*, (2011).
152. Templeton SP, Kim TS, O'Malley K, Perlman S. Maturation and localization of macrophages and microglia during infection with a neurotropic murine coronavirus. *Brain Pathol*, 18(1), 40-51 (2008).
153. Das Sarma J. Microglia-mediated neuroinflammation is an amplifier of virus-induced neuropathology. *J Neurovirol*, 20(2), 122-136 (2014).
154. Yamasaki R, Lu H, Butovsky O *et al.* Differential roles of microglia and monocytes in the inflamed central nervous system. *J Exp Med*, (2014).
155. Armstrong RC, Le TQ, Flint NC, Vana AC, Zhou YX. Endogenous cell repair of chronic demyelination. *J Neuropathol Exp Neurol*, 65(3), 245-256 (2006).
156. Keirstead HS, Blakemore WF. The role of oligodendrocytes and oligodendrocyte progenitors in CNS remyelination. *Adv Exp Med Biol*, 468, 183-197 (1999).
157. Blakemore WF, Keirstead HS. The origin of remyelinating cells in the central nervous system. *J Neuroimmunol*, 98(1), 69-76 (1999).
158. Liu L, Darnall L, Hu T, Choi K, Lane TE, Ransohoff RM. Myelin repair is accelerated by inactivating CXCR2 on nonhematopoietic cells. *J Neurosci*, 30(27), 9074-9083 (2010).
159. Murtie JC, Zhou YX, Le TQ, Vana AC, Armstrong RC. PDGF and FGF2 pathways regulate distinct oligodendrocyte lineage responses in experimental demyelination with spontaneous remyelination. *Neurobiol Dis*, 19(1-2), 171-182 (2005).
160. McTigue DM, Tripathi RB. The life, death, and replacement of oligodendrocytes in the adult CNS. *J. Neurochem.*, 107(1), 1-19 (2008).
161. Carbajal KS, Miranda JL, Tsukamoto MR, Lane TE. CXCR4 signaling regulates remyelination by endogenous oligodendrocyte progenitor cells in a viral model of demyelination. *Glia*, 59(12), 1813-1821 (2011).
162. Tsai HH, Frost E, To V *et al.* The chemokine receptor CXCR2 controls positioning of oligodendrocyte precursors in developing spinal cord by arresting their migration. *Cell*, 110(3), 373-383 (2002).

163. Armstrong RC, Le TQ, Frost EE, Borke RC, Vana AC. Absence of fibroblast growth factor 2 promotes oligodendroglial repopulation of demyelinated white matter. *J Neurosci*, 22(19), 8574-8585 (2002).
164. Robinson S, Tani M, Strieter RM, Ransohoff RN, Miller RH. The chemokine growth-regulated oncogene-alpha promotes spinal cord oligodendrocyte precursor proliferation. *Journal of Neuroscience*, 18(24), 10457-10463 (1998).
165. Williams JL, Patel JR, Daniels BP, Klein RS. Targeting CXCR7/ACKR3 as a therapeutic strategy to promote remyelination in the adult central nervous system. *J Exp Med*, 211(5), 791-799 (2014).
166. Gold R, Linington C, Lassmann H. Understanding pathogenesis and therapy of multiple sclerosis via animal models: 70 years of merits and culprits in experimental autoimmune encephalomyelitis research. *Brain*, 129(Pt 8), 1953-1971 (2006).
167. Stromnes IM, Goverman JM. Active induction of experimental allergic encephalomyelitis. *Nature protocols*, 1(4), 1810-1819 (2006).
168. Dumas A, Amiable N, de Rivero Vaccari JP *et al.* The inflammasome pyrin contributes to pertussis toxin-induced IL-1beta synthesis, neutrophil intravascular crawling and autoimmune encephalomyelitis. *PLoS Pathog*, 10(5), e1004150 (2014).
169. Carbonetti NH. Pertussis toxin and adenylate cyclase toxin: key virulence factors of Bordetella pertussis and cell biology tools. *Future microbiology*, 5(3), 455-469 (2010).
170. Berard JL, Wolak K, Fournier S, David S. Characterization of relapsing-remitting and chronic forms of experimental autoimmune encephalomyelitis in C57BL/6 mice. *Glia*, 58(4), 434-445 (2010).
171. Stromnes IM, Goverman JM. Passive induction of experimental allergic encephalomyelitis. *Nature protocols*, 1(4), 1952-1960 (2006).
172. Rumble J, Segal BM. In vitro polarization of T-helper cells. *Methods Mol Biol*, 1193, 105-113 (2014).
173. Muranski P, Restifo NP. Essentials of Th17 cell commitment and plasticity. *Blood*, 121(13), 2402-2414 (2013).
174. Reboldi A, Coisne C, Baumjohann D *et al.* C-C chemokine receptor 6-regulated entry of TH-17 cells into the CNS through the choroid plexus is required for the initiation of EAE. *Nat Immunol*, 10(5), 514-523 (2009).
175. t Hart BA, Gran B, Weissert R. EAE: imperfect but useful models of multiple sclerosis. *Trends in molecular medicine*, 17(3), 119-125 (2011).
176. Brucklacher-Waldert V, Stuerner K, Kolster M, Wolthausen J, Tolosa E. Phenotypical and functional characterization of T helper 17 cells in multiple sclerosis. *Brain*, 132(Pt 12), 3329-3341 (2009).
177. Durelli L, Conti L, Clerico M *et al.* T-helper 17 cells expand in multiple sclerosis and are inhibited by interferon-beta. *Ann Neurol*, 65(5), 499-509 (2009).
178. Tzartos JS, Friese MA, Craner MJ *et al.* Interleukin-17 production in central nervous system-infiltrating T cells and glial cells is associated with active disease in multiple sclerosis. *Am J Pathol*, 172(1), 146-155 (2008).
179. Hesselgesser J, Halks-Miller M, DelVecchio V *et al.* CD4-independent association between HIV-1 gp120 and CXCR4: functional chemokine receptors are expressed in human neurons. *Curr Biol*, 7(2), 112-121 (1997).

180. Horuk R, Martin AW, Wang Z *et al.* Expression of chemokine receptors by subsets of neurons in the central nervous system. *J Immunol*, 158(6), 2882-2890 (1997).
181. Flynn G, Maru S, Loughlin J, Romero IA, Male D. Regulation of chemokine receptor expression in human microglia and astrocytes. *J Neuroimmunol*, 136(1-2), 84-93 (2003).
182. Filipovic R, Jakovcevski I, Zecevic N. GRO-alpha and CXCR2 in the human fetal brain and multiple sclerosis lesions. *Dev Neurosci*, 25(2-4), 279-290 (2003).
183. Omari KM, John GR, Sealfon SC, Raine CS. CXC chemokine receptors on human oligodendrocytes: implications for multiple sclerosis. *Brain*, 128(Pt 5), 1003-1015 (2005).
184. Araujo DM, Cotman CW. Trophic effects of interleukin-4, interleukin-7 and interleukin-8 on hippocampal neuronal cultures - potential involvement of glial-derived factors. *Brain Res.*, 600(1), 49-55 (1993).
185. Limatola C, Ciotti MT, Mercanti D, Santoni A, Eusebi F. Signaling pathways activated by chemokine receptor CXCR2 and AMPA-type glutamate receptors and involvement in granule cells survival. *Journal of Neuroimmunology*, 123(1-2), 9-17 (2002).
186. Saas P, Walker PR, Quiquerez AL *et al.* A self-defence mechanism of astrocytes against Fas-mediated death involving interleukin-8 and CXCR2. *Neuroreport*, 13(15), 1921-1924 (2002).
187. Robinson S, Tani M, Strieter RM, Ransohoff RM, Miller RH. The chemokine growth-regulated oncogene-alpha promotes spinal cord oligodendrocyte precursor proliferation. *J Neurosci*, 18(24), 10457-10463 (1998).
188. Filipovic R, Zecevic N. The effect of CXCL1 on human fetal oligodendrocyte progenitor cells. *Glia*, 56(1), 1-15 (2008).
189. Tsai HH, Frost E, To V *et al.* The chemokine receptor CXCR2 controls positioning of oligodendrocyte precursors in developing spinal cord by arresting their migration. *Cell*, 110(3), 373-383 (2002).
190. Padovani-Claudio DA, Liu LP, Ransohoff RM, Miller RH. Alterations in the oligodendrocyte lineage, myelin, and white matter in adult mice lacking the chemokine receptor CXCR2. *Glia*, 54(5), 471-483 (2006).
191. Kerstetter AE, Padovani-Claudio DA, Bai L, Miller RH. Inhibition of CXCR2 signaling promotes recovery in models of multiple sclerosis. *Experimental Neurology*, 220(1), 44-56 (2009).
192. Marsh DR, Flemming JM. Inhibition of CXCR1 and CXCR2 chemokine receptors attenuates acute inflammation, preserves gray matter and diminishes autonomic dysreflexia after spinal cord injury. *Spinal cord*, 49(3), 337-344 (2011).
193. Kang Z, Wang C, Zepp J *et al.* Act1 mediates IL-17-induced EAE pathogenesis selectively in NG2+ glial cells. *Nat Neurosci*, 16(10), 1401-1408 (2013).
194. Omari KM, Lutz SE, Santambrogio L, Lira SA, Raine CS. Neuroprotection and remyelination after autoimmune demyelination in mice that inducibly overexpress CXCL1. *Am J Pathol*, 174(1), 164-176 (2009).
195. Wiekowski MT, Chen SC, Zalamea P *et al.* Disruption of neutrophil migration in a conditional transgenic model: evidence for CXCR2 desensitization in vivo. *J Immunol*, 167(12), 7102-7110 (2001).

196. Sui Y, Potula R, Dhillon N *et al.* Neuronal apoptosis is mediated by CXCL10 overexpression in simian human immunodeficiency virus encephalitis. *Am J Pathol*, 164(5), 1557-1566 (2004).
197. Zhang B, Chan YK, Lu B, Diamond MS, Klein RS. CXCR3 mediates region-specific antiviral T cell trafficking within the central nervous system during west nile virus encephalitis. *Journal of Immunology*, 180(4), 2641-2649 (2008).
198. Zhang B, Patel J, Croyle M, Diamond MS, Klein RS. TNF-alpha-dependent regulation of CXCR3 expression modulates neuronal survival during West Nile virus encephalitis. *Journal of Neuroimmunology*, 224(1-2), 28-38 (2010).
199. Klein RS, Lin E, Zhang B *et al.* Neuronal CXCL10 directs CD8(+) T-cell recruitment and control of West Nile virus encephalitis. *Journal of Virology*, 79(17), 11457-11466 (2005).

CHAPTER TWO

Complementary roles of Fas-associated death domain (FADD) and receptor interacting protein kinase-3 (RIPK3) in T-cell homeostasis and antiviral immunity

Lu JV, Weist BM, van Raam BJ, Marro BS, Nguyen LV, Srinivas P, Bell BD, Luhrs KA, Lane TE, Salvesen GS, Walsh CM

Abstract

Caspase-8 (casp8) is required for extrinsic apoptosis, and mice deficient in casp8 fail to develop and die in utero while ultimately failing to maintain the proliferation of T cells, B cells, and a host of other cell types. Paradoxically, these failures are not caused by a defect in apoptosis, but by a presumed proliferative function of this protease. Indeed, following mitogenic stimulation, T cells lacking casp8 or its adaptor protein FADD (Fas-associated death domain protein) develop a hyperautophagic morphology, and die a programmed necrosis-like death process termed necroptosis. Recent studies have demonstrated that receptor-interacting protein kinases (RIPKs) RIPK1 and RIPK3 together facilitate TNF-induced necroptosis, but the precise role of RIPKs in the demise of T cells lacking FADD or casp8 activity is unknown. Here we demonstrate that RIPK3 and FADD have opposing and complementary roles in promoting T-cell clonal expansion and homeostasis. We show that the defective proliferation of T cells bearing an interfering form of FADD (FADDdd) is rescued by crossing with RIPK3$^{-/-}$ mice, although such rescue ultimately leads to lymphadenopathy. Enhanced recovery of these double-mutant T cells following stimulation demonstrates that FADD, casp8, and RIPK3 are all essential for clonal expansion, contraction, and antiviral responses. Finally, we demonstrate that caspase-mediated cleavage of RIPK1-containing necrosis inducing complexes (necrosomes) is sufficient to prevent necroptosis in the face of death receptor signaling. These studies highlight the "two-faced" nature of casp8 activity, promoting clonal expansion in some situations and apoptotic demise in others.

2.1 Introduction

Following ligation of death receptors (DR), death domain-containing members of the TNF receptor superfamily recruit proteins that are essential for promoting DR-induced apoptosis [1]. These include caspase-8 (casp8), a noncatalytic paralogue of casp8 called c-FLIP, and the adaptor protein FADD (Fas-associated death domain protein). Curiously, loss of any of these proteins leads to early embryonic lethality and significant defects in hematopoiesis and activated lymphocyte survival [2]. Furthermore, T-cell–specific expression of an interfering form of FADD containing only the death domain of this adaptor (FADDdd) leads to defective T-cell clonal expansion and altered thymopoiesis[3-5]. These findings suggest that the signaling molecules that promote apoptosis following DR function serve additional roles that are linked, but unrelated to apoptosis. Recently, it was discovered that the defective survival of T cells lacking active casp8 is associated with a hyperautophagic morphology, and that such T cells die from an alternative form of cell death mediated by receptor-interacting protein kinase-1 (RIPK1) [6,7].

For several years, it has been known that triggering DRs in the absence of caspase activity can lead to a nonapoptotic form of cell death that resembles necrosis [8,9] that requires the serine/threonine kinase activity of RIPK1 [10]. By using a small-molecule library, Yuan and colleagues identified a family of molecules termed necrostatins that are capable of binding to RIPK1 and blocking DR-induced necrosis [11], a process defined as necroptosis. RNAi screening of genes responsible for DR-induced necroptosis validated that RIPK1 is required for this alternative form of cell death [12] by forming a complex with RIPK3 termed the necrosome [13] in the absence of casp8 function [14-16]. Thus, it is now clear that both RIPK1 and RIPK3 are functionally required for the elaboration of

necroptotic signaling following DR ligation in cells lacking the capacity to activate caspases. As RIPK1 and RIPK3 have both been shown to be targets for casp8 activity, it has been suggested that failure in casp8-mediated cleavage of RIPK1 and RIPK3 may lead preferentially to necroptosis [13,17].

Although our previous work has demonstrated that FADDdd-expressing and casp8-deficient T cells succumb to RIPK1-dependent necroptosis, we wished to assess the potential involvement of RIPK3 in this process. Interestingly, although FADD is required, the classic DRs are unlikely to be involved in the demise of such mutant T cells, as antagonizing them failed to block the induction of casp8 activity following T-cell mitogenic stimulation [18]. Thus, we sought to establish the in vivo impact of non–DR-induced necroptosis to T-cell–mediated immune function in the context of T cells lacking the capacity to activate casp8. Importantly, because mice bearing a germline RIPK1 deletion succumb to perinatal lethality [19], we chose instead to cross FADDdd-expressing mice [4] with RIPK3$^{-/-}$ mice, as the latter strain develops in an overtly normal fashion, and RIPK3$^{-/-}$ T cells display no obvious activation defects [20]. We find that a RIPK3 deficiency acts as a second site suppressor mutation in the context of FADDdd-expressing T cells, and prevents acute necroptosis of these cells following mitogenic stimulation. This RIPK3 deficiency also restores in vivo T-cell–mediated antiviral activity observed in FADDdd transgenic mice [21], but promotes development of lymphoproliferative disease. RIPK1 and RIPK3 both appear to be cleaved following T-cell antigenic stimulation, and we demonstrate that blockade of RIPK1 processing is sufficient to promote DR-induced necroptosis.

2.2 Results

To investigate the role of RIPK3 in T-cell development and homeostasis, spleens, lymph nodes, and thymi were harvested from WT mice, mice expressing FADDdd in thymocytes and T cells [4], RIPK3$^{-/-}$ mice [20], and RIPK3$^{-/-}$ × FADDdd mice for initial comparison of CD4^{+} and CD8^{+} T-cell ratios. WT naive splenocytes typically display a 2:1 CD4:CD8 ratio, whereas FADDdd splenocytes display a 4:1 CD4:CD8 ratio as a result of defective CD8^{+} accumulation and homeostasis [21]. Loss of RIPK3 signaling in FADDdd T cells restored the CD4:CD8 ratio to WT levels in spleen and lymph nodes (**Figure 2.1A**), and rescued the diminished fraction of FADDdd CD44^{High}/CD62L^{High} T cells or central memory T cells (T_{CM}; **Figure 2.1B**). These dual mutant mice also displayed an enhanced fraction of CD44^{High}/CD62L^{Low} effector T cells (**Figure 2.1C**), potentially because of defective clearance of autoreactive T cells. We observed no significant differences in the fractions of CD4, CD8, CD4/CD8 double positive, or CD4/CD8 double-negative (DN) populations among the four genotypes (**Figure 2.1D**). FADDdd T cells display a partial block during thymopoiesis at the CD4^{-}CD8^{-}CD25^{+}CD44^{-} (DN3) stage associated with expression of the pre-Tα/T-cell receptor (TCR)-β complex [4]. Failure to express the pre-Tα/TCRβ complex leads to thymocyte death, whereas successful surface expression promotes proliferation and differentiation into the CD25^{-}/CD44^{-} "DN4" stage [22]. As expected, we observed an enhanced DN3 population and a paucity of DN4 cells in FADDdd thymocytes, whereas WT, RIPK3$^{-/-}$, and FADDdd × RIPK3$^{-/-}$ thymocytes developed normal fractions of DN3 cells (**Figure 2.1E** and **Figure 2.S1**).

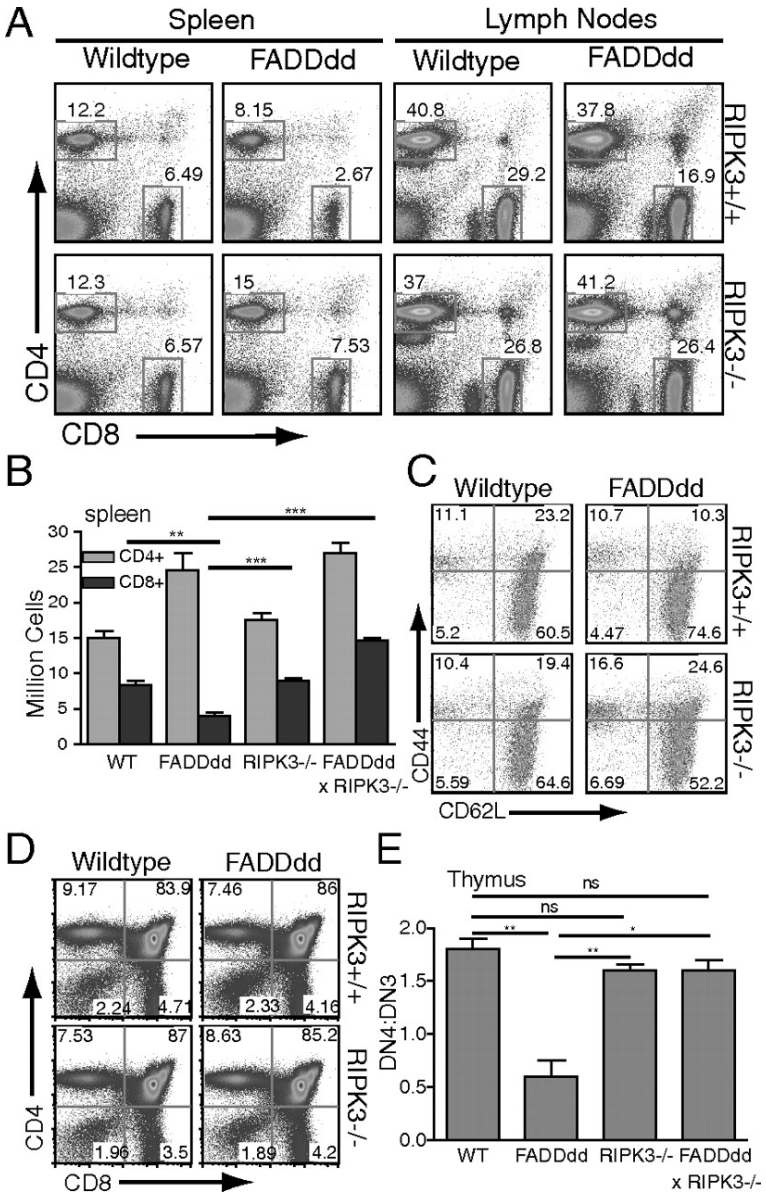

Figure 2.1. CD8⁺ T-cell homeostasis restored in FADDdd × RIPK3$^{-/-}$ mice. (*A*) Spleen and lymph node cells were analyzed by flow cytometry for CD4⁺ vs. CD8⁺ populations. Numbers represent percentage of cells staining in each gate. (*B*) Graph displays number of CD4⁺ and CD8⁺ cells in the spleen, representative of three separate experiments. Error bars represent SEM (***P* < 0.01 and ****P* < 0.001 vs. WT CD8⁺). (*C*) Decreased CD8⁺ memory T cell population in FADDdd mice restored with RIPK3 deficiency. CD8⁺ gated splenocytes analyzed for CD44⁺CD62L⁻ (*D*). Thymocyte DN population shown by anti-CD4 and anti-CD8 staining; numbers represent percentage of cells per quadrant. (*E*) Graph displays DN4:DN3 population in thymocytes of indicated genotypes, representative of three experiments (**P* < 0.05 and ***P* < 0.01). Error bars indicate SEM.

Previous studies have demonstrated that FADDdd or casp8$^{-/-}$ T cells display defective clonal expansion following antigen receptor stimulation [2] as a result of the induction of necroptotic cell death [6,7]. With recent evidence demonstrating that both RIPK1 and RIPK3 are involved in promoting necroptotic death following DR ligation [23], we sought to determine if RIPK3 may participate in the necroptotic death of FADDdd T cells. Splenocytes from FADDdd × RIPK3$^{-/-}$ mice were labeled with carboxyfluorescein succinimidyl ester (CFSE) and cultured with α-CD3/-CD28 for 3 d to detect the T-cell proliferative response. As observed previously, FADDdd T cells had a diminished proliferative response, as assessed by accumulation of live CD8^{+}/CFSE^{Lo} T cells (**Figure 2.2A**). In contrast, FADDdd × RIPK3$^{-/-}$ T cells displayed an enhanced proliferative response, correlating with a reduced fraction of 7-actinomycin D (7AAD) high T cells, demonstrating that the loss of RIPK3 rescued the defective clonal expansion and death of FADDdd T cells (**Figure 2.2B**). Although treatment with the RIPK1 inhibitor Nec-1 restored FADDdd T-cell proliferation to levels comparable to RIPK3$^{-/-}$ T cells, the loss of both FADD and RIPK3 signaling led to an appreciable enhancement in recovery of live proliferating T cells (**Figure 2.2C**). Further assessment of the role of FADD in peripheral tolerance revealed that, upon restimulation through the TCR, FADDdd and FADDdd × RIPK3$^{-/-}$ T cells are resistant to restimulation-induced cell death (RICD) (**Figure 2.2D**). However, loss of RIPK3 signaling, alone or in the context of the FADDdd mutation, led to little enhanced recovery of live T cells upon restimulation, demonstrating that the death pathway induced during RICD is almost entirely FADD-directed, casp8-mediated apoptosis.

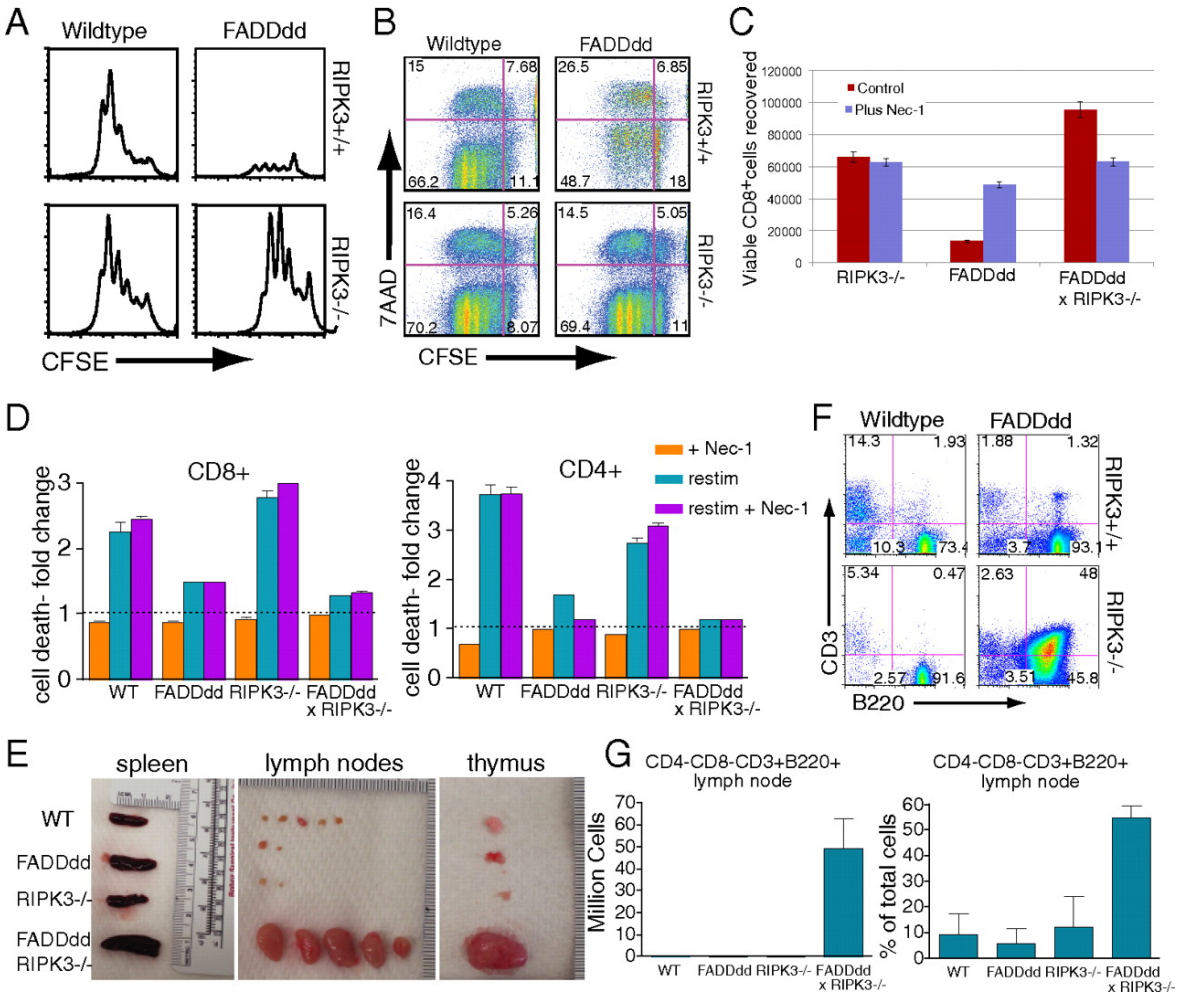

Figure 2.2. RIPK3 deficiency restores proliferation and survival of FADDdd CD8⁺ T cells. (*A*) CFSE analysis of CD8⁺ T cells treated with α-CD3 (145-2C11; 1 μg/mL) plus αCD28 (200 ng/mL). Splenocytes were stained and analyzed by cytometry after 3 d. Shown are plots for CFSE vs. cell numbers of CD8⁺ splenocytes. (*B*) Rescue of enhanced death phenotype of FADDdd CD8⁺ T cells by RIPK3 deficiency. Plots for CFSE vs. 7-AAD of CD8 cells; upper and lower left quadrants represent populations that have divided and are dead or alive, respectively. (*C*) Recovery of live CD8⁺ T cells in FADDdd × RIPK3$^{-/-}$ vs. WT cultures following 3 d stimulation. Activated splenocytes treated with or without 10 μM necrostatin-1 (Nec-1) added at start of culture. Graph represents percent viable CD8⁺ cells recovered ± SEM. (*D*) Fold change in cell death of CD4⁺ or CD8⁺ cells upon restimulation (restim) with or without Nec-1 relative to death observed in activated cells (1 μg 1 × 10^5 cells αCD3, 200 ng/mL αCD28) not subjected to restimulation (dotted line). Error bars represent SEM (**P* < 0.05, ***P* < 0.01, and ****P* < 0.001 vs. WT restimulation). (*E*) Lymphoid tissue from aged (40 wk) mice of indicated genotypes. (*F*) FACS plots display percentage of double-negative population that are CD3⁺ B220⁺ in mice of indicated genotypes. (*G*) Graphs represent counts or percentage of total live cells (after RBC lysis) that are CD4⁻CD8⁻CD3⁺B220⁺. Error bars represent SEM; *n* = 3 of each genotype.

Mice and human subjects lacking functional Fas receptor (CD95) or Fas-ligand (CD95L) develop lymphoproliferative disease and autoimmune lymphoproliferative syndromes, respectively, as well as an accumulation of $CD4^-$, $CD8^-$, $CD3^+$, $B220^+$ T lymphocytes. Similarly, older FADDdd × $RIPK3^{-/-}$ mice displayed a slight splenomegaly with frank lymphadenopathy and enlarged thymi (**Figure 2.2E**), coupled with a dramatic increase of $CD4^-$, $CD8^-$, $CD3^+$, $B220^+$ T lymphocytes (**Figure 2.2F and G**). Histological analyses revealed lymphocyte infiltrates within livers of the DKO mice (**Figure 2.S2**). These findings demonstrate that, although RICD drives a mostly apoptotic form of death, chronic loss of both DR-induced apoptosis and necroptosis leads to recapitulation of the lymphoproliferative phenotype observed in mice lacking functional Fas or FasL.

FADDdd mice are incapable of mounting an effective immune response against viral pathogens, including lymphocytic choriomeningitis virus and murine hepatitis virus (MHV) [21]. To address the consequence of the loss of both RIPK3 and FADD signaling during an antiviral response, FADDdd × $RIPK3^{-/-}$ mice were injected intraperitoneally with 2×10^5 pfu of MHV and killed 7 d after infection. Tetramer staining of T cells in the liver showed infiltration of virus-specific T cells to the infected tissue, which was not evident in FADDdd mice as expected, but restored in FADDdd × $RIPK3^{-/-}$ mice (**Figure 2.3A**). To determine whether FADD and RIPK3 play a role in cytotoxic T lymphocyte (CTL) activity, in vivo and in vitro CTL assays were performed by using target cells pulsed with nonspecific [ovalbumin (OVA)] or virus-specific immunodominant (S510) peptides. To assess in vivo killing activity, C57BL56/J splenocytes were pulsed with low and high concentrations of CFSE, followed by peptide pulsing with S510 and OVA peptides, respectively. One hour after injection of pulsed splenocytes into 7 d mock- and MHV-infected mice, spleens were

harvested to assess the recovery of S510- vs. OVA-pulsed target cells. Whereas FADDdd mice failed to kill S510-pulsed target cells because of defective accumulation of effector cells, killing activity was similar among WT, RIPK3$^{-/-}$, and FADDdd × RIPK3$^{-/-}$ mice (**Figure 2.3B and C**). As with restoration of virus-specific effector cells, deletion of RIPK3 in FADDdd mice rescued their defective clearance of MHV (**Figure 2.3D**).

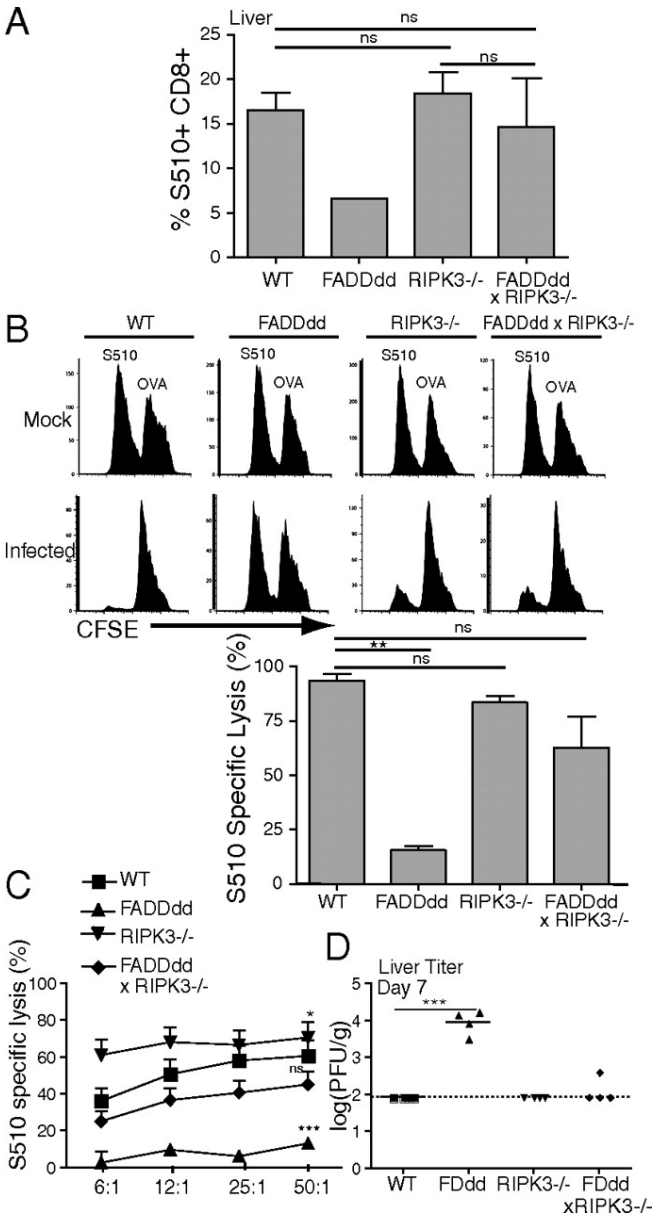

Figure 2.3. FADDdd × RIPK3$^{-/-}$ mice exhibit normal immune response to murine hepatitis virus (MHV) infection. (*A*) T cells from livers of infected mice were stained with MHV-specific (S510) tetramer. Graph represents percentage of S510-positive cells of total CD8^{+} cells. (*B*) Nonspecific and specific target cells were labeled with CFSE$^{hi/low}$, respectively, and adoptively transferred into infected and sham mice for in vivo CTL analysis shown by FACS plots. Graph displays percent specific lysis (**$P < 0.01$). (*C*) Splenocytes from infected and sham mice were incubated with specific/nonspecific target cells for 4 h to measure in vitro CTL activity. Graph represents percent specific lysis. Considered a significant difference with respect to WT specific lysis (*$P < 0.01$, ***$P < 0.001$). (*D*) Livers from infected mice were harvested 7 d after infection for viral titer analysis. Error bars indicate SEM (***$P < 0.001$).

To address the T-cell–intrinsic role of both RIPK3 and FADD signaling during an antiviral response, we performed MHV infection studies in immunodeficient $Rag2^{-/-}$ × $IL2R\gamma c^{-/-}$ mice reconstituted with purified T cells from the four genotypes. 2.5×10^6 T cells were adoptively transferred into $Rag2^{-/-}$ × $IL2R\gamma_c^{-/-}$ mice, and rested for 7 d before injected intraperitoneally with 2×10^5 pfu of MHV. Although overall splenocyte numbers 7 d after infection were approximately similar in uninfected mice, indicating no defect in homeostatic proliferation, FADDdd × $RIPK3^{-/-}$ possessed a greater number of splenocytes relative to other mice, consistent with a potential defect in lymphocyte homeostasis following viral infection (**Figure 2.4A**). To evaluate the generation of virus-specific T cells, IFN-γ production was analyzed after a 6-h in vitro restimulation of splenocytes with the immunodominant $CD8^+$ T-cell epitope, the MHV S510 peptide. $RIPK3^{-/-}$ and FADDdd × $RIPK3^{-/-}$ mice developed comparable numbers of IFN-γ–expressing splenic CTLs as WT mice, whereas the recovery of these virus-specific T cells was significantly diminished in FADDdd spleens (**Figure 2.4B**). These findings demonstrate that the loss of RIPK3 rescued the expansion capacity of antiviral T cells expressing FADDdd. Consistent with this, the diminished fraction of effector/memory $CD8^+$ ($CD44^{High}/CD62L^{Low}$) T cells observed after infection in FADDdd splenocytes was restored to WT levels in FADDdd × $RIPK3^{-/-}$ mice (**Figure 2.S3**).

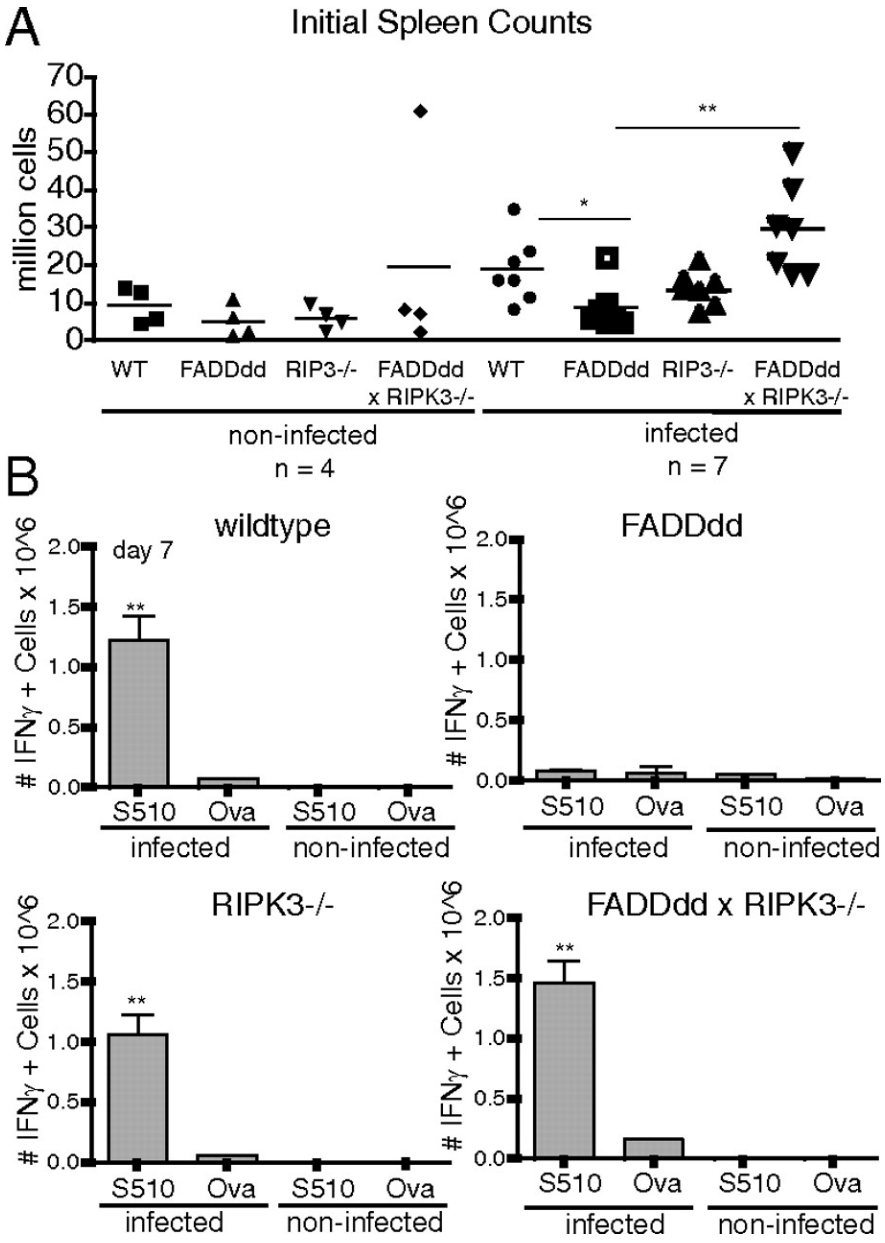

Figure 2.4. T-cell–intrinsic FADD and RIPK3 activity required for antiviral response to murine hepatitis virus (MHV) infection. (*A*) Initial splenocyte counts of infected and control mice in indicated genotypes (**P* < 0.05 and ***P* < 0.01). (*B*) FADDdd × RIPK3$^{-/-}$ adoptive transfer mice and controls were infected intraperitoneally with MHV. IFN-γ levels in splenocytes of infected and control mice were determined by intracellular IFN-γ staining 7 d after infection. Splenocytes were restimulated 6 h with S510 or OVA peptides and stained for CD8. IFN-γ(+) cells were calculated by multiplying total splenocytes by percentage of IFN-γ cells (***P* < 0.01 vs. infected FADDdd S510).

Processing of RIPK1 and/or RIPK3 by casp8, itself activated by FADD [and possibly cFLIP [24]], is thought to prevent necroptosis [13,17]. Considering that casp8 catalytic activity is required for T-cell clonal expansion [18], processing of RIPK1 or RIPK3, both of which are targets of casp8 [25,26], was assayed following T-cell antigenic stimulation. We detected cleaved RIPK1 and RIPK3 in viable OT-I OVA-specific T cells following stimulation with OVA peptide or anti-Fas [27] (**Figure 2.5A**). This led us to pose the broader question of whether processing of RIPK1 and/or RIPK3 may also occur during DR-induced apoptosis vs. necroptosis. We treated Jurkat T cells lacking FADD [28], which are known to be highly sensitive to DR-induced necroptosis [10](**Figure 2.S4**), and $FADD^{-/-}$ Jurkat cells transfected with full length FADD ($FADD^{REC}$; **Figure 2.5B**) with TNF-α or TRAIL and detected RIPK1 (and PARP1) cleavage fragments in $FADD^{REC}$ cells (**Figure 2.5C**).

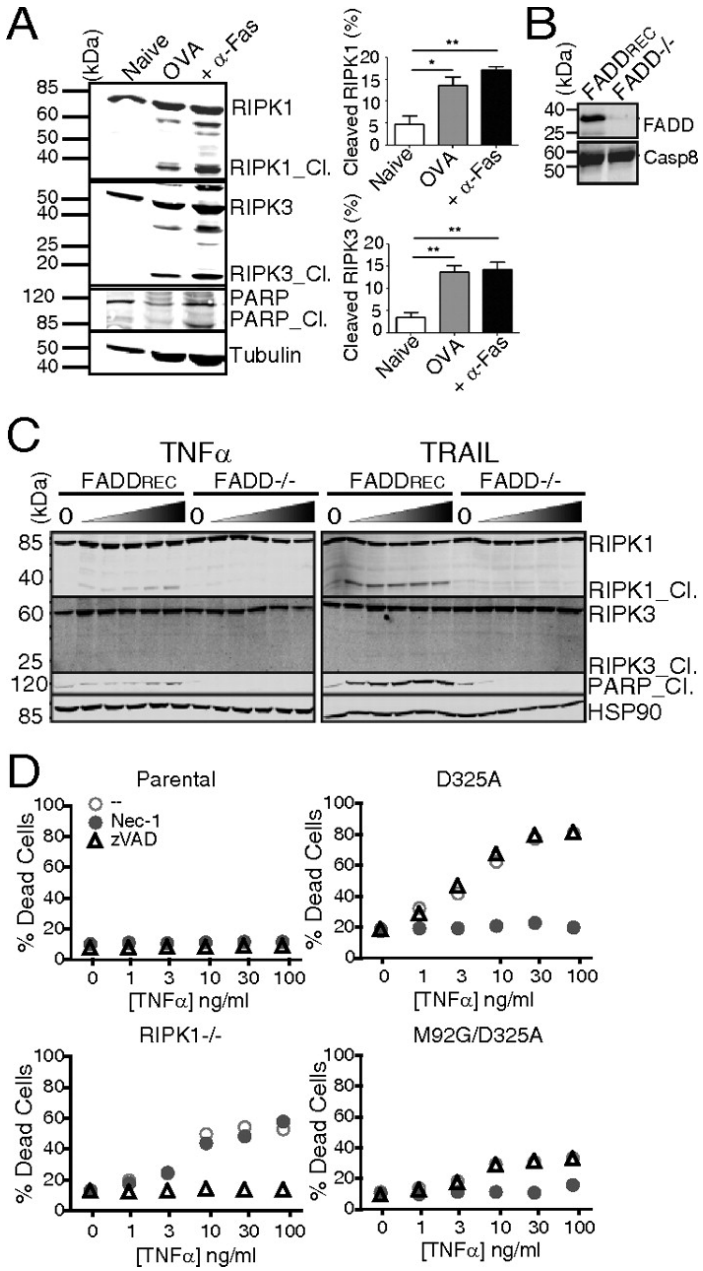

Figure 2.5. RIPK1/RIPK3 cleavage following TCR vs. DR ligation. (*A*) OT-I T cells [27] were stimulated with OVA peptide for 72 h and stimulated without or with α-Fas or left untreated (naive); immunoblots were hybridized with α-RIPK1 and α-RIPK3 to detect processing. Graphs represent percent RIPK1/3 cleavage (**P* < 0.05 and ***P* < 0.01). (*B*) Reconstitution of FADD-deficient Jurkat cells [28] (FADD$^{-/-}$) with full-length FADD (FADD^{REC}), and blots of lysates probed with α-FADD and α-casp8. (*C*) Western blot of RIPK1 and RIPK3 cleavage in FADD$^{-/-}$ and FADD^{REC} Jurkat cells; HSP90 used as loading control. RIPK1_ Cl., PARP_ Cl., cleaved RIPK1 and PARP1, respectively. (*D*) Parental, RIPK1$^{-/-}$; D325A RIPK1, M92G/D325A RIPK1 Jurkat cells treated with TNFα, Nec-1 (10 μM), or z-VAD-FMK (20 μM) and stained with 7AAD and annexin-V to detect death.

To assess the potential that casp8-mediated processing of RIPK1 prevents the elaboration of a necroptotic response following DR ligation, we treated RIPK1-deficient Jurkat cells [29] stably reconstituted with cleavage-resistant RIPK1_D325A or kinase dead/cleavage-resistant RIPK1_M92G/D325A [rendered catalytically inactive by a kinase "gatekeeper" mutation [30]; (**Figure 2.S5**) with TNF-α ± Nec-1 or zVAD-FMK (**Figure 2.5D**). RIPK1$^{-/-}$ cells were sensitized to TNF-induced apoptosis, which was rescued with the addition of zVAD-FMK. In contrast, cells expressing noncleavable RIPK1_D325A were sensitized to TNF-induced necroptosis, which was rescued by Nec-1. Blocking kinase activity of cleavage-resistant RIPK1 (M92G/D325A) diminished TNF-induced necroptotic death observed in RIPK1_D325A reconstituted RIPK1$^{-/-}$ Jurkat cells. Ectopic expression of RIPK1_D325A in RIPK1-sufficient Jurkat cells failed to shift TNF-induced apoptosis to necroptosis (**Figure 2.S6**). Thus, uncleaved RIPK1 does not act in a dominant fashion to promote necroptosis. Presumably, only a small fraction of activated RIPK1, recruited via association with FADD or other adaptors, is necessary for a necroptotic response to TNF. These results provide evidence that direct inactivation of RIPK1 and/or RIPK3, through a FADD-dependent mechanism, differentiates between apoptosis and necroptosis, and RIPK1 activity is required to promote necroptosis.

2.3 Discussion

Our findings here demonstrate that RIPK3 acts in concert with RIPK1 in promoting the necroptotic demise of T cells lacking the nonapoptotic casp8 activity that is normally observed following mitogenic signaling [6,7,18]. Thus, early casp8 catalytic activity within T cells acts to prevent the elaboration of signaling from an RIPK1/RIPK3 containing necrosome [13] in a manner similar to that observed following DR signaling. Although T-cell–intrinsic casp8 and FADD activity are required for antiviral T-cell responses, loss of RIPK3 restores the ability of FADDdd T cells to control MHV infection, suggesting that casp8 and RIPK3 play additional opposing roles during antiviral immune responses.

Unlike the case for DR signaling, the process that leads to RIPK1/RIPK3-containing necrosome formation is currently unclear. We previously observed RIPK1 recruitment to complexes that likely exist on autophagosomal membranes [6] and found that extracellular blockade of DR ligation fails to rescue casp8$^{-/-}$ or FADDdd-expressing T cells[18]. This suggests that the nucleation of RIPK1/RIPK3 necrosomes occurs in a manner independent of DR signaling. Here, we demonstrate that RIPK3, like RIPK1 [6,7], promotes necroptotic death of FADDdd T cells following their activation. Our findings contrast with a recent publication that suggested RIPK3 signaling is not involved in the necroptotic demise of T cells lacking FADD [31] based on the fact that RIPK3 failed to coimmunoprecipitate with RIPK1. Given that our results demonstrate a requirement for RIPK3 in TCR-induced necroptosis, it is possible that, whereas the upstream pathways that promote the nucleation of RIPK1/RIPK3 containing necrosomes may be unique following DR ligation vs. T-cell mitogenesis, the downstream pathways are likely similar.

Here we present data that demonstrate an essential role for DR-induced apoptotic death during reactivation-induced cell death, a process that has previously been shown to require Fas signaling [32]. We emphasize that loss of RIPK3 signaling had little impact on this; FADDdd was highly effective in blocking T-cell RICD. In contrast, the loss of RIPK3 in FADDdd T cells led to a significant increase of live proliferating T cells following mitogenic stimulation. Although Nec-1 treatment also rescued the expansion of FADDdd T cells, it did not lead to embellished recovery of proliferating cells vs. WT T cells. This result suggests that RIPK3 may have independent functions in T cells that may have been previously overlooked. Alternatively, Nec-1 treatment may have off-target effects that limit T-cell expansion.

Although RIPK3$^{-/-}$ T cells were shown to develop and proliferate relatively normally in previous studies [20]and in our work presented here, Moquin and Chan found that RIPK3$^{-/-}$ mice fail to promote efficient inflammatory responses to vaccinia virus infection[17]. This may be a likely consequence of the expression of the caspase inhibitory protein SPI-2, a protein related to poxvirus CrmA, and possible assembly of necrosomes in an antiviral inflammatory environment. In contrast, we note here that RIPK3$^{-/-}$ mice were also capable of controlling murine hepatitis virus (MHV) infection. In previous studies, FADDdd expressing mice failed to adequately respond to viral infection, and this was likely a result of defective CD8^{+} T-cell responses [21]. Supporting this conclusion, the T-cell–intrinsic loss of RIPK3 restored the ability of FADDdd mice to efficiently clear MHV infections (**Figure 2.S4**). Thus, the primary defect in FADDdd-expressing mice to MHV infection is in the expansion/survival of MHV-specific T cells. Furthermore, as direct infection of RIPK3$^{-/-}$ mice led to efficient viral clearance, our results call into question a

general requirement for RIPK3 signaling in antiviral immunity. Importantly, the immune defects seen in FADDdd mice were rescued with a RIPK3 deficiency, although older FADDdd × RIPK3$^{-/-}$ mice bear a phenotypic resemblance to Fas-deficient (lpr/lpr) mice. These data indicate casp8-dependent apoptosis and RIPK1/3-dependent necroptosis are both necessary to maintain homeostasis within the adaptive immune system.

These studies emphasize a primary role for RIPK3 in promoting TCR-induced necroptosis in T cells lacking catalytically active casp8 [18]. The simplest interpretation is that RIPK1 and/or RIPK3 are inactivated by casp8 directly [13]when brought into close apposition. Supporting this, we observed cleavage of both RIPK1 and RIPK3 in antigenically stimulated primary T cells, but only RIPK1 cleavage was detected in Jurkat T cells treated with DR ligands (**Figure 2.5**). Expression of cleavage-resistant RIPK1 was sufficient to convert TNF-induced apoptosis into necroptosis, whereas kinase-dead RIPK1 diminished TNF-induced necroptosis and apoptosis. Thus, a failure in caspase-mediated cleavage of RIPK1 alone is sufficient to promote necroptosis following DR ligation. Following the submission of our manuscript, several other laboratories have reported parallel findings in the context of T cells, supporting our studies here [33-36]. Taken together, our findings show that casp8 activity is essential for controlling RIPK1/3-dependent necroptosis in activated T cells, and that RIPK1/3 processing orchestrates the switch between apoptotic vs. necrotic cell death. Furthermore, these findings demonstrate that RIPK3-induced necroptotic activity leads to the early demise of FADDdd T cells, and this blocks antiviral immunity and the development of lymphoproliferative disease in mice lacking FADD signaling in T cells.

2.4 Methods

Mice. FADDdd transgenic mice [4] were crossed with RIPK3$^{-/-}$ mice [20], the latter provided by Kim Newton and Vishva Dixit at Genentech (South San Francisco, CA). Rag2$^{-/-}$ × γc and C57BL6/J (B6) mice were obtained from Jackson Laboratories. Mice were bred and maintained in accordance with the institutional animal use and care committee at the University of California, Irvine, vivarium.

T-Cell Assays/Infections. T cells were activated as described previously [37]. In some cases, 10 μM Nec-1 was added at the start of culture to block necroptosis [6]. For transfer, T cells from mice of the indicated genotypes were isolated by depletion of B220^{+}, CD11b^{+} and MHCII^{+} cells with magnetic beads (Miltenyi), and injected i.v. at a dose of 2.5 × 10^{6} cells per Rag2$^{-/-}$ × IL-2Rγc$^{-/-}$ mouse. For infection, 2 × 10^{5} pfu MHV (strain JHM-DM) was injected intraperitoneally into mice. PBS solution was injected into "mock" controls. Intracellular staining, viral titer plaque assays, and statistical analyses were performed by using methods reported previously [38].

RICD and CTL Assay. Restimulation was by using an approach based on a previous publication [39] by using 1 × 10^{5} cells per well and proceeded overnight before staining with 7-AAD. For the in vivo CTL assay, mice were infected, and, after 7d, CTL activity was assessed as described previously [40]. B6 splenocytes were pulsed with 5 μM OVA or S510 peptide as target cells and resuspended at 20 × 10^{6}/mL for CFSE labeling. OVA/S510-pulsed cells were labeled with 2.5 and 0.5 μM CFSE, respectively, and mixed at a 1:1 ratio to obtain a cell suspension of 100 × 10^{6}/mL. Target cells (100 μL) were transferred i.p. into each infected mouse, and the assay was allowed to proceed 75 min before harvesting spleens for FACS. The specific lysis percentage was defined as 100*[1 − R(sham) /

R(infected)], with R representing the ratio of $CFSE^{hi}$ to $CFSE^{lo}$. In vitro, EL4 target cells were pulsed with peptides as stated earlier. OVA-pulsed/S510-pulsed EL4 cells were labeled with 2.5 μM CFSE and 5 μM EF670, respectively (10 min., 37 °C; eBioscience), and mixed at equal volumes. To prepare effectors, splenocytes of infected mice were RBC-lysed and plated in 96-well round-bottom plates at 100 μL/well before the addition of 100 μL target cells. Plates were incubated at 37 °C, 5% CO_2, for 4 h before FACS analysis. The specific lysis percentage was determined as 100*[1 − R(infected) / R(no effectors)], with R representing the ratio of EF670 to CFSE.

Retroviral Infection. Jurkat cells were infected with retroviral supernatants by using methods reported previously [6]. Two days after infection, cells were treated with Nec-1 (10 μM), zVAD-FMK (20 μM), CHX (5 μg/mL), TNF-α (20 ng/mL), and etoposide (50 μM). Fourteen hours after treatment, cells were stained with annexin V, anti-Thy1, and 7-AAD for FACS analysis.

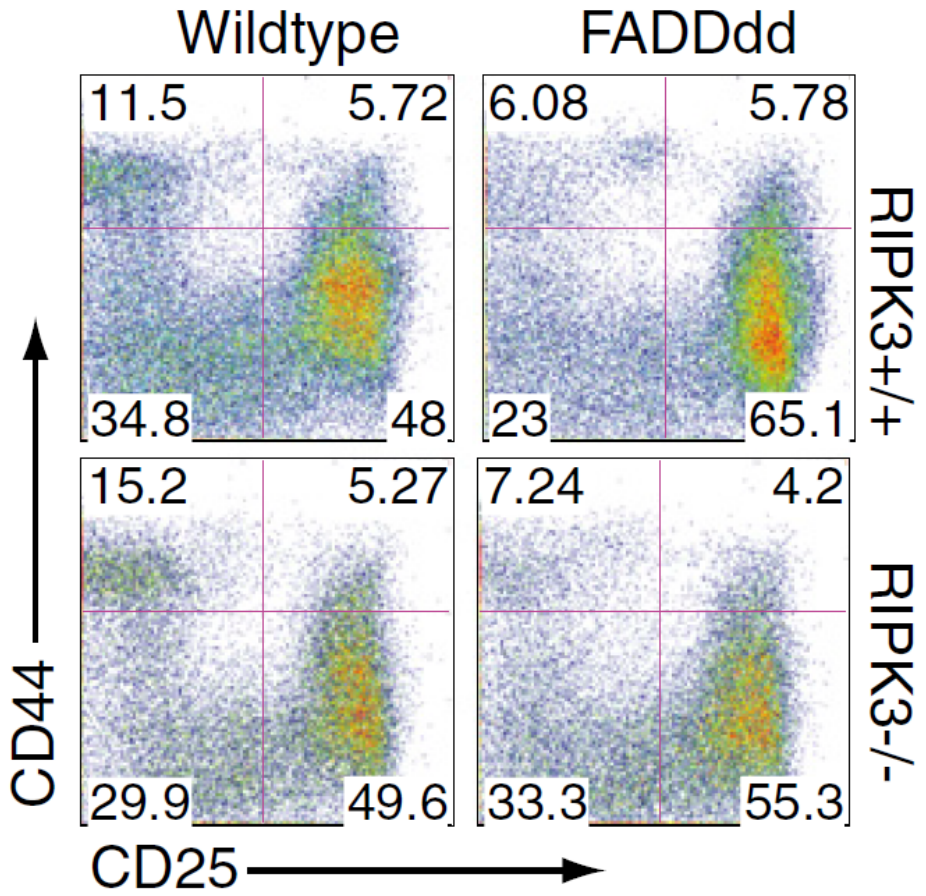

Figure 2.S1. Rescue of DN4:DN3 ratio by a RIPK3 deficiency on the FADDdd genetic background. DN thymocyte populations defined by CD25 and CD44 expression reveals restored DN4 population in FADDdd x RIPK3$^{-/-}$ mice. The data shown are representative of three separate experiments.

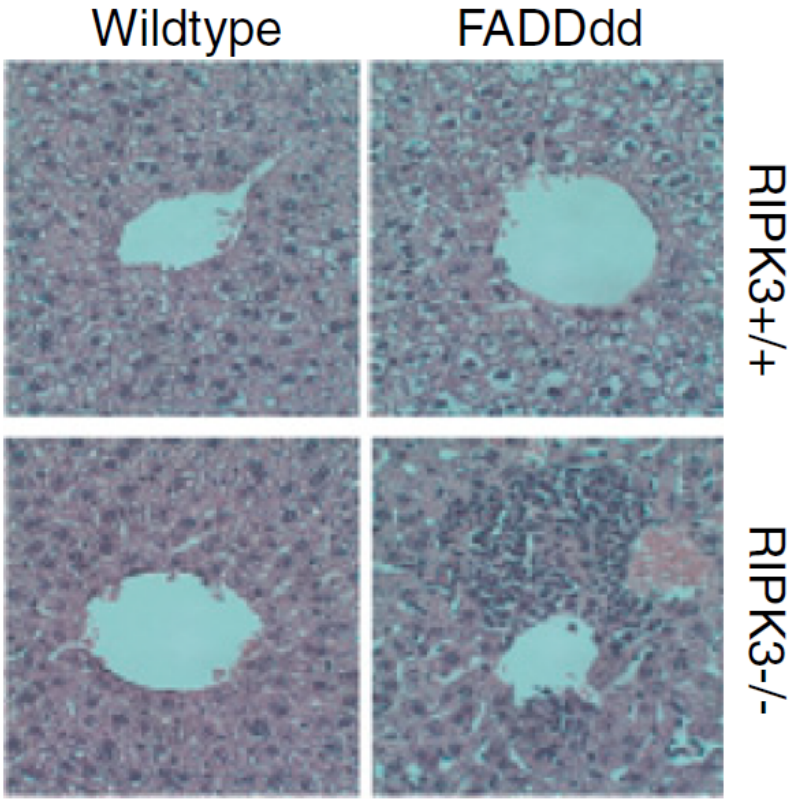

Figure 2.S2. Liver inflammation in aged FADDdd x RIPK3$^{-/-}$ mice. H&E-stained liver sections from 8-mo-old mice of indicated genotypes.

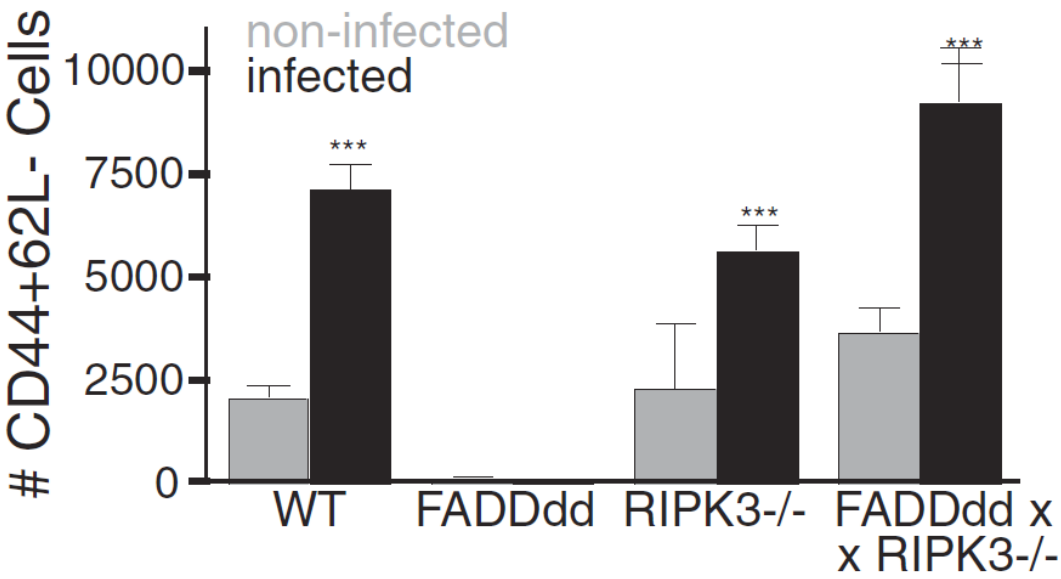

Figure 2.S3. Restoration of antiviral effector/memory T cells in FADDdd x RIPK3$^{-/-}$ mice. Analysis of CD8+ effector/memory populations defined by CD44, CD62L 7 d after infection. Error bars represent SEM. Considered a significant difference with respect to infected FADDdd. (***P < 0.001).

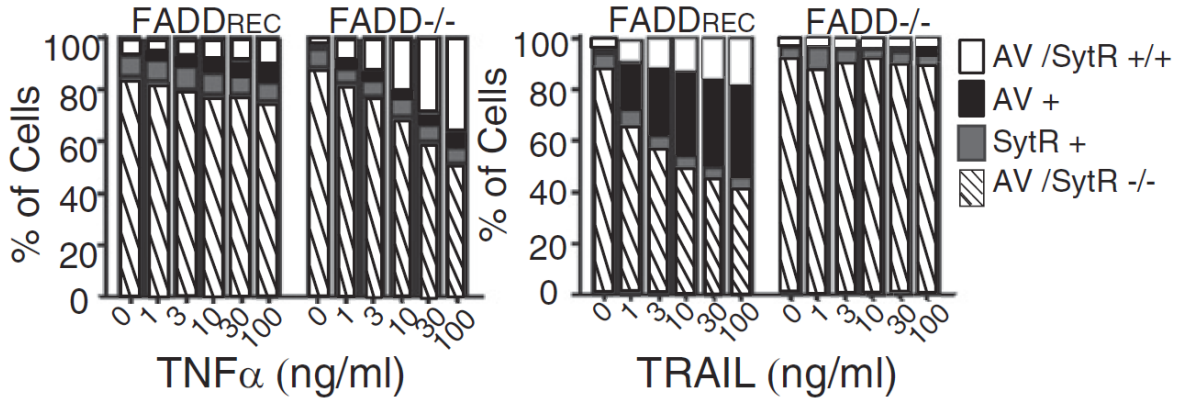

Figure 2.S4. Jurkat T cells lacking FADD are sensitive to DR-induced necroptosis. FADD$^{-/-}$ and FADD-reconstituted Jurkat cells were treated with TNF-α or TRAIL for 18 h at indicated concentrations, followed by staining with annexin V (AV) and Sytox Red (SytR) to detect cell death.

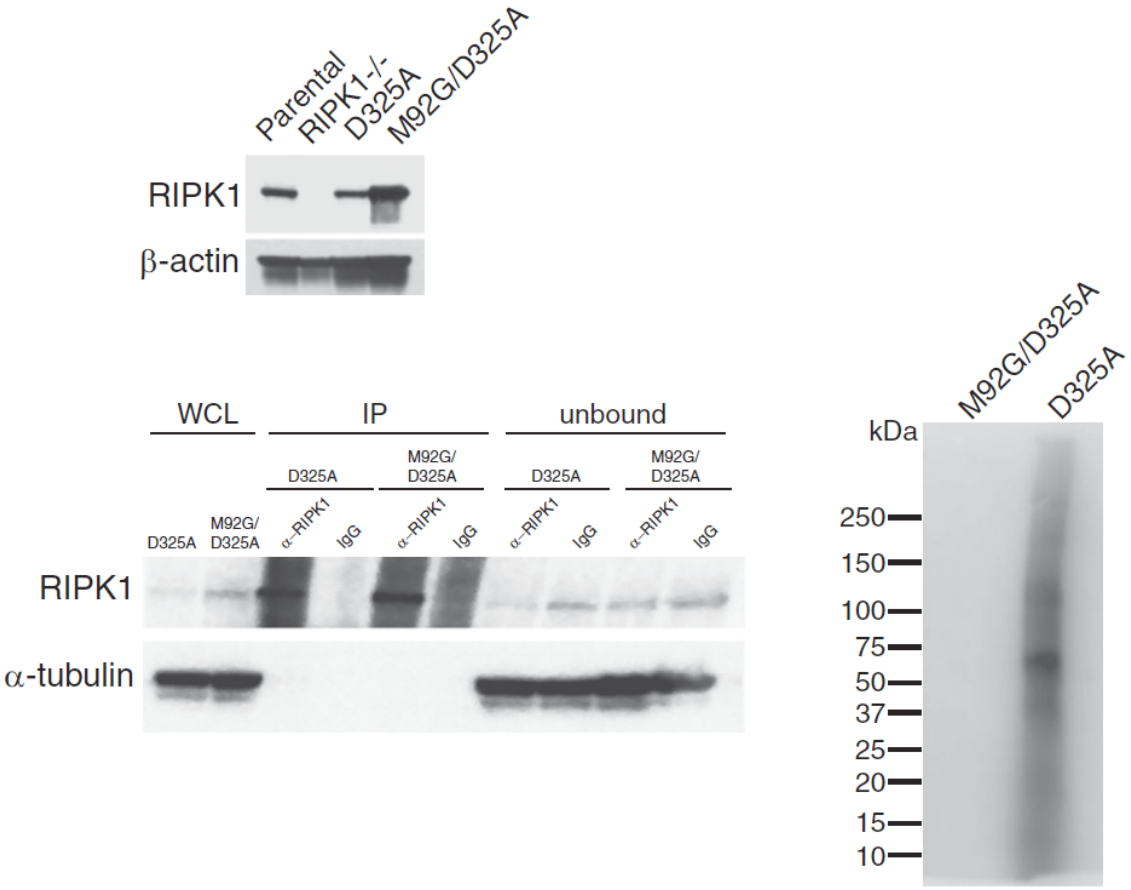

Figure 2.S5. **RIPK1-deficient Jurkat cells reconstituted with cleavage-resistant RIPK1 mutants.** *Top*: Reconstitution of RIPK1-deficient Jurkat cells ($RIPK1^{-/-}$) with cleavage-resistant (D325A RIPK1), kinase-dead/cleavage-resistant (M92G/D325A RIPK1); blots of lysates probed with anti-RIPK1. *Bottom Left*: $RIPK1^{-/-}$ Jurkat cells reconstituted with D325A RIPK1 or M92G/D325A RIPK1 were treated with TNF-α (40 ng/mL) for 2 h before immunoprecipitation of RIPK1; blots of lysates probed with anti-RIPK1. *Bottom Right*: in vitro kinase assay of immunoprecipitated RIPK1 (*Bottom Left*) shows no autophosphorylation with M92G/D325A RIPK1 double mutation, indicating that M92G mutation blocks RIPK1 kinase activity.

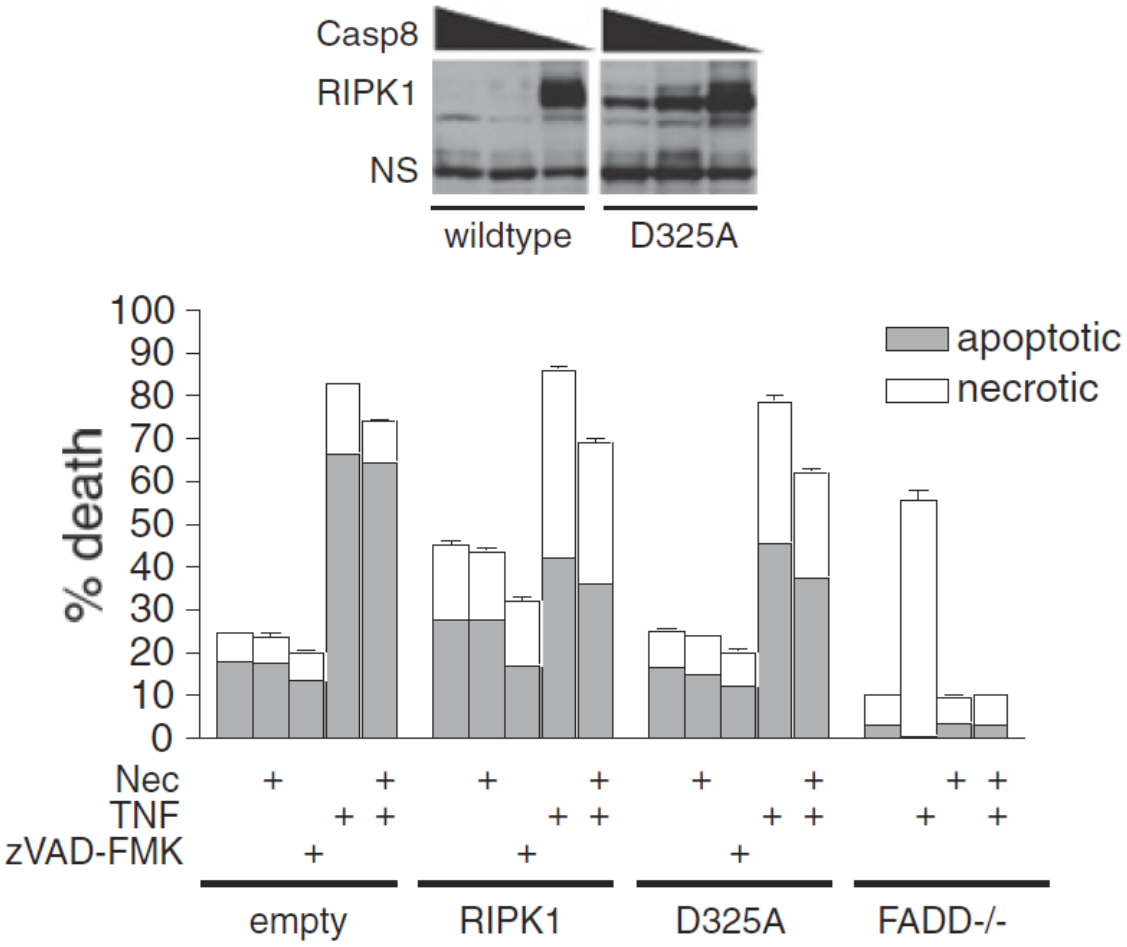

Figure 2.S6. **Ectopic expression of cleavage-resistant RIPK1 does shift TNF-induced apoptosis to necroptosis in RIPK1-sufficient Jurkat cells.** *Top*: Casp8 was cotransfected from high to low concentrations along with WT RIPK1 or RIPK1_D325A to show that the latter is resistant to cleavage. *Bottom*: Parental Jurkat cells were infected retrovirally with pMit-empty, -RIPK1, and -RIPK1 D325A and treated with combinations of z-VAD-FMK (20 μM), necrostatin-1 (Nec; 10 μM), and TNF-α (20 ng/mL) for 14 h. Cells were stained with 7AAD and annexin-V to detect apoptotic vs. necrotic cells.

Acknowledgments

The authors thank Kim Newton and Vishva Dixit (Genentech) for RIPK3$^{-/-}$ mice, David Fruman and Aimee Edinger for review of this manuscript, and Huy Q. Nguyen, Isaac H. Chu, and Alan Nguyen for technical assistance. This work was supported by National Institutes of Health Grants AI50506 (to C.M.W.), AI63419 (to C.M.W.), CA69381 (to G.S.S.), and NS41249 (to T.E.L.).

Competing interest

The authors declare no conflict of interest.

Author's Contributions

J.V.L., B.J.v.R., B.S.M., T.E.L., G.S.S., and C.M.W. designed research; J.V.L., B.M.W., B.J.v.R., B.S.M., L.V.N., P.S., B.D.B., and K.A.L. performed research; B.M.W., B.J.v.R., P.S., B.D.B., and K.A.L. contributed new reagents/analytic tools; J.V.L., B.S.M., T.E.L., G.S.S., and C.M.W. analyzed data; and J.V.L., T.E.L., G.S.S., and C.M.W. wrote the paper.

2.5 References

1. Ashkenazi A, Dixit VM. Death receptors: Signaling and modulation. *Science*, 281(5381), 1305-1308 (1998).
2. Siegel RM. Caspases at the crossroads of immune-cell life and death. *Nat Rev Immunol*, 6(4), 308-317 (2006).
3. Newton K, Harris AW, Bath ML, Smith KG, Strasser A. A dominant interfering mutant of FADD/MORT1 enhances deletion of autoreactive thymocytes and inhibits proliferation of mature T lymphocytes. *EMBO J*, 17(3), 706-718 (1998).
4. Walsh CM, Wen BG, Chinnaiyan AM, O'Rourke K, Dixit VM, Hedrick SM. A role for FADD in T cell activation and development. *Immunity*, 8(4), 439-449 (1998).
5. Zornig M, Hueber AO, Evan G. p53-dependent impairment of T-cell proliferation in FADD dominant-negative transgenic mice. *Curr Biol*, 8(8), 467-470 (1998).
6. Bell BD, Leverrier S, Weist BM *et al.* FADD and caspase-8 control the outcome of autophagic signaling in proliferating T cells. *Proc Natl Acad Sci U S A*, 105(43), 16677-16682 (2008).
7. Ch'en IL, Beisner DR, Degterev A *et al.* Antigen-mediated T cell expansion regulated by parallel pathways of death. *Proc Natl Acad Sci U S Ag* 105(45), 17463-17468 (2008).
8. Kawahara A, Ohsawa Y, Matsumura H, Uchiyama Y, Nagata S. Caspase-independent cell killing by Fas-associated protein with death domain. *J Cell Biol*, 143(5), 1353-1360 (1998).
9. Vercammen D, Beyaert R, Denecker G *et al.* Inhibition of caspases increases the sensitivity of L929 cells to necrosis mediated by tumor necrosis factor. *J Exp Med*, 187(9), 1477-1485 (1998).
10. Holler N, Zaru R, Micheau O *et al.* Fas triggers an alternative, caspase-8-independent cell death pathway using the kinase RIP as effector molecule. *Nat Immunol*, 1(6), 489-495 (2000).
11. Degterev A, Huang Z, Boyce M *et al.* Chemical inhibitor of nonapoptotic cell death with therapeutic potential for ischemic brain injury. *Nat Chem Biol*, 1(2), 112-119 (2005).
12. Hitomi J, Christofferson DE, Ng A *et al.* Identification of a molecular signaling network that regulates a cellular necrotic cell death pathway. *Cell*, 135(7), 1311-1323 (2008).
13. Declercq W, Vanden Berghe T, Vandenabeele P. RIP kinases at the crossroads of cell death and survival. *Cell*, 138(2), 229-232 (2009).
14. Zhang DW, Shao J, Lin J *et al.* RIP3, an Energy Metabolism Regulator That Switches TNF-Induced Cell Death from Apoptosis to Necrosis. *Science*, 325(5938), 332-336 (2009).
15. He SD, Wang L, Miao L *et al.* Receptor Interacting Protein Kinase-3 Determines Cellular Necrotic Response to TNF-alpha. *Cell*, 137(6), 1100-1111 (2009).
16. Cho YS, Challa S, Moquin D *et al.* Phosphorylation-driven assembly of the RIP1-RIP3 complex regulates programmed necrosis and virus-induced inflammation. *Cell*, 137(6), 1112-1123 (2009).
17. Moquin D, Chan FK. The molecular regulation of programmed necrotic cell injury. *Trends Biochem Sci*, 35(8), 434-441 (2010).

18. Leverrier S, Salvesen GS, Walsh CM. Enzymatically active single chain caspase-8 maintains T-cell survival during clonal expansion. *Cell Death Differ*, (2010).
19. Kelliher MA, Grimm S, Ishida Y, Kuo F, Stanger BZ, Leder P. The death domain kinase RIP mediates the TNF-induced NF-kappaB signal. *Immunity*, 8(3), 297-303 (1998).
20. Newton K, Sun X, Dixit VM. Kinase RIP3 is dispensable for normal NF-kappa Bs, signaling by the B-cell and T-cell receptors, tumor necrosis factor receptor 1, and Toll-like receptors 2 and 4. *Mol Cell Biol*, 24(4), 1464-1469 (2004).
21. Beisner DR, Chu IH, Arechiga AF, Hedrick SM, Walsh CM. The requirements for Fas-associated death domain signaling in mature T cell activation and survival. *J Immunol*, 171(1), 247-256 (2003).
22. Fehling HJ, Krotkova A, Saint-Ruf C, von Boehmer H. Crucial role of the pre-T-cell receptor alpha gene in development of alpha beta but not gamma delta T cells. *Nature*, 375(6534), 795-798 (1995).
23. Vandenabeele P, Declercq W, Van Herreweghe F, Vanden Berghe T. The role of the kinases RIP1 and RIP3 in TNF-induced necrosis. *Sci Signal*, 3(115), re4 (2010).
24. Pop C, Oberst A, Drag M *et al.* FLIP(L) induces caspase 8 activity in the absence of interdomain caspase 8 cleavage and alters substrate specificity. *The Biochemical journal*, 433(3), 447-457 (2011).
25. Lin Y, Devin A, Rodriguez Y, Liu ZG. Cleavage of the death domain kinase RIP by caspase-8 prompts TNF-induced apoptosis. *Genes Dev*, 13(19), 2514-2526 (1999).
26. Feng S, Yang Y, Mei Y *et al.* Cleavage of RIP3 inactivates its caspase-independent apoptosis pathway by removal of kinase domain. *Cell Signal*, 19(10), 2056-2067 (2007).
27. Hogquist KA, Jameson SC, Heath WR, Howard JL, Bevan MJ, Carbone FR. T cell receptor antagonist peptides induce positive selection. *Cell*, 76(1), 17-27 (1994).
28. Juo P, Woo MS, Kuo CJ *et al.* FADD is required for multiple signaling events downstream of the receptor Fas. *Cell Growth Differ*, 10(12), 797-804 (1999).
29. Ting AT, Pimentel-Muinos FX, Seed B. RIP mediates tumor necrosis factor receptor 1 activation of NF-kappaB but not Fas/APO-1-initiated apoptosis. *EMBO J*, 15(22), 6189-6196 (1996).
30. Shah K, Liu Y, Deirmengian C, Shokat KM. Engineering unnatural nucleotide specificity for Rous sarcoma virus tyrosine kinase to uniquely label its direct substrates. *Proc Natl Acad Sci U S A*, 94(8), 3565-3570 (1997).
31. Osborn SL, Diehl G, Han SJ *et al.* Fas-associated death domain (FADD) is a negative regulator of T-cell receptor-mediated necroptosis. *Proc Natl Acad Sci U S A*, 107(29), 13034-13039 (2010).
32. Siegel RM, Chan FK, Chun HJ, Lenardo MJ. The multifaceted role of Fas signaling in immune cell homeostasis and autoimmunity. *Nat Immunol*, 1(6), 469-474 (2000).
33. Oberst A, Pop C, Tremblay AG *et al.* Inducible dimerization and inducible cleavage reveal a requirement for both processes in caspase-8 activation. *J Biol Chem*, 285(22), 16632-16642 (2010).
34. Kaiser WJ, Upton JW, Long AB *et al.* RIP3 mediates the embryonic lethality of caspase-8-deficient mice. *Nature*, (2011).
35. Zhang H, Zhou X, McQuade T, Li J, Chan FK, Zhang J. Functional complementation between FADD and RIP1 in embryos and lymphocytes. *Nature*, (2011).

36. Ch'en IL, Tsau JS, Molkentin JD, Komatsu M, Hedrick SM. Mechanisms of necroptosis in T cells. *J Exp Med*, 208(4), 633-641 (2011).
37. Arechiga AF, Bell BD, Leverrier S *et al.* A Fas-associated death domain protein/caspase-8-signaling axis promotes S-phase entry and maintains S6 kinase activity in T cells responding to IL-2. *J Immunol*, 179(8), 5291-5300 (2007).
38. Ramos SJ, Hardison JL, Stiles LN, Lane TE, Walsh CM. Anti-viral effector T cell responses and trafficking are not dependent upon DRAK2 signaling following viral infection of the central nervous system. *Autoimmunity*, 40(1), 54-65 (2007).
39. Ramaswamy M, Dumont C, Cruz AC *et al.* Cutting edge: Rac GTPases sensitize activated T cells to die via Fas. *J Immunol*, 179(10), 6384-6388 (2007).
40. Barber DL, Wherry EJ, Ahmed R. Cutting edge: rapid in vivo killing by memory CD8 T cells. *J Immunol*, 171(1), 27-31 (2003).

CHAPTER THREE

Inducible expression of CXCL1 from astrocytes amplifies demyelination that is associated with increased neutrophil infiltration into the CNS following CNS viral infection

Brett S. Marro and Thomas E. Lane

Abstract

The functional role of the ELR$^+$ chemokine CXCL1 in host defense and following infection of the central nervous system (CNS) with the neurotropic JHM strain of mouse hepatitis virus (JHMV) was examined. Mice in which expression of CXCL1 is under the control of a tetracycline-inducible promoter active within GFAP-positive cells were generated and this allowed for selectively increasing CNS expression of CXCL1 in response to JHMV infection and evaluating the effects on neuroinflammation, control of viral replication, and demyelination. Inducible expression of CNS-derived CXCL1 resulted in increased levels of CXCL1 protein within the serum, brain and spinal cord that correlated with increased frequency of Ly6G$^+$CD11b$^+$ neutrophils present within the CNS. Elevated levels of CXCL1 did not affect generation of virus-specific T cells and there was no difference in control of JHMV replication compared to control mice indicating T cell infiltration into the CNS is CXCL1-independent. Sustained CXCL1 expression resulted in increased mortality that correlated with increased neutrophil infiltration, diminished numbers of mature oligodendrocytes, and increased demyelination. Neutrophil ablation in CXCL1-transgenic mice reduced the severity of demyelination, but did not completely abrogate the increase in disease severity in mice that overproduced CXCL1. These findings demonstrate that sustained neutrophil infiltration into the CNS is associated with increased demyelination in a model of viral-induced neurologic disease.

3.1 Introduction

Inoculation of susceptible mice with the neurotropic J2.2v-1 JHM strain of mouse hepatitis virus (JHMV) into the central nervous system (CNS) results in wide-spread dissemination of viral particles, leading to infection and replication within glial cells. This is followed by infiltration of virus-specific T lymphocytes that control viral replication through cytokine secretion and cytolytic activity [1]. Sterilizing immunity is not achieved as viral antigen and viral RNA are detected within white matter tracts of surviving mice resulting in demyelination that is amplified by inflammatory T cells and macrophages. In response to infection, numerous cytokines/chemokines are secreted by inflammatory leukocytes and resident cells of the CNS, generating an inflammatory milieu that contributes to host defense while also promoting disease. Our previous work has defined the functional roles for chemokines and chemokine receptors in orchestrating leukocyte recruitment into the CNS in response to JHMV infection that aid in host defense as well as their contribution to demyelination [2-5].

Among the chemokines expressed during acute and chronic JHMV-induced neurologic disease are the ELR-positive CXC chemokines CXCL1, CXCL2 and CXCL5 and its signaling receptor CXCR2 [4,6]. Following JHMV infection of the CNS, expression of CNS-derived ELR-positive ligands promote the migration of CXCR2-expressing neutrophils ($Ly6G/C^{high}CD11b^{+}$) to the blood-brain-barrier (BBB), where they can assist in breaking down structural components of the glial limitans through release of matrix metalloproteinases (MMPs) from preformed granules. Indeed, our laboratory has recently demonstrated that antibody-mediated neutralization of CXCR2 within JHMV-infected mice prevented PMN migration to the CNS, and this was associated with a significant increase in

mortality and inefficient control of virus replication as a result of impaired parenchymal access of virus-specific T cells [4]. Anti-CXCR2 treatment was also found to diminish macrophage recruitment to the CNS as well, making it challenging to define the precise contributions of both immune cell subsets in establishing host-defense while also promoting disease when CXCR2 signaling is neutralized. To extend on these findings, other studies have demonstrated that neutrophil depletion in JHMV infected mice in which monocyte trafficking to the CNS is compromised does not alter early CNS inflammation, clinical disease severity or death, but rather limits parenchymal access of leukocytes at later times following infection, suggesting that neutrophils and monocytes may act separately to shape adaptive immunity following JHMV infection of the CNS [7,8].

The present study was undertaken to expand our understanding of how ELR-positive chemokines influence host defense and disease progression following JHMV infection of the CNS. To this end, we have generated mice in which expression of CXCL1 is under the control of a tetracycline-inducible promoter that is active within GFAP-positive cells that express an enhanced version of the reverse tetracycline transactivator (rtTA*M2) protein. The successful generation of these pBI-CXCL1-rtTA mice has allowed us to selectively increase CNS expression of CXCL1 in adult mice following JHMV-induced disease and evaluate the effects on neuroinflammation, control of viral replication, and demyelination.

3.2 Methods

pBI-CXCL1 vector construction. CXCL1 cDNA incorporating *XhoI* and *NheI* restriction site ends was generated from the brains of C57BL/6 mice infected with 250PFU JHMV. CXCL1 cDNA was cloned into a pBI-MCS-EGFP plasmid [9] downstream of a bi-directional tetracycline responsive element (TRE). The purified pBI-CXCL1 plasmid was linearized following an overnight incubation with *AatII* and *AseI* restriction enzymes to generate a 3350bp fragment containing the pBI-CXCL1 construct.

Virus and mice. pBI-CXCL1 transgenic mice were generated by the University of California, Irvine transgenic mouse facility through DNA microinjection of fertilized C56BL/6 eggs using the linearized pBI-CXCL1 construct [9]. The five resulting founder transgenic (tg) mice where mated to wildtype C57BL/6 mice to indentify F1 offspring containing the transgene. To generate double transgenic mice, hemizygous pBI-CXCL1 transgenics were crossed to hemizygous GFAP-rtTA*M2 mice (JAX), resulting in double transgenic mice (pBI-CXCL1-rtTA), single tgs (rtTA-GFAP or pBI-CXCL1) or WT. Double transgenic mice were phenotypically normal and breeder progeny displayed normal Mendelian genetics. Age-matched 5-6 week old single tg or double tg mice were infected intracerebrally (i.c.) with 250 plaque forming units (PFU) of JHMV strain J2.2v-1 in 30ul of sterile HBSS. SHAM infected animals received 30ul HBSS via i.c. injection. For viral titer analysis, one half of each brain or whole spinal cord was homogenized and used in a plaque assay as previously described [10].

Primary astrocyte cultures. Cortices from postnatal day 1 double tg and single tg mice were dissected and triterated according to previously published protocols [11]. In brief, following removal of the meninges, cortical tissue was minced with a razor and placed in

pre-warmed DMEM containing papain in order to completely dissociate the tissue. Following further dissociation with a Pasteur pipette, single cell suspensions were added to poly-d-lysine coated culture flasks and grown for nine days in DMEM supplemented with 10% FBS. Flasks were then transferred to an orbital shaker in a 5% CO_2 tissue culture incubator and shaken for approximately 16 hours at 220 rpm in order to remove loosely adherent contaminating cells. Cells were passaged in 0.05% trypsin and replated. When cells regained confluency, 10uM Ara C (Sigma, St Louis, MO) was added for three days to kill dividing cells. Cells were passaged again and added to 24-well culture dishes or Nunc™ Lab-Tek II Chamber slides (ThermoFisher Scientific, Waltham, MA).

Semi-quantitative RT-qPCR. Total cDNA from brains and spinal cords of sham and JHMV infected mice at days 4, 7, and 12 p.i. was generated via Superscript III (Life Tech., Carlsbad, CA) following homogenization in Trizol (Life Tech., Carlsbad, CA). To determine relative CXCL1 mRNA expression, real-time SYBR green analysis was performed using mouse β-actin and mouse CXCL1 primers using a Roche Lightcycler 480 [12]. CXCL1 expression was determined by normalizing the expression of each sample to β-actin and then quantifying fold change relative to sham infected double tg mice. Expression of CCL2, CCL5, CXCL3, CXCL5, CXCL9, CXCL10, Il-10, Il-1α, Il-1β, Il-2, Il-6, TNFα, IL-17α and IFN-γ was determined using a Mouse Cytokine and Chemokine RT^2 Profiler PCR array (Qiagen Inc, Valencia, CA).

ELISA. Assessment of CXCL1protein within the supernatants of Dox-treated astrocyte cultures was determined using a CXCL1 (KC) DuoSet sandwhich ELISA kit (R&D Systems, Minneapolis, MN) according to manufacturer specifications. To determine CXCL1 protein levels within the spinal cords of double and single tg mice, spinal cords were homogenized in RIPA buffer and clarified by high-speed centrifugation. Following quantification of total

protein, samples were diluted in RIPA buffer to a standard protein concentration before performing the ELISA assay.

Flow cytometry. Flow cytometry was performed to immunophenotype inflammatory cells entering the CNS using established protocols [3,13] . In brief, single cell suspensions were generated from tissue samples by grinding with frosted microscope slides. Immune cells were enriched by a 2-step percoll cushion (90% and 63%) and cells were collected at the interface of the two percoll layers. Before staining with the fluorescent antibodies, isolated cells were incubated with anti-CD16/32 Fc block (BD Biosciences, San Jose, CA) at a 1:200 dilution. Immunophenotyping was performed using either Rat anti-mouse IgG or armenian hamster anti-mouse IgG antibodies for the following cell surface markers: F4/80 (Serotec, Raleigh, NC), MHV S510-tetramer (NIH), MHV M133-Tetramer (NIH) and CD4, CD8, Ly6g, CD11b,IFN- γ, CD44, CD45, CD69, CD80 and MHC-II (BD Biosciences, San Jose, CA).

Sodium fluorescein (NaF) BBB permeability assay. Mice received 100ul of 10% sodium fluorescein (NaF) in PBS via intraperitoneal injection. After 30 minutes, mice were euthanized and perfused with 30ml PBS to remove NaFl from the vasculature. Brains and spinal cords were dissected, weighed and homogenized in PBS. Homogenates were clarified by centrifugation at 500xg for 10 minutes at 4°c. A 1:1 ratio of supernatant was combined with 15% TCA and incubated for 24 hours at 4°c. Samples were centrifuged and supernatants were neutralized with 5N NaOH. Fluorescence intensity was assessed with a Synergy H1 (BioTek, Winooski, VT) set at a 485nm excitation.

Clinical severity and histopathology. Clinical disease severity was assessed using a 4 point scoring scale as previously described [3]. Mice were euthanized according to IACUC guidelines and perfused with 30ml of 4% paraformaldehyde (PFA). Spinal cords were

removed, fixed overnight in 4% PFA at 4°c and separated into eight 1.5mm sections. Each μM section was cryoprotected in 20% sucrose for five days before embedding in OCT. Eight thick coronal sections were cut and stained with luxol fast blue (LFB) and H&E. Percent demyelination for each mouse was determined by taking the average demyelination of eight spinal cord coronal sections using Image J software (NIH).

Immunofluorescence. Spinal cord sections were processed as above. For immunofluorescence, slides were first desiccated for at least two hours and blocked with 5% Normal Donkey Serum with or without 0.3% Triton-X 100. Primary antibodies were incubated overnight at 4°c: goat anti - CXCL1 1:50 (R&D Systems, Minneapolis, MN), rabbit anti – GFAP 1:500 (Life Technologies, Carlsbad, CA), rat anti – Ly-6B.2 1:100 (Serotec, Raleigh, NC), rabbit anti - Iba11:500 (Wako Chemicals, Richmond, VA) , rabbit anti – GST-π 1:1000 (MBL, Woburn, MA).

Neutrophil depletion. Mice received either 250μg anti-Ly6g clone 1A8 or isotype control (BioXCell, West Lebanon, NH) via intraperitoneal injection every other day beginning at day 5 p.i. Targeted depletion of neutrophils was confirmed by flow staining of circulating neutrophils at defined times post-treated with Ly6g-specific antibody.

3.3 Results

Generation and characterization of pBI-CXCL1-rtTA double-transgenic mice.

To experimentally induce CXCL1 overproduction from astrocytes to examine effects on host defense and disease in response to JHMV infection of the CNS, transgenic mice were engineered to utilize the tetracycline-controlled transcriptional activation system. In brief, the human glial fibrillary acidic protein (hGFAP) promoter drove expression of a modified version of the reverse tetracycline transactivator protein (rtTA*M2). In the presence of doxycycline, transcription initiates at a tet-operon leading to production of recombinant CXCL1 mRNA transcripts. Double transgenic (tg) mice (pBI-CXCL1-rtTA) were generated and genotyped to confirm that they incorporated both constructs **(Figure 1A)**. To determine if doxycycline (Dox) could selectively induce CXCL1 expression, astrocytes were derived from post-natal day 1 (P1) cortices of double tg and single tg mice (i.e., lacking GFAP-rtTA element), and cultured in the presence of Dox for 24-hours. Following Dox treatment (100ng/ml), increased expression of CXCL1 in double tg cultures was detected by immunofluorescent staining with no CXCL1-positive cells detected in the vehicle treated double tg cultures (**Figure 1B**). In addition, following 24-hours of Dox treatment of double tg cultures, supernatants revealed elevated CXCL1 protein levels compared to vehicle treated double tg astrocytes as well as Dox treated single tg astrocytes (**Figure 1C**). These data confirm that recombinant CXCL1 can be induced in response to Dox and that there is minimal activity of the tetracycline responsive element in the absence of Dox treatment.

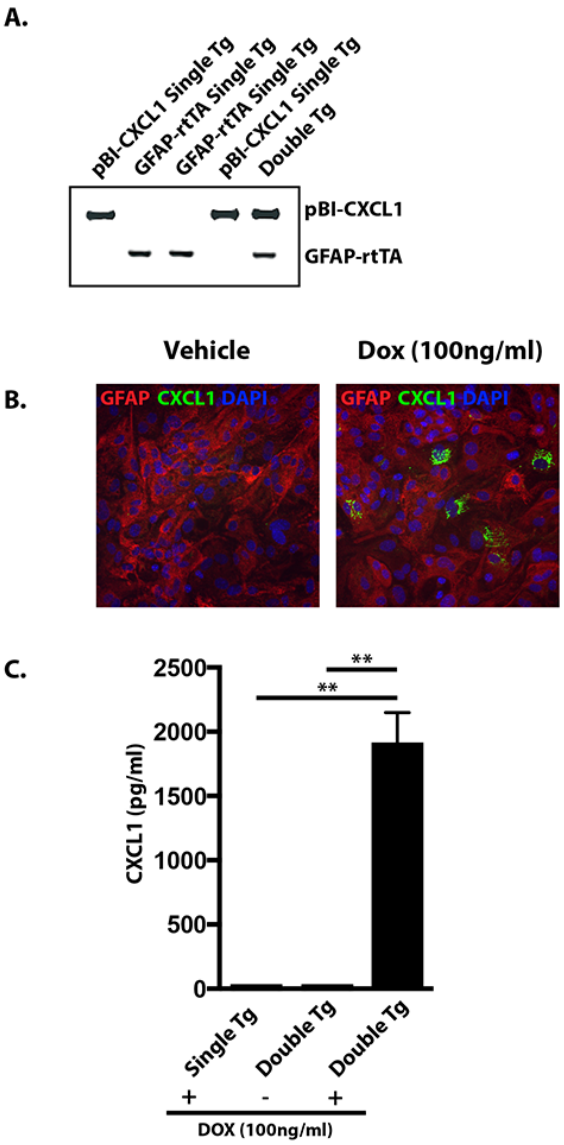

Figure 3.1. Generation and *in vitro* characterization of a doxycycline inducible, astrocyte-specific CXCL1 overexpressing mouse line. Double transgenic (double tg) mice utilizing the Tet-On doxycycline (Dox) inducible system were generated by crossing hemizygous hGFAP-rtTA*M2 mice to a transgenic mouse line incorporating a tetracycline responsive element driving expression of CXCL1 (pBI-CXCL1) **(A)**. To test the inducibility of CXCL1 from astrocytes derived from double tg mice, cortex tissue from double tg and single tg post-natal day 1 (P1) mice was dissociated and enriched for astrocytes. Following 24-hours of Dox (100ng/ml) treated double tg astrocyte cultures, immunofluorescence confirmed CXCL1 expression within GFAP-positive astrocytes while vehicle treatment yielded no CXCL1 fluorescence **(B)**. Supernatants from Dox-treated double tg and single tg astrocytes cultures were collected and levels of CXCL1 were measured by ELISA. In the presence of Dox, double tg cultures yielded significantly elevated CXCL1 protein levels,

while single tg cultures did not, suggesting the CXCL1 inducible system is functional **(C)**. Data from panel ***C*** represents supernatants pooled from triplicate wells derived from three separate double tg and single tg mouse cultures. Data is presented as average±SEM ; **p<0.01

Dox treatment of double tg mice elevates CXCL1 mRNA and protein within the CNS.

In response to JHMV infection of C57BL/6 mice, the ELR chemokines CXCL1, CXCL2, CXCL5 are upregulated within the brain and spinal cord [4,14]. We next tested whether treatment with Dox resulted in overproduction of CXCL1 within the brains and spinal cords of JHMV infected double tg mice. Double tg or single tg mice were infected i.c. with JHMV (250 PFU) and subsequently treated daily with Dox (50mg/kg) via i.p. injection starting at day 2 post-infection (p.i.) and continuing through day 12 p.i. (**Figure 2A**). Dox treatment resulted in increased mRNA transcripts specific for CXCL1 in the brains of infected double tg mice at days 4, 7, and 12 p.i. compared to single tg mice (**Figure 2B**). Similarly, CXCL1 transcripts were elevated in the spinal cords at days 4, 7 ($p<0.05$), and 12 ($p<0.01$) p.i. when compared to single tg mice (**Figure 2B**). To confirm that that CXCL1 mRNA was derived from the transgene and not from germline-encoded CXCL1, we employed qPCR primers that specifically anneal to a UTR region specific for endogenous CXCL1 mRNA and not transgenic CXCL1. As shown in **Figure 2C**, there was only a marginal increase in endogenously produced CXCL1 mRNA transcripts when compared to transgene-encoded CXCL1. These results confirm that increased CXCL1 mRNA transcripts are derived from the CXCL1 transgene. CNS-derived CXCL1 in Dox-treated double tg mice resulted increased CXCL1 protein in both the spinal cord (**Figure 2D**) as well as serum (**Figure 2E**) compared to single tg mice at day 7 p.i.. Immunofluorescent staining confirmed increased CXCL1 protein present within the CNS and astrocytes as the primary cellular source in Dox-treated double tg mice (**Figure 2F**). Finally, overproduction of recombinant CXCL1 within the CNS of JHMV infected mice did not result in increased expression of other proinflammatory cytokines and chemokines within the SC (**Figure 2G**) or brain (**data not shown**). These

data demonstrate that double tg mice are responsive to Dox treatment resulting in increased levels of CXCL1 derived within the CNS and this corresponds to elevated levels of circulating CXCL1 within the serum. However, CXCL1 overproduction does not impact the expression other pro-inflammatory factors involved in JHMV host-defense and disease.

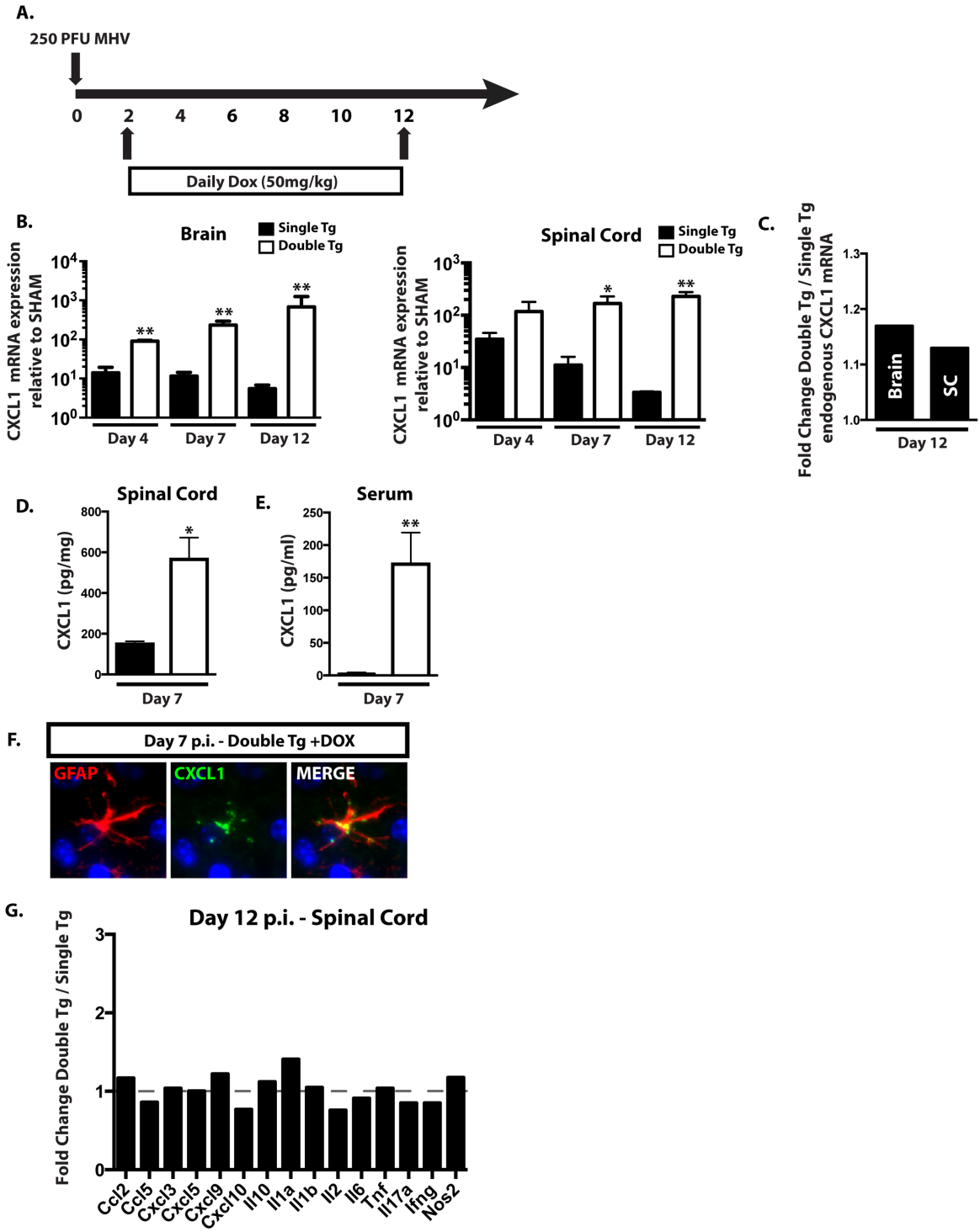

Figure 3.2. CXCL1 is induced *in vivo* following administration of doxycycline into double transgenic mice during acute JHMV infection. To test the ability of doxycycline (Dox) to induce CXCL1 overproduction *in vivo*, double tg and single tg mice were infected with 250 PFU JHMV and treated daily with 50mg/kg Dox starting at day 2 post-infection (p.i.) **(A)**. Mice were sacrificed at days 4, 7 and 12 p.i. Administration of Dox to double tg

mice resulted in a significant increase in the expression of CXCL1 mRNA compared to Dox-treated single tg mice within the brain at days 4, 7 and 12 p.i. as measured by RT-qPCR **(B)**. Within the SC, Dox-treated double tg mice had statistically significant increases in CXCL1 mRNA expression over Dox-treated single tg mice at days 7 and 12 p.i. Transcript levels from single and double tg mice were normalized to b-Actin and are relative to SHAM infected double tg mice **(B)**. CXCL1 transgene expression within the brain and spinal cord did not impact endogenous CXCL1 production within Dox-treated double tg mice compared to Dox-treated single tgs **(C)**. Overproduction of CXCL1 protein was observed within the SC at day 7 p.i. within double tg mice **(D)** and this correlated with an increase in CXCL1 protein within the blood serum at day 7 p.i. as measured by ELISA **(E)**. Immunofluorscence analysis of spinal cord tissue from Dox-treated double tg mice confirmed that astrocytes were the source of CXCL1 production at day 7 p.i. **(F)**. To determine if overexpression of CXCL1 affected other genes involved in host-defense chronic neurologic disease induced following JHMV infection, a pro-inflammatory gene-array was utilized with cDNA derived from the brains and spinal cords of double tg and single tg mice **(G)**. Data from panel ***B*** represents 2 experiments with a minimum of 4 mice per group. All RT-qPCR samples were run in triplicate. Panel ***D*** and ***E*** represents a minimum of 3 mice per group. Superarray data was compiled utilized the average value of two mice per group run in duplicate. Data is presented as average$\pm$SEM; *$p<0.05$, **$p<0.01$

CXCL1 overexpression increases morbidity in double tg mice.

Dox-induced overexpression of CXCL1 within the CNS resulted in a statistically significant increase in clinical disease severity (**Figure 3A**) and this correlated with an increase in mortality (**Figure 3B**). This was not associated with impaired ability to control viral infection within either the brain or spinal cords as similar viral titers were detected at days 4 and 7 p.i. in double tg and single tg mice (**Figures 3C and D**). Furthermore, both double tg and single tg animals reduced CNS viral titers to below detectable titers as measured by plaque assay within the brain by day 12 p.i. (**Figure 3C**) while the viral titers within the spinal cord at day 12 p.i. were near the limit of detection **(Figure 3D)**. Moreover, no differences were observed with viral RNA load between double tg and single tg mice at day 12 p.i. (**data not shown**). These data indicate that the augmented clinical disease severity in Dox-treated double tg mice is not a result of an inability to control viral replication within the CNS.

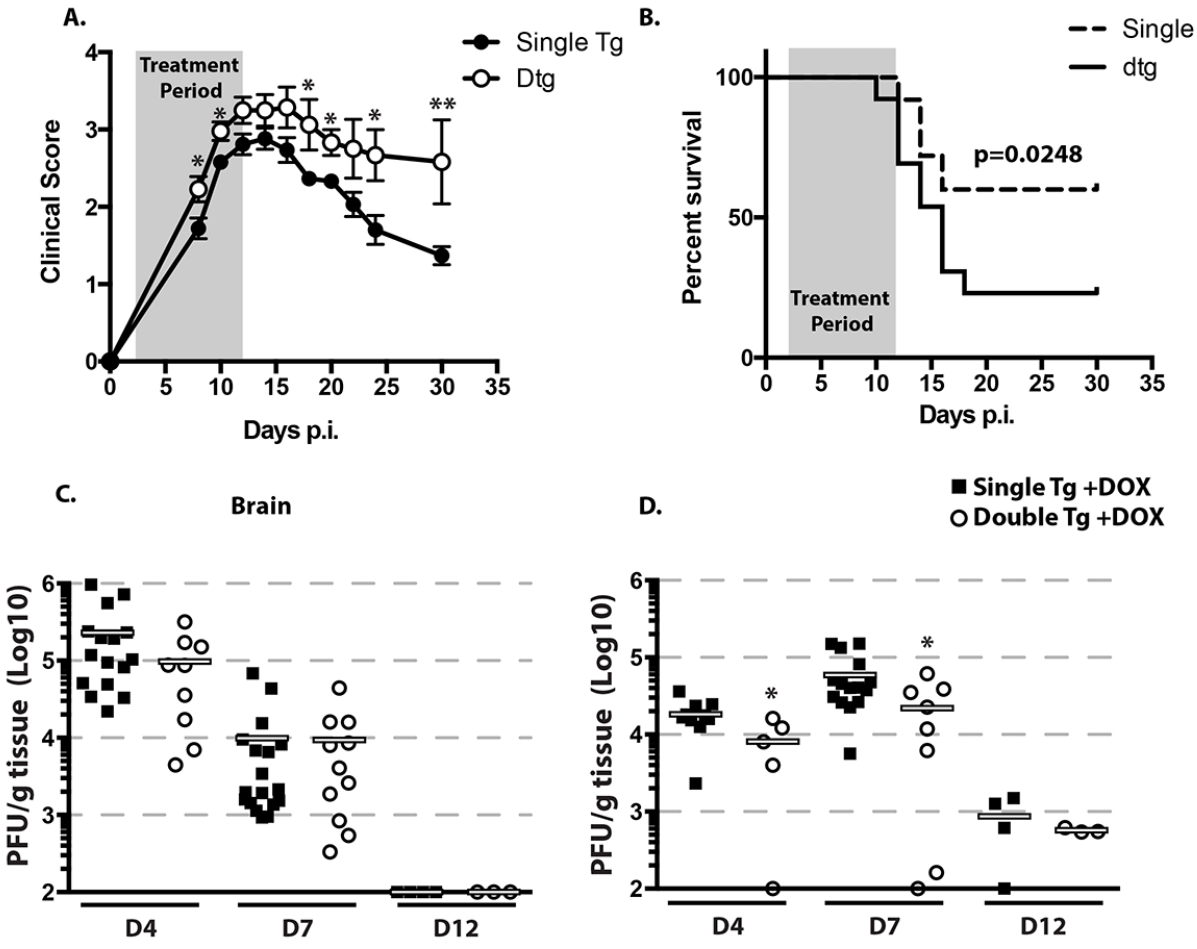

Figure 3.3. CXCL1 overproduction amplifies JHMV-induced clinical disease and mortality but is not a result of delayed viral clearance. Double tg and single tg mice were infected with 250 PFU JHMV and treated with 50mg/kg Dox daily starting at day 2 p.i. through day 12 p.i. Clinical severity was assessed until day 30 p.i. using a 4 point scale **(A).** Dox treatment of double tg mice lead to significantly increased mortality compared to doxycycline treated single tg controls **(B)**. Viral titers of Dox-treated double tg and single tg mice were measured by plaque assay **(C)**. Clinical disease and mortality scoring represents an average of double tg and single tg mice. For panels ***A*** and ***B***, n=23 single tg mice and n=12 double tg mice. *p<0.05, **p<0.01

Neutrophil migration to the CNS is increased in Dox-treated double tg mice.

We have previously shown that neutrophils migrate into the CNS of JHMV-infected mice through a CXCR2-dependent mechanism [4]. Therefore, we determined if Dox-induced CXCL1 overexpression within the CNS resulted in enhanced mobilization of neutrophils to the CNS in response to JHMV infection. JHMV-infected double tg and single tg mice were i.c. infected with virus, treated with Dox and mice were sacrificed at days 4 and 7 p.i. and neutrophil ($Ly6G^{high}CD11b^{+}$) levels in blood were measured by flow cytometry. CXCL1 overexpression from the CNS resulted in significantly increased frequency of neutrophils within the blood at days 4 ($p<0.05$) and 7 ($p<0.001$) in double tg mice compared to infected single tg controls (**Figure 4A**). Dox-induced CXCL1 production in JHMV-infected double tg mice also resulted in a significant increase in neutrophil frequency within the brain at days 4 ($p<0.0001$) and 7 ($p<0.01$) p.i. (**Figure 4B**). Similarly, there was an increase in neutrophil frequency within spinal cords of double tg mice at days 4 ($p<0.01$) and 7 ($p<0.05$) p.i. compared to single tg mice (**Figure 4B**). Immunofluorescence staining for neutrophils (Ly-6B.2) supported the flow cytometric data and revealed increased numbers of neutrophils accumulating within the meninges of double transgenic mice at day 7 p.i. (**Figure 4C**).

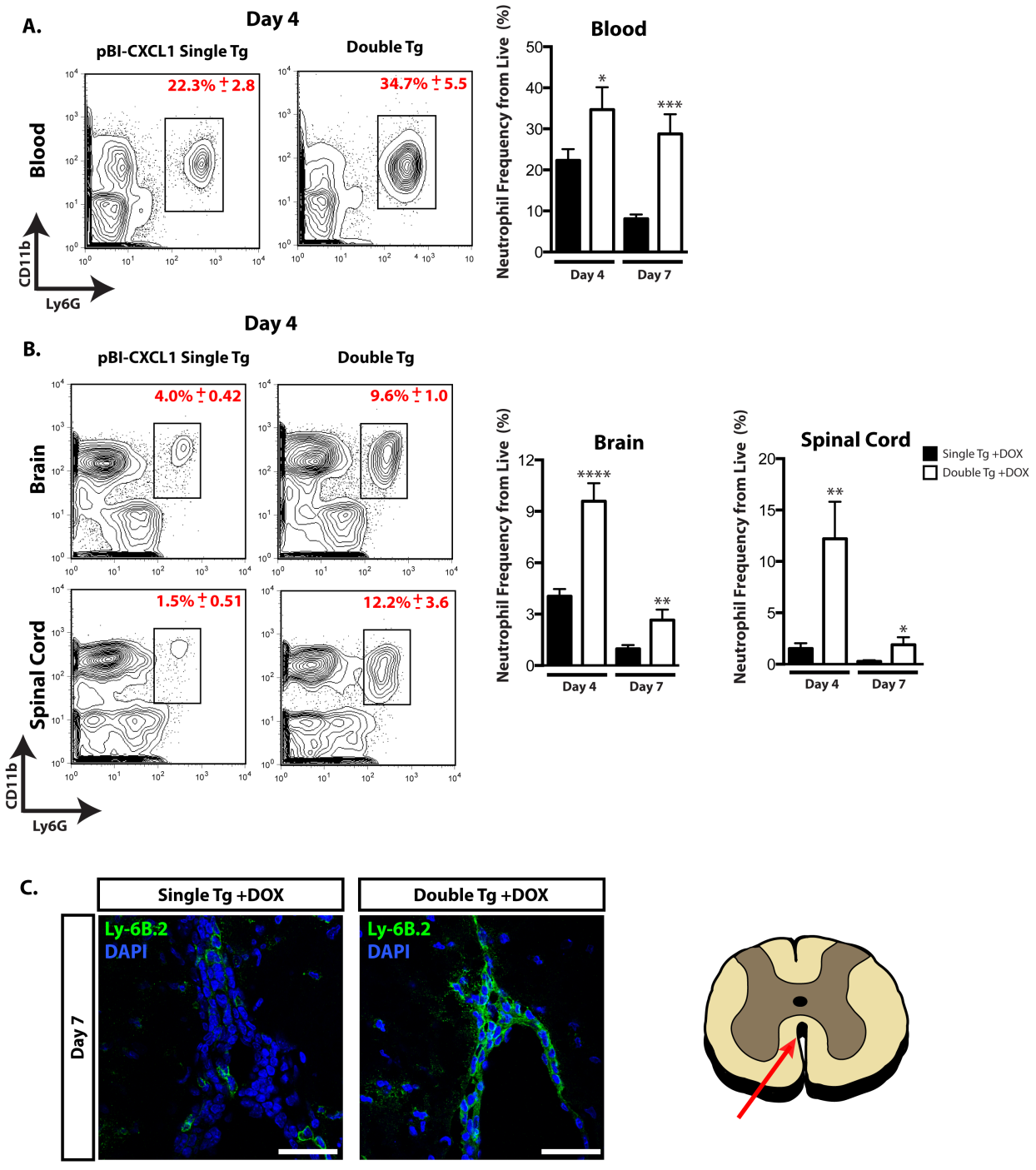

Figure 3.4. CXCL1 overproduction from astrocytes mobilizes neutrophils and directs them to the CNS. Blood from Dox-treated JHMV-infected double tg and single tg mice was isolated at day 4 and day 7 p.i. and used for flow cytometric analysis. The frequency of CD11b+Ly6G+ neutrophils were significantly higher within the blood at day 4 and 7 p.i. indicating sustained neutrophil mobilization following Dox treatment **(A)**. Neutrophil migration to the brains and spinal cords of both groups were assessed by flow cytometry at day 4 and 7 post-infection **(B)**. A significant increase in neutrophil frequency within the

brain and spinal cord was observed in Dox-treated double tg mice at both time-points **(B)**. Immunofluorescence analysis indicated that Ly-6B.2-positive neutrophils were primarily located at the ependymal lining and perivascular space at the spinal cord, with minimal neutrophil presence within the parenchyma **(C)**. Panels ***A*** and ***B*** represents 3 independent experiments with a minimum of 3 mice per group per experiment at each time-point analyzed. Data is presented as average$\pm$SEM; *p<0.05, **p<0.01, ***p<0.001 ****p<0.0001

Overexpression of CXCL1 does not amplify T cell or macrophage infiltration into the CNS.

The increased presence of neutrophils within the CNS of double tg mice suggested that there would also be a corresponding increase in BBB permeability. Rather, no differences were observed in BBB permeability within the brain or spinal cord at day p.i. as measured by NaF uptake **(Figure 5A)**. Similar observations were recorded at day 7 p.i, (**data not shown**). Immunophenotyping of cells infiltrating into the brains and spinal cords was performed at defined times following JHMV infection and Dox treatment to determine if CXCL1 overproduction influenced the accumulation of other cellular subsets. Examination of brains at days 4, 7, and 12 p.i. revealed no differences in frequencies of $CD45^{hi}$-positive cells between infected double and single tg mice (**Figure 5B**) although there were elevated numbers of total $CD45^{hi}$ cellular infiltrates at day 4 within the spinal cord (**Figure 5C**) and is a result of the increased neutrophil frequency at this time-point. Moreover, there were no differences in either frequencies or numbers of CD4+ and CD8+ T cells or virus-specific CD4+ and CD8+ T cells within the brains of infected double and single tg mice (**Figure 5B**). Within the spinal cord, we detected no differences in the frequencies CD4+ and CD8+ T cells at day 7 and 12 p.i. or the total number of virus-specific T cells 12 days p.i. in infected double and single tg mice (**Figure 5C**). In addition, no differences were detected in the expression of the activation marker CD69 on T lymphocytes present within the spinal cords at day 12 p.i. (**Figure 5D**).

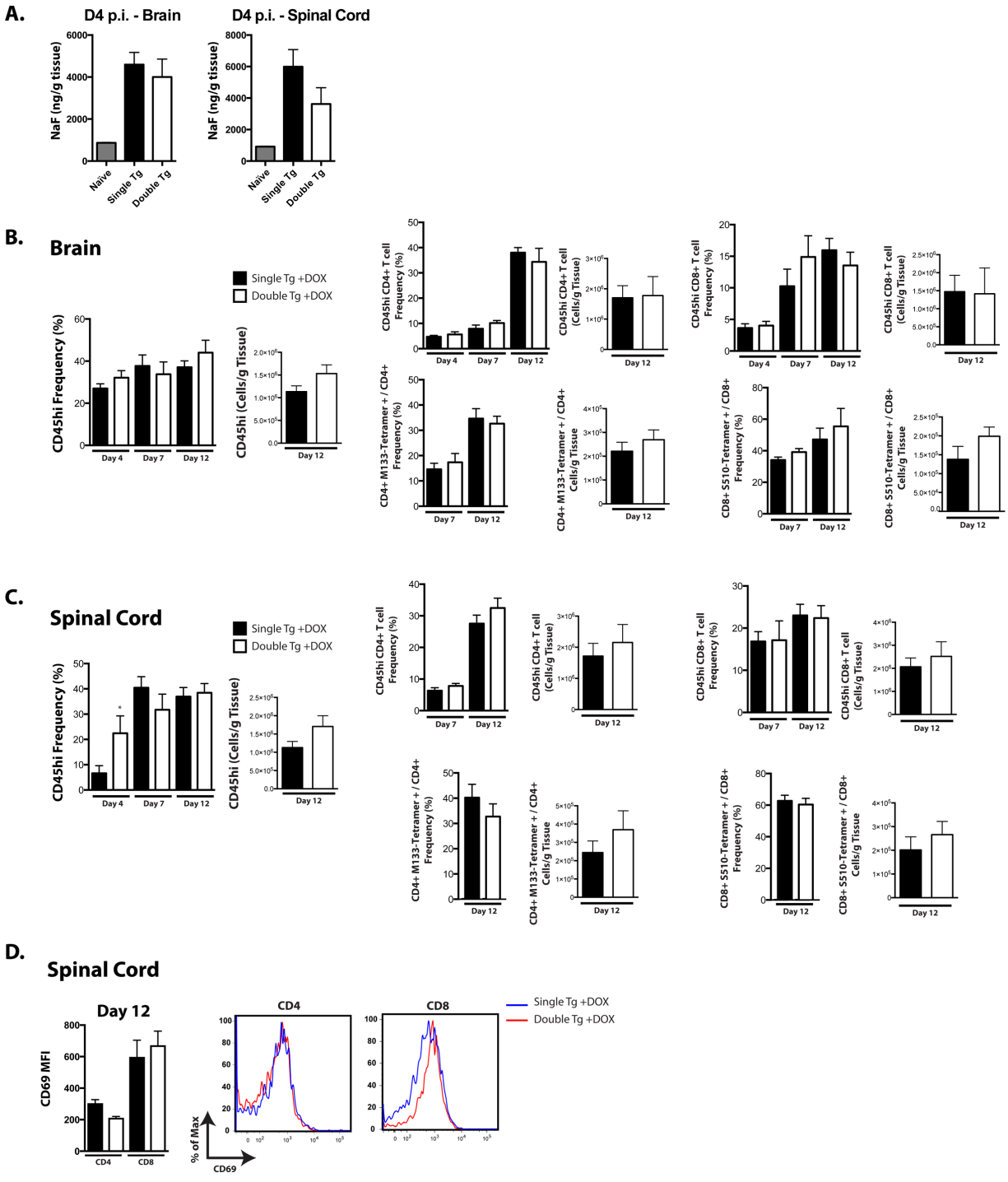

Figure 3.5. CXCL1 overproduction from the CNS does not affect T cell infiltration into the CNS. At day 4 p.i., brains and spinal cords from Dox-treated double tg and single tg mice treated with NaFl were removed and total NaFl uptake was measured **(A)** Single cell suspensions from the brains and spinal cords from Dox-treated JHMV-infected double tg and single tg mice were isolated and assessed for T cell infiltration by Flow cytometry **(B-**

C). No statistical difference was observed in the frequency of CD45hi inflammatory infiltrates within the brain at day 4, 7 or 12 post-infection (p.i.) or the frequency of CD4+ and CD8+ T cells within the brain at day 4, 7 or 12 p.i. **(B)**. At day 4 post-infection, the frequency of CD45hi infiltrates at day 4 post-infection was significantly higher in JHMV-infected Dox-treated double tg mice and is likely a result of the enhanced neutrophil as a result of CXCL1 transgene expression **(C)**. However, the frequency of CD4+ and CD8+ T cells were not impacted as a result of enhanced neutrophil accumulation within the SC **(C)**. CD69 expression on CD4+ and CD8+ T cells within the spinal cord was unchanged between double tg and single tg mice at day 12 p.i. **(D).** Flow cytometric data represents 3 independent experiments with a minimum of 3 mice per group per experiment at each time-point. Data is presented as average$\pm$SEM; *$p<0.05$

Examination of macrophage ($CD45^{hi}F4/80^{+}$) accumulation within either the brain or spinal cords between infected double and single tg mice revealed no differences at any time point examined (**Figure 6A**). Moreover, CNS-infiltrating macrophages displayed no differences in the expression of MHC class II or CD80 (**Figure 6B**). Although similar frequencies and numbers of microglia ($CD45^{lo}F480^{+}$) were present within the brains of infected mice (**Figure 6C**) at day 12 p.i., there was a significant ($p<0.05$) increase in microglia present within the spinal cords of infected double tg mice compared to single tg animals (**Figure 6C**). Collectively, these findings argue that overexpression of CXCL1 within the CNS does not significantly affect infiltration and activation of T cells or macrophages yet does increase numbers of microglia within the spinal cord.

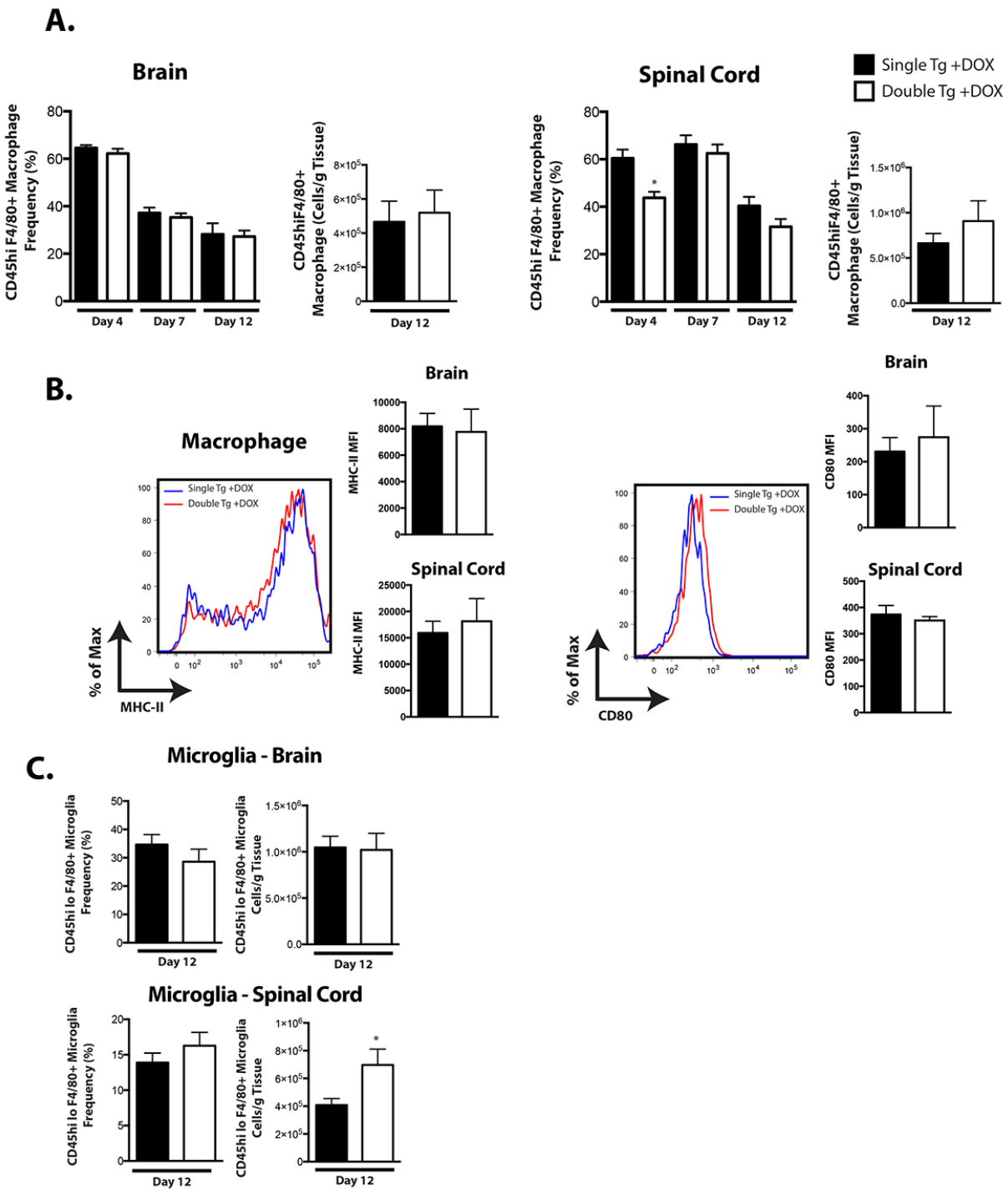

Figure 3.6. Macrophages are not impacted following CXCL1 overproduction from the CNS but microglia show increased numbers. The frequency of macrophages out of CD45hi cellular infiltrates within the brain and spinal cord remained unchanged in double tg mice treated with Dox **(A)**. Macrophage frequencies were lower and day 4 p.i, within the spinal cord as is likely reflected by the increase in neutrophils at this time-point **(A)**. Total

macrophage numbers within the brain and spinal cord of double tg mice were also similar compared to single tg mice at day 12 p.i. **(A)** No differences were observed in the median fluorescence intensity (MFI) of MHC-II and CD80 within the brain or spinal cord of double tg and single tg mice **(B)**. Total microglia was elevated within the double tg mice within the spinal cords at day 12 p.i. **(C)**. Flow cytometric data represents 3 independent experiments with a minimum of 3 mice per group per experiment at each time-point. Data is presented as average$\pm$SEM *$p<0.05$

Demyelination is increased in response to elevated CNS expression of CXCL1.

Examination of spinal cords from JHMV-infected Dox-treated double tg mice revealed an overall increase ($p<0.05$) in the severity of demyelination when compared to infected single tg animals (**Figure 6A**). Analysis of defined spinal cord sections revealed increased demyelination along the length of the spinal cords of infected double transgenic mice compared to single tg mice although pathology was enhanced within the cervical/thoracic region and to a lesser extent within the lumbar regions (**Figure 7A**). The increase in demyelination in double tg was associated with a significant ($p<0.05$) loss of mature oligodendrocytes (as determined by expression of GST-π) within the spinal cords (**Figure 7B**). Furthermore, Iba-1 staining revealed enriched numbers of macrophages/microglia within demyelinating white matter tracts in double tg mice compared to single tg mice (**Figure 7C**). These data indicate that the increased clinical disease observed in Dox-treated double tg mice correlates with enhanced spinal cord demyelination.

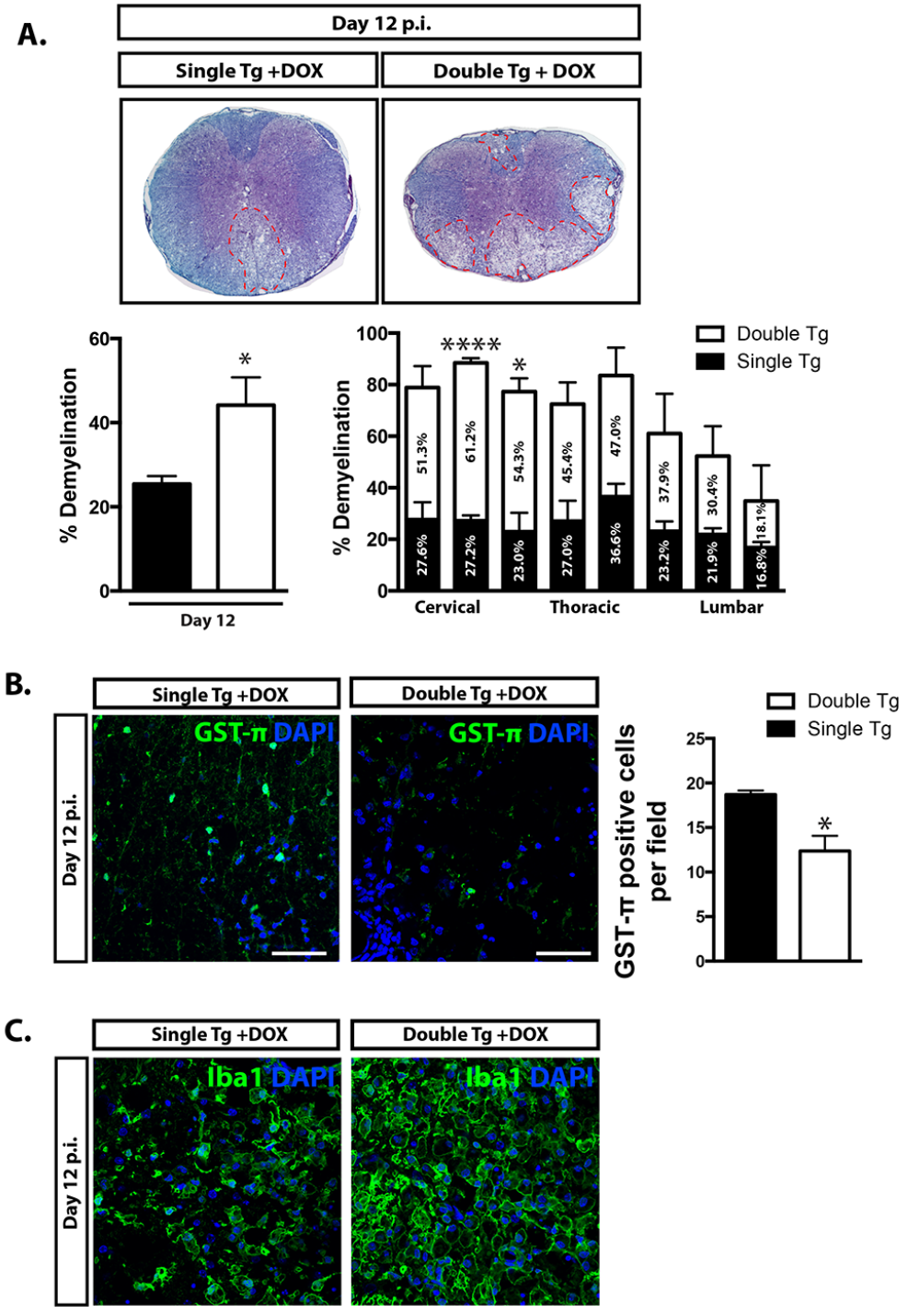

Figure 3.7. Histopathological analysis of spinal cords of double tg mice reveals an increase in demyelination and reduced total numbers of mature oligodendrocytes. White matter demyelination within the spinal cords of Dox-treated double tg mice is significantly elevated compared to single tg controls **(A)**. Upon closer investigation, cervical regions of the double tg had significantly more white matter. This correlated with a reduced number of mature GST-π-positive oligodendrocytes within the spinal cord of

double tg mice **(B)**. Within double tg mice, areas of significant white matter damage showed dense populations of Iba1-positive macrophages **(C)**.. Panel A and B represent 1 experiment with a minimum of 5 mice per group. Data is presented as average$\pm$SEM; *p<0.05, ****p<0.0001

Neutrophil accumulation within the spinal cord correlates with increased demyelination.

We next determined if neutrophil infiltration into the CNS was associated with the increase in both clinical and histologic disease in double tg mice. Flow cytometric data indicated that neutrophil frequencies within the spinal cords of infected double tg were significantly increased ($p<0.01$) as well as their total numbers ($p<0.001$) at day 12 p.i. compared to single tg mice (**Figure 8A**). CXCL1 expression, as determined by immunohistochemical staining, was elevated within the spinal cords of Dox-treated double-tg mice as compared to treated single tg mice (**Figure 8B**). In double tg mice, a significant increase in neutrophils ($p<0.05$) were detected within the spinal cord parenchyma of double tg mice compared to single tg mice (**Figure 8B**). Notably, neutrophils were enriched within more cervical regions of the spinal cord undergoing demyelination while these cells were relatively absent in demyelinating lesions in single tg mice **(Figure 8B)**. To determine if the robust parenchymal presence of neutrophils within the spinal cords of double tg mice was associated with the enhanced lesion load, we eliminated neutrophils from the periphery using anti-Ly6g mAb injection beginning at day 5 p.i. **(Figure 8C)**. Flow analysis of immune cell infiltrates within the spinal cord confirmed neutrophil depletion following anti-Ly-6g treatment **(Figure 8C)**. A small but significant decrease ($p<0.05$) in the clinical score of anti-Ly-6g treated mice compared to isotype-treated double tg mice was observed at day 12 p.i. Supporting our previous findings that double tg mice display increase in white matter demyelination compared to single tg mice was the observation that isotype-treated double tg mice displayed a significant increase ($p<0.05$) in the percentage of total white matter demyelination compared to isostype-treated single tg

mice **(Figure 8D)**. However, anti-Ly-6g treatment of double tg mice did not result in a significant decrease in demyelination, suggesting that neutrophil depletion starting at day 5 p.i. is not protective against the amplified pathology observed in isotype-treated mice (**Figure 8D**).

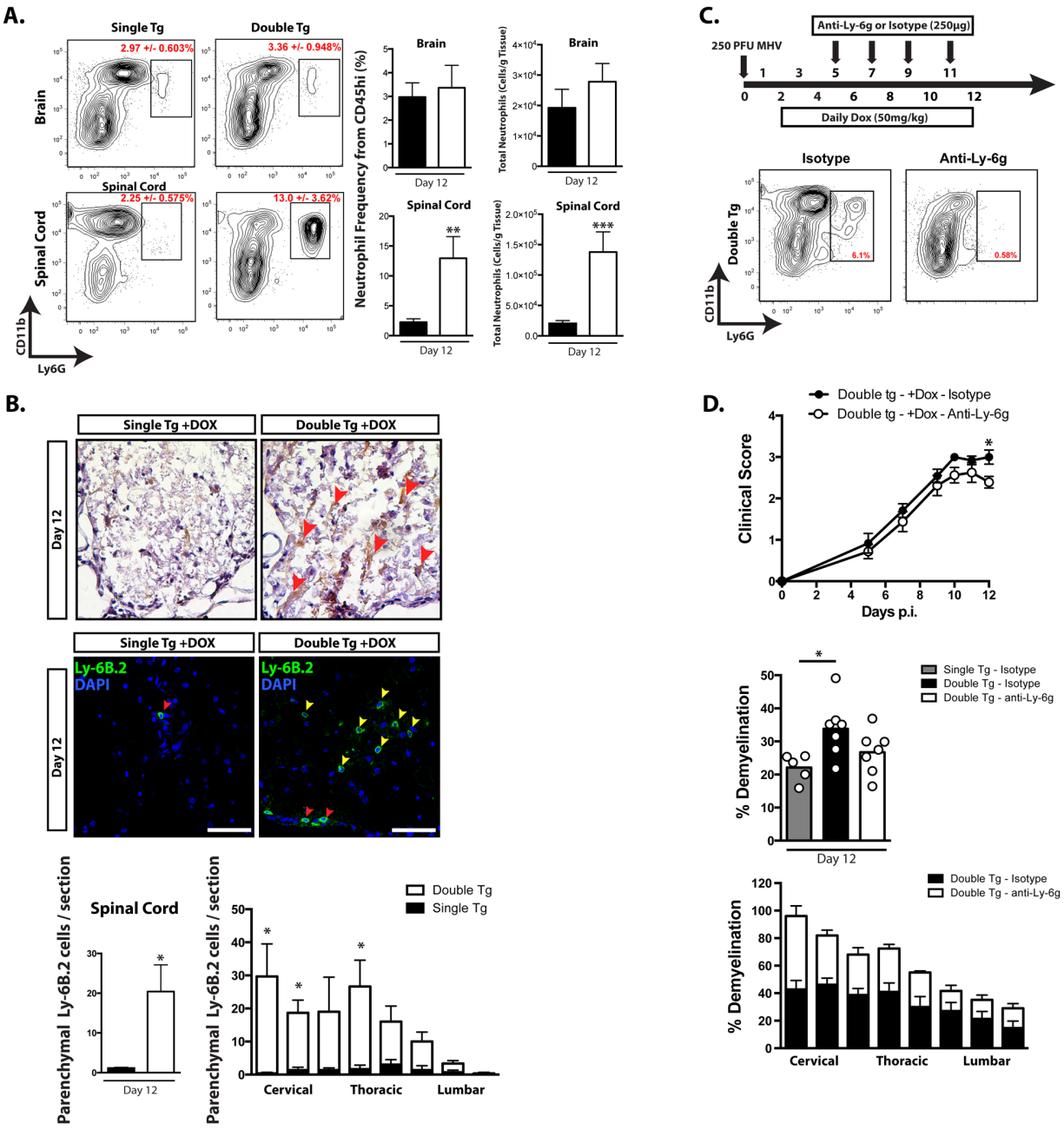

Figure 3.8. Neutrophils are found within parenchymal regions of the spinal cord in double tg mice and their elimination only partially reduces overall pathology. At day 12 post-infection (p.i.) brains and spinal cords were isolated and single cell suspensions were prepared from double tg and single tg mice infected with JHMV. Flow cytometric analysis revealed a significant increase in the frequency and total number of neutrophils within the spinal cord of double tg mice **(A)**. Immunofluorescence analysis revealed a significant increase in the number of Ly6B.2-neutrophils located within CXCL1 rich parenchymal regions of demyelinated white matter of double tg mice **(B)**. To determine if

neutrophils are contributing to the increase in pathology observed in double tg mice, neutrophils were eliminated from double tg and single tg mice with the use of an Anti-Ly-6g neutralizing antibody and their clinical scores were assessed to day 12 post-infection **(C)**. A significant increase in demyelination was observed in isotype-treated double tg mice compared to isotype-treated single tg mice, and a partial decrease in clinical disease was observed in Ly-6g treated double tg mice compared to double tg isotype controls. Panel ***A*** represents 3 independent experiments with a minimum of 3 mice per group per experiment. Immunofluoresence analysis in Panel ***B*** represents 1 experiment with a minimum of 5 mice per group. Clinical scoring data from Panel ***C*** represents combined data from 2 independent experiments. n=7 for isotype-treated groups and n=7 for anti-Ly-6g-treated group. Data from panel D represents 2 independent experiments. n=5 for isotype-treated single tg mice, n=7 for isotype-treated double tg mice and n=7 for anti-Ly-6g treated mice. Data is presented as average$\pm$SEM; *$p<0.05$, **$p<0.01$, ***$p<0.001$

3.4 Discussion

The ELR-positive CXC chemokines (CXCL1-3 and CXCL5-8) are high affinity ligands for their cognant receptor CXCR2. This signaling axis serves critical functions in host-defense and disease, as it is the dominant chemotactic pathway for neutrophil homing to sites of inflammation. CXCL1, CXCL2 and CXCL5 are upregulated within the CNS shortly following JHMV infection and control neutrophil migration to the BBB, resulting in peak accumulation by 3 days p.i. [4] The importance of neutrophils in host-defense to JHMV infection has been investigated with the use of antibodies that either eliminate neutrophils from the periphery or prevent their chemotaxis to the CNS. Many of these studies [4,15,16] have implicated the short-lived neutrophils as a primarily cellular source for the protease MMP9 during acute JHMV infection. However, no studies have investigated how chronic ELR-chemokine overproduction from the CNS impacts neutrophil function as well as host-defense and disease following JHMV infection.

The successful generation of a Dox-dependent CXCL1 expressing transgenic mouse has allowed for selective CXCL1 production from astrocytes within mice infected JHMV. Dox administration resulted in elevated CXCL1 transgene expression within the brains and spinal cords of double tg mice, correlating with rapid and robust neutrophil migration to the CNS compared to Dox-treated controls. As a result of CXCL1 transgene expression, double tg mice displayed sustained increase in clinical disease severity congruent with an increase in mortality. This observation shares similarities to mice infected with the lethal DM-JHMV variant that is characterized by a severe disease whereby neutrophils dominate the immune cell composition early following infection [16].

Over-accumulation of neutrophils in the CNS did not result in an increase in BBB permeability or affect the expression of proinflammatory factors that could potentially attract inflammatory leukocytes. Indeed, we observed no statistical difference in the frequencies of macrophages or T cells between double tg and single tg mice at day 12 p.i. These results are partially supported by Savarin and colleagues [7,8] who have provided evidence that neutrophils are not essential for promoting access of inflammatory leukocytes into the CNS as neutropenic mice or MMP9-deficient mice infected with the sublethal JHMV variant do not show appreciable differences in the early recruitment of $CD45^{hi}$ into the parenchyma. Overall, these data indicate that the increased presence of neutrophils within the CNS following JHMV infection does not influence BBB integrity and has no impact on the recruitment of other inflammatory cells from the periphery.

An increase in total white matter demyelination was observed at day 12 p.i. in Dox-treated double tg mice and this correlated with an overall decrease in the total number of GST-pi positive mature oligodendrocytes. Our findings revealed a significant parenchymal presence of neutrophils associated with regions of severe demyelination in infected double tg mice. In the context of sublethal JHMV infection on the CNS of wildtype mice, Ly6B.2-positive neutrophils are primarily localized to the endothelial luminal surface and are not found in appreciable numbers in parenchymal regions (**unpublished observations**). Neutrophils are known to possess an arsenal of toxic species that can impact cell survival such as neutrophil elastase, cathepsin G and matrix metalloproteinases [17]. Moreover, respiratory burst from the neutrophil phagosome and the generation nitric oxide as well as reactive oxygen species (ROS) through the NADPH oxidase complex can contribute to both vascular and parenchymal damage, resulting in bystander destruction of axons and

oligodendrocytes within white matter tissue [18,19]. This has been demonstrated in mouse models of ischemic injury where inhibition of the NADPH complex results in less injury to vascular endothelium and reduced cellular damage within brain parenchyma [20]. Furthermore, neutrophils are implicated in exacerbating lesion development within spinal cords on patients with neuromyelitis optica (NMO) [21], and inhibition of neutrophil elastase, a serine protease released from the primary granules of neutrophils, in mouse models of NMO resulted in reduced neuroinflammation and myelin loss. [22,23]. The potential destructive force of neutrophils has also been demonstrated using neurovirulent JHM recombinant viruses as neutrophil depletion or inhibition of nitric oxide synthase (NOS) correlated with reduced apoptosis of glial cells within the brain [24]. Another scenario is that neutrophils could be promoting pathology by drawing in macrophages within more cervical regions of the spinal cord. Within the EAE model of chronic neurologic disease, neutrophils have recently been reported to have a role in maturating local APCs within the CNS [25]. We observed dense clusters of macrophages in heavily demyelinated white matter regions that also contained significant neutrophil populations in double tg mice.

Ransohoff and colleagues [26] have shown that chronic overexpression of CXCL1 from oligodendrocytes within naïve mice results in a neurologic disease associated with microglia and astrocytic reactivity as a result of pronounced neutrophil accumulation within the brain. Indeed, we observed increased numbers of microglia within infected double tg mice and astrocytes displayed distinct phenotypic changes within heavily demyelinated regions including truncated morphologies and hypertrophy (**unpublished observations**). To determine if neutrophils were contributing to the increase in morbidity

in double tg mice, we eliminated neutrophils with the use of an anti-Ly6-g antibody starting at day 5 p.i. as this represents a time where there is only a minor neutrophil presence within the CNS in control animals. Neutrophil depletion in Dox-treated double tg mice resulted in a small improvement in clinical disease at day 12 p.i. compared to control animals and this was associated with a decrease in the severity of demyelination. These findings argue that sustained neutrophil infiltration into the CNS enhances clinical disease severity that is associated with an increase in white matter destruction. Moreover, the results presented here are consistent with a recent report from Segal and colleagues [27] and argue that therapies targeting neutrophil accumulation within the CNS may offer novel alternative therapies for treating neuroinflammatory diseases.

Within the context of the human demyelinating disease MS, neutrophils may contribute promoting disease, as the neutrophil chemoattractant CXCL8 is detected within the cerebrospinal fluid (CSF) of MS patients [28]. Furthermore, it was recently demonstrated that circulating neutrophils within MS patients display phenotypic changes that are characterized by a more activated state [29]. However, neutrophils are not abundantly found within active MS lesions and are not considered an important component in augmenting the pathology within newly formed lesions [30]. Despite this, neutrophils may have functional roles during the pre-clinical phase of the disease before focal demyelinating lesions are generated.

3.5 References

1. Bergmann CC, Lane TE, Stohlman SA. Coronavirus infection of the central nervous system: host-virus stand-off. *Nat Rev Microbiol*, 4(2), 121-132 (2006).
2. Liu MT, Chen BP, Oertel P *et al.* The T cell chemoattractant IFN-inducible protein 10 is essential in host defense against viral-induced neurologic disease. *J Immunol*, 165(5), 2327-2330 (2000).
3. Lane TE, Liu MT, Chen BP *et al.* A central role for CD4(+) T cells and RANTES in virus-induced central nervous system inflammation and demyelination. *J Virol*, 74(3), 1415-1424 (2000).
4. Hosking MP, Liu L, Ransohoff RM, Lane TE. A protective role for ELR+ chemokines during acute viral encephalomyelitis. *PLoS Pathog*, 5(11), e1000648 (2009).
5. Lane TE, Asensio VC, Yu N, Paoletti AD, Campbell IL, Buchmeier MJ. Dynamic regulation of alpha- and beta-chemokine expression in the central nervous system during mouse hepatitis virus-induced demyelinating disease. *J Immunol*, 160(2), 970-978 (1998).
6. Hosking MP, Tirotta E, Ransohoff RM, Lane TE. CXCR2 signaling protects oligodendrocytes and restricts demyelination in a mouse model of viral-induced demyelination. *PLoS One*, 5(6), e11340 (2010).
7. Savarin C, Stohlman SA, Atkinson R, Ransohoff RM, Bergmann CC. Monocytes regulate T cell migration through the glia limitans during acute viral encephalitis. *J Virol*, 84(10), 4878-4888 (2010).
8. Savarin C, Stohlman SA, Rietsch AM, Butchi N, Ransohoff RM, Bergmann CC. MMP9 deficiency does not decrease blood–brain barrier disruption, but increases astrocyte MMP3 expression during viral encephalomyelitis. *Glia*, 59(11), 1770-1781 (2011).
9. Yu J, Zhang L, Hwang PM, Rago C, Kinzler KW, Vogelstein B. Identification and classification of p53-regulated genes. *Proc Natl Acad Sci U S A*, 96(25), 14517-14522 (1999).
10. Hirano N, Murakami T, Fujiwara K, Matsumoto M. Utility of mouse cell line DBT for propagation and assay of mouse hepatitis virus. *The Japanese journal of experimental medicine*, 48(1), 71-75 (1978).
11. Schwartz JP, Wilson DJ. Preparation and characterization of type 1 astrocytes cultured from adult rat cortex, cerebellum, and striatum. *Glia*, 5(1), 75-80 (1992).
12. Tirotta E, Duncker P, Oak J *et al.* Epstein-Barr virus-induced gene 3 negatively regulates neuroinflammation and T cell activation following coronavirus-induced encephalomyelitis. *J Neuroimmunol*, 254(1-2), 110-116 (2013).
13. Blanc CA, Rosen H, Lane TE. FTY720 (fingolimod) modulates the severity of viral-induced encephalomyelitis and demyelination. *Journal of neuroinflammation*, 11, 138 (2014).
14. Hosking MP, Tirotta E, Ransohoff RM, Lane TE. CXCR2 Signaling Protects Oligodendrocytes and Restricts Demyelination in a Mouse Model of Viral-Induced Demyelination. *PLoS One*, 5(6), 12 (2010).
15. Zhou J, Marten NW, Bergmann CC, Macklin WB, Hinton DR, Stohlman SA. Expression of matrix metalloproteinases and their tissue inhibitor during viral encephalitis. *J Virol*, 79(8), 4764-4773 (2005).

16. Zhou J, Stohlman SA, Hinton DR, Marten NW. Neutrophils promote mononuclear cell infiltration during viral-induced encephalitis. *J Immunol*, 170(6), 3331-3336 (2003).
17. Mantovani A, Cassatella MA, Costantini C, Jaillon S. Neutrophils in the activation and regulation of innate and adaptive immunity. *Nature Reviews Immunology*, 11(8), 519-531 (2011).
18. Hampton MB, Kettle AJ, Winterbourn CC. Inside the neutrophil phagosome: oxidants, myeloperoxidase, and bacterial killing. *Blood*, 92(9), 3007-3017 (1998).
19. Weiss SJ. Tissue destruction by neutrophils. *N Engl J Med*, 320(6), 365-376 (1989).
20. Chen H, Song YS, Chan PH. Inhibition of NADPH oxidase is neuroprotective after ischemia-reperfusion. *Journal of cerebral blood flow and metabolism : official journal of the International Society of Cerebral Blood Flow and Metabolism*, 29(7), 1262-1272 (2009).
21. Lucchinetti CF, Mandler RN, McGavern D *et al.* A role for humoral mechanisms in the pathogenesis of Devic's neuromyelitis optica. *Brain*, 125(Pt 7), 1450-1461 (2002).
22. Zhang H, Bennett JL, Verkman AS. Ex vivo spinal cord slice model of neuromyelitis optica reveals novel immunopathogenic mechanisms. *Ann Neurol*, 70(6), 943-954 (2011).
23. Saadoun S, Waters P, MacDonald C *et al.* Neutrophil protease inhibition reduces neuromyelitis optica-immunoglobulin G-induced damage in mouse brain. *Ann Neurol*, 71(3), 323-333 (2012).
24. Iacono KT, Kazi L, Weiss SR. Both spike and background genes contribute to murine coronavirus neurovirulence. *Journal of Virology*, 80(14), 6834-6843 (2006).
25. Steinbach K, Piedavent M, Bauer S, Neumann JT, Friese MA. Neutrophils amplify autoimmune central nervous system infiltrates by maturing local APCs. *J Immunol*, 191(9), 4531-4539 (2013).
26. Tani M, Fuentes ME, Peterson JW *et al.* Neutrophil infiltration, glial reaction, and neurological disease in transgenic mice expressing the chemokine N51/KC in oligodendrocytes. *J Clin Invest*, 98(2), 529-539 (1996).
27. Rumble JM, Huber AK, Krishnamoorthy G *et al.* Neutrophil-related factors as biomarkers in EAE and MS. *J Exp Med*, 212(1), 23-35 (2015).
28. Ishizu T, Osoegawa M, Mei FJ *et al.* Intrathecal activation of the IL-17/IL-8 axis in opticospinal multiple sclerosis. *Brain*, 128(Pt 5), 988-1002 (2005).
29. Naegele M, Tillack K, Reinhardt S, Schippling S, Martin R, Sospedra M. Neutrophils in multiple sclerosis are characterized by a primed phenotype. *J Neuroimmunol*, 242(1-2), 60-71 (2012).
30. Lassmann H, Bruck W, Lucchinetti CF. The immunopathology of multiple sclerosis: an overview. *Brain Pathol*, 17(2), 210-218 (2007).

CHAPTER FOUR

Inducible ablation of *Cxcr2* in oligodendroglia attenuates autoimmune, but not viral, mediated neuroinflammation and demyelination

Brett S. Marro, Jonathan J. Grist, Daniel J. Doty, Richard M. Ransohoff, Robert S. Fujinami, and Thomas E. Lane

Abstract

The present study examines the functional role of CXCR2 signaling in oligodendroglia in two pre-clinical models of the human demyelinating disease multiple sclerosis (MS). We have generated mice (*Plp-Cre-ER^{T2}; Cxcr2$^{fl/fl}$* mice) in which *Cxcr2* is inducibly ablated within oligodendrocyte lineage cells in adult mice following treatment with tamoxifen. Deletion of *Cxcr2* in oligodendroglia resulted in markedly reduced disease severity in MOG_{35-55}-induced EAE, a model in which inflammatory Th1/Th17 cells are important in amplifying demyelination. Loss of CXCR2 signaling in oligodendroglia resulted in a dramatic decrease in neuroinflammation characterized by limited infiltration of neutrophils, macrophages, and T cells and a significant reduction in the severity of demyelination. Gene expression profiles revealed that ablation of *Cxcr2* in oligodendroglia resulted in muted expression of proinflammatory genes including CXCL1, CCL2, CXCL10, IFN-γ and IL-17A within the CNS. Antigen recall responses indicated no differences in secretion of IFN-γ and/or IL-17A by MOG_{35-55} peptide stimulated T cells indicating that the reduced clinical and histopathology observed in tamoxifen-treated *Plp-Cre-ER^{T2}; Cxcr2$^{fl/fl}$* mice was the result of compromised leukocyte trafficking to the CNS. In marked contrast, loss of CXCR2 signaling in oligodendroglia in mice infected with the neurotropic JHM strain of mouse hepatitis virus (JHMV), a disease mediated by virus-specific Th1 lymphocytes infiltrating into the CNS, did not affect pro-inflammatory gene expression within the CNS nor limit the severity of neuroinflammation or demyelination. These findings argue for a previously unappreciated role for CXCR2 signaling in oligodendrocyte lineage cells in autoimmune-mediated demyelination by amplifying neuroinflammation via regulation of pro-inflammatory gene expression within the CNS.

4.1 Introduction

Multiple sclerosis (MS) is a chronic neurodegenerative disease characterized by multifocal regions of neuroinflammation, demyelination, axonal loss, and transient remyelination that ultimately results in extensive neurologic disability [1]. Animal models of MS indicate that central nervous system (CNS) infiltration of neutrophils, monocyte/macrophages, and inflammatory T cells, including those that are autoreactive to specific proteins embedded in the myelin sheath, are important in disease initiation and maintaining demyelination [2,3]. In support of this is evidence that drugs designed to limit immune cell infiltration into the CNS impedes new lesion formation in MS patients [4,5] and improve clinical outcome associated with dampened demyelination in animal models of MS [6-9]. Therefore, understanding the signaling events that shape immune cell trafficking into and within the CNS offer new insights for identification of novel targets for therapeutic intervention.

Through use of preclinical mouse models of MS, chemokines and chemokine receptors have been implicated as important in attracting activated immune cells into the CNS and have been considered relevant targets for clinical intervention for MS patients [10-19]. As an example, administration of anti-CXCL10 antisera in JHMV infected mice with established demyelination within the spinal cord inhibited the trafficking of CD4+ T cells into the CNS, resulting in reduced clinical disease severity [20,21]. These findings are supported by a study in which blockade of CXCR3, the receptor for CXCL10, also abrogated the recruitment of inflammatory CD4+ T cells into the CNS [22]. In addition, CXCL10 has also been implicated in recruiting antibody-secreting cells (ASCs) into the CNS of JHMV-infected mice [23]. Within the context of EAE-induced demyelination, antibody-mediated

blockade of CXCL10 signaling was initially reported to diminish CD4+ T cell recruitment into the CNS parenchyma, leading to reduced clinical disease severity in mice that were induced with EAE via the adoptive transfer model [24]. However, later findings suggested that anti-CXCL10 treatment had no effect on EAE disease [25] or even amplifies disease severity [26].

A second chemokine signaling axis that serves important functions within the EAE and JHMV models of chronic neurologic disease is through CXCR2. This is a receptor for ELR-positive CXC chemokines (e.g., CXCL1 and CXCL2) and is expressed on polymorphonuclear neutrophils (PMN) as well as glia and neurons [27-31]. CXCR2 signaling on neutrophils promotes demyelination in experimental autoimmune encephalomyelitis (EAE) and cuprizone-induced demyelination [16,32]. These findings not only emphasized the importance of the innate immune response in demyelination but also illustrated that blocking CXCR2 signaling impeded neutrophil recruitment to the CNS and subsequently dampened the severity of demyelination. CXCR2 has additional roles that extend beyond influencing neutrophil activity as it is expressed on immature oligodendrocyte progenitor cells (OPCs) as well as mature myelinating oligodendrocytes [33]. Signaling through CXCR2 is believed to influence OPC proliferation and differentiation [34], control the positional migration of OPCs during the development of the mouse spinal cord [35] as well as regulating the numbers of OPCs to ensure the structural integrity of the white matter during CNS development [35]. Indeed, mice devoid of CXCR2 exhibit a paucity of OPCs and structural misalignments that persist into adulthood of the mouse, resulting in reduced numbers of mature oligodendrocytes and total myelin within the white matter [36]. Within the context of mouse models of demyelination, recent studies have

demonstrated paradoxical roles for CXCR2 signaling within the CNS. Some findings indicate CXCR2 as an inhibitory cue for myelin production by oligodendrocytes [37,38], while others have suggested that CXCR2 signaling is a survival mechanism for OPCs to prevent apoptosis induced by cytotoxic factors secreted during an inflammatory response [29,39-41].

Many of these studies have employed either germline-deficient mice deleted of *Cxcr2* or the use of CXCR2 neutralizing antibodies and small molecule antagonists to assess how CXCR2 signaling functions on oligodendrocytes. Although these studies have provided important insights into the role of CXCR2 in development and disease, potential off-target effects of using CXCR2-targeting antibodies and compounds exist since microglia, astrocytes, and neurons may also express CXCR2. Therefore, the present study was undertaken to better understand how selective deletion of *Cxcr2* within oligodendroglia in adult mice influences neuroinflammatory demyelination using two well-accepted pre-clinical models of MS. To accomplish this goal, we have utilized a tamoxifen-inducible *Cre-ER^{T2}* mouse model in which the proteolipid (*Plp*) enhancer element drives expression of an inducible form of CRE recombinase, generating mice that can be induced to selective ablate *Cxcr2* in oligodendroglia lineage cells (*Plp-Cre-ER^{T2}; Cxcr2$^{fl/fl}$* mice) following tamoxifen treatment. Here, we demonstrate that loss of *Cxcr2* in oligodendroglia results in a marked reduction in clinical disease severity following EAE-induction by immunization with myelin oligodendrocyte glycoprotein (MOG) peptide 35-55 (MOG_{35-55}) and this was associated with dampened neuroinflammation and demyelination. Overall numbers of MOG_{35-55}-specific CD4+ T cells within lymphatic tissues was not affected in *Plp-Cre-ER^{T2}; Cxcr$^{fl/fl}$* mice following MOG_{35-55} immunization indicating the clinical and histologic benefits of CXCR2

deletion on oligodendroglia was not the result of intrinsic problems in T cell responses. Rather, proinflammatory gene expression profiles were dramatically reduced within the brains of MOG_{35-55} immunized *Plp-Cre-ER^{T2}; Cxcr2 $^{fl/fl}$* mice advocating for a previously unappreciated role for oligodendroglia in disease through influencing neuroinflammation. In contrast, CNS infection of tamoxifen-treated *Plp-Cre-ER^{T2}; Cxcr2 $^{fl/fl}$* mice with the neurotropic JHM strain of mouse hepatitis virus (JHMV), which results in a Th1/IFN-γ -mediated demyelinating disease, did not attenuate neuroinflammation or demyelination. Therefore, these findings indicate the beneficial effects of ablating CXCR2 signaling in oligodendroglia CXCR2 are selective depending upon the model system employed and antigens that promote the inflammation. More importantly, these data argue for a previously unappreciated role for CXCR2 signaling on oligodendroglia in initiating an autoimmune-mediated, demyelinating disease by enhancing the expression of proinflammatory gene profiles within the CNS and our findings support strategies for targeting CXCR2 for treatment of MS.

4.2 Materials and Methods

Mice and tamoxifen treatement. *Plp-Cre-ER$^{T2\ +/+}$ :: Cxcr2$^{fl/fl}$* mice were kindly donated by Dr. Richard Ransohoff (Cleveland Clinic). Mice were crossed to the reporter strain B6.Cg-*Gt(ROSA)26Sor$^{tm9(CAG\text{-}tdTomato)Hze}$*/J (JAX) to generate *Plp-Cre-ER$^{T2\ +/+}$ :: Cxcr2$^{fl/fl}$ :: R26-stop-Td$^{+/-}$* mice (*Cxcr2$^{fl/fl}$*). Tamoxifen was prepared resuspending at 10mg/ml in prewarmed sesame seed oil. The mixture was placed on an orbital shaker at 37°c and shaken overnight to completely dissolve solution. 4-week old *Cxcr2$^{fl/fl}$* mice received 1mg/ml tamoxifen twice daily for five days via i.p. injection. Mice were rested for two weeks prior to MOG_{35-55} immunization or virus infection to reduce any immunomodulatory effects of tamoxifen.

Primary oligodendrocyte cultures. Cortices from postnatal day 1 *Plp-Cre-ER$^{T2\ +/+}$ :: Cxcr2$^{fl/fl}$ :: R26-stop-Td$^{+/-}$* mice (*Cxcr2$^{fl/fl}$*) were dissected and processed according to previously published protocols[42]. In brief, following removal of the meninges, cortical tissue was minced with a razor and placed in pre-warmed DMEM containing papain in order to completely dissociate the tissue. Following further aspiration through a Pasteur pipette, single cell suspensions were added to poly-d-lysine coated culture flasks and grown for nine days in DMEM supplemented with 10% FBS. Flasks were then transferred to an orbital shaker in a 5% CO_2 tissue culture incubator and shaken for approximately 16 hours at 220 rpm in order to remove loosely adherent OPCs. Media containing OPCs was transferred to 10 cm dishes for 30 minutes to remove strongly adherent astroglial contaminants. OPCs were transferred to a 15ml conical and centrifuged at 300xg for 5 minutes. Cells were counted and plated onto matrigel-coated Nunc™ Lab-Tek II Chamber slides (ThermoFisher Scientific, Waltham, MA) at 50,000 OPCs per chamber in N2 media supplemented with 3, 3', 5-Triiodo-L-thyronine sodium salt hydrate (T3 Sigma). After two days, fresh media was

used supplemented with (Z)-4-Hydroxytamoxifen (4-OHT Sigma) at 100nM to induce Cre-mediated recombination. Cells were cultured for an additional six days.

EAE induction. Complete Freund's adjuvant (CFA) was prepared by mixing 10mL incomplete Freund's adjuvant (Thermo Scientific, Rockford, IL) with 40mg M tuberculosis H37 (BD Biosciences, San Jose, CA) to make a 4mg/ml solution of CFA. MOG_{35-55} peptide was prepared by resuspending in PBS at 1 μmol/mL. A 1:1 CFA-MOG mixture was generating an emulsified by homogenization. To induce EAE, mice received two subcutaneous 100uL injections of the CFA-MOG mixture and 100uL of pertussis toxin (Ptx) (LIST Biological, Campbell, CA) via retroorbital injection. Mice received a second injection of PTx at day two post-immunization [43].

Adoptive Transfer EAE. 7-week old wildtype C57BL/6 mice (JAX) were immunized with MOG_{35-55} peptide in CFA without pertussis toxin. After 10 days, mice were euthanized and inguinal, brachial, axillary and cervical lymph nodes were isolated and processed to generate single cell suspensions. A total of $2.5x10^8$ cells were seeded into a T75 in the presence of 50ug/ml MOG_{35-55} peptide, 8ng/ml IL-23 (Peprotech, Rocky Hill, NJ), 10ng/ml Il-1a (Peprotech, Rocky Hill, NJ)) and 10ug/ml anti-IFN- γ (BioXCell, West Lebanon, NH). Flasks were placed at 37c 5% CO2 for 4 days. To isolate polarized CD4+ T cells, CD4+ positive selection was performed via MACS purification (Miltenyi Biotec Inc, San Diego, CA). Purified CD4+ T cells were resuspended to a concentration of $1.5x10^7$ cell/ml in cold PBS. To induce EAE, tamoxifen-pretreated *Plp-Cre-ER$^{T2\ +/+}$:: Cxcr2$^{fl/fl}$:: R26-stop-Td$^{+/-}$* or *Plp-Cre-ER$^{T2\ +/+}$:: Cxcr2$^{fl/fl}$:: R26-stop-Td$^{+/-}$* control mice were injected with 200ul of cells ($3x10^6$ total cells) via intraperitoneal injection. Clinical symptoms developed 8-10 days following adoptive transfer.

***Ex vivo* MOG_{35-55} peptide and PMA/Ionomycin stimulation assay**. Spleens and inguinal lymph nodes (ILN) were isolated from experimental mice and processed to generate single cell suspensions. A total of $1x10^6$ cells mononuclear cells were added to each well of a 96-well plate in the presence of either 20ug/ml MOG_{35-55} peptide and Golgiplug (BD Biosciences, San Jose, CA) and stimulated for 6-hours or 50ng/ml PMA (Sigma, St Louis, MO) + 2ug/ml Ionomycin (Sigma, St Louis, MO) for 5 hours. Following the incubation period, cells were stained for surface and intracellular antigens.

Virus infection. *Plp-Cre-ER$^{T2\ +/+}$ :: Cxcr2$^{fl/fl}$ :: R26-stop-Td$^{+/-}$*, mice were infected intracerebrally (i.c.) with 250 plaque forming units (PFU) of JHMV strain J2.2v-1 in 30ul of sterile HBSS.

PCR array and semi-quantitative RT-qPCR. Proinflammatory gene expression was determined using a Mouse Cytokine and Chemokine RT^2 Profiler PCR array (Qiagen Inc, Valencia, CA). For RT-qPCR analysis, total cDNA from brains and spinal cords of MOG_{35-55} immunized mice at day 8 and 11 post-immunization was generated via Superscript III (Life Tech., Carlsbad, CA) after homogenization in Trizol (Life Tech., Carlsbad, CA). Real-time SYBR green analysis was performed using mouse b-Actin control primers and primers specific to mouse CCL2, CCL5, CXCL1, CXCL2, CXCL10, IFN- γ and IL-17A using a Roche Lightcycler 480. Fold change in expression was determined by normalizing the expression of each sample to β-Actin and then quantifying fold change relative to naïve mice.

Flow cytometry. Flow cytometry was performed to assess the composition of inflammatory cells entering the CNS using established protocols [44,45]. In brief, single cell suspensions were generated from tissue samples by grinding with frosted microscope slides. Immune cells were enriched by a 2-step percoll cushion (90% and 63%) and cells

were collected at the interface of the two percoll layers. Before staining with the fluorescent antibodies, isolated cells were incubated with anti-CD16/32 Fc block (BD Biosciences, CA) at a 1:200 dilution. Immunophenotyping was performed using either rat anti-mouse IgG or armenian hamster anti-mouse IgG antibodies for the following cell surface markers: F4/80 (Serotec, Raleigh, NC), MHV S510-tetramer (NIH), MHV M133-Tetramer (NIH) and CD4, CD8, Ly6g, CD11b, IFN-γ, IL-17A, CD44, and CD45 (BD Biosciences, San Jose, CA) .

Clinical severity and histopathology. Clinical disease severity for JHMV infected mice was assessed using a 4-point scoring scale as previously described [44] while clinical disease severity for EAE-induced mice was assessed using a 5-point scale (REF). Mice were euthanized according to IACUC guidelines and perfused with 30ml of 4% paraformaldehyde (PFA). Spinal cords were removed, fixed overnight in 4% PFA at 4°c and separated into eight 1.5mm sections. Each section was cryoprotected in 20% sucrose for five days before embedding in OCT. Eight micron thick coronal sections were cut and stained with luxol fast blue (LFB) as well as hematoxylin and eosin (H&E). Percent demyelination for each mouse was determined by taking the total average demyelination within the white matter of eight SC coronal sections using Image J software (NIH). Tissue pathology scoring for MOG_{35-55} immunized mice is based on a previously described protocol [46]. In brief, anterior, posterior and lateral locations of each spinal cord sections were assessed for meningitis, perivascular cuffing and demyelination and normalized to the number of observed sections.

Immunohistochemistry. Spinal cord sections were desiccated at room temperature (RT) for 2 hours before beginning the staining process. Slides were then washed in PBS and blocked with 5% normal donkey serum (NDS) for 1 hours at RT. Rabbit anti-GFAP (Invitrogen, Carlsbad, CA) was diluted to 1:200 in 5% NDS and stained overnight at 4c. Slides were washed in PBS and biotin-conjugated donkey anti-rabbit was added at a 1:50 dilution. The DAB process was completed using the Vectastain ABC Kit (Vector Laboratories, Burlingame, CA).

4.3 Results

Generation and characterization of *PLP-Cre-ER^{T2}; Cxcr2 $^{fl/fl}$* mice.

To further elucidate the role of CXCR2 signaling on oligodendroglia during demyelination, we sought to ablate *Cxcr2* specifically within oligodendrocytes and their progenitors and assess its impact on EAE, a model of autoimmune-mediated inflammatory demyelination, as well as JHMV-induced neurologic disease. To carry this out, we employed a *Plp-Cre-ER$^{T2\ +/+}$ :: Cxcr2 $^{fl/fl}$* mouse line that can utilize the recombination activity of Cre recombinase to selectively ablate *Cxcr2* [47-50]. These transgenic mice contain the proteolipid protein (PLP) regulatory element driving expression of Cre-ER^{T2} [51]. The PLP regulatory element contains a DNA sequence downstream of the transcription start site of the *Plp* gene that has previously been shown to induce transgene expression and accurately reflect endogenous PLP expression both spatially and temporally [51]. Moreover, loxP sites were incorporated to surround *Exon* 2 and *Exon 3* at the *Cxcr2* locus, allowing for Cre-mediated recombination and ablation of *Cxcr2*. Liu and colleagues [32] have recently shown that active Cre expression within neutrophils *in vivo* can efficiently ablate the modified *Cxcr2* locus, leading to dramatically reduced CXCR2 expression. To aid in visualizing cells that have active Cre-recombinase, *Plp-Cre-ER$^{T2\ +/+}$ :: Cxcr2 $^{fl/fl}$* transgenic mice were crossed to a tamoxifen-inducible *Rosa26*-Tdtomato red reporter line on the C57BL/6 background to generate *Plp-Cre-ER$^{T2\ +/+}$ :: Cxcr2 $^{fl/fl}$ :: R26-stop-Td $^{+/-}$* mice, herein referred to as *Cxcr2 $^{fl/fl}$*.

To confirm that genetic ablation of *Cxcr2* and induction of Tdtomato red expression is specific to oligodendrocyte-lineage cells, oligodendrocyte precursor cells (OPCs) were generated from post-natal day 1 (P1) *Cxcr2* $^{fl/fl}$ mice. Following 6 days of OPC differentiation in the presence of 4-OHT (100nM), Cre-mediated recombination was confirmed at the *Cxcr2* locus following PCR amplification of genomic DNA with primers that generate an amplicon only following recombination of *Cxcr2* (**Figure 1A**). In addition, Tdtomato expression was found to be highly expressed within O1+ OPCs following addition of 4-OHT treatment (**Figure 1B**). To determine the cellular specificity of Cre *in vivo,* 4-week old *Cxcr2* $^{fl/fl}$ mice were treated daily with 1mg tamoxifen via intraperitoneal (i.p.) twice daily for 5-days. Two weeks following the first treatment day, mice were sacrificed to determine if Cre activity was specific to oligodendroglia. Following tamoxifen treatment, recombination was detected within the brain of transgenic mice but no amplicon was generated within within the spleen, liver or kidney (**Figure 1C**). Furthermore, PCR amplicons were also detected within the spinal cords following tamoxifen treatment (**Figure 1C**). Finally, Tdtomato expression was selectively expressed within GST-π – positive mature oligodendrocytes within the spinal cord, thus confirming that Cre activity is specific to oligodendrocyte lineage cells.

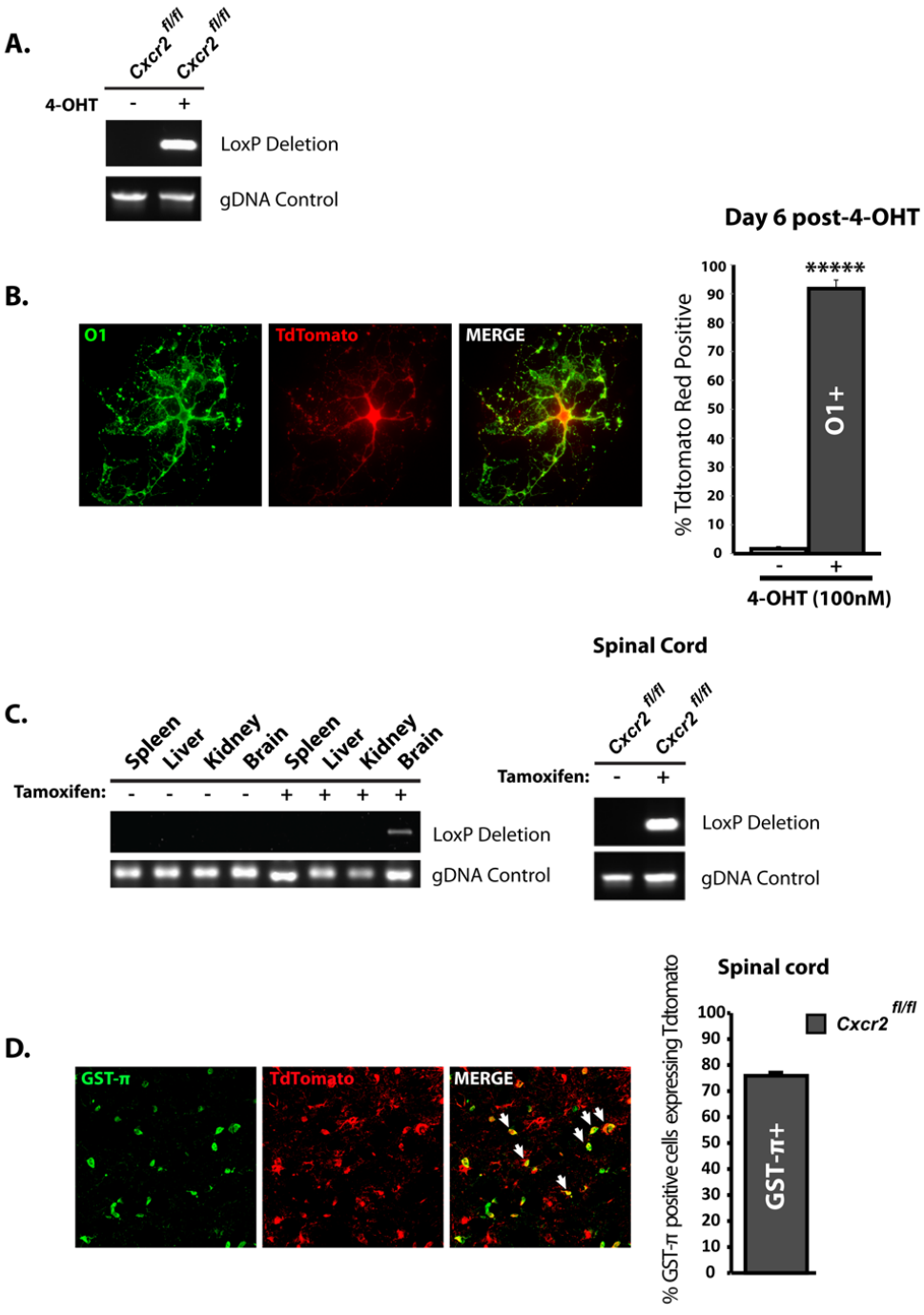

Figure 4.1. Cre-mediated recombination is detected *in vitro* and *in vivo*.
Oligodendrocyte-enriched cultures derived from post-natal day 1 (P1) *Cxcr2* $^{fl/fl}$ mice were cultured in the presence of 100nM 4-hydroxytamoxifen (4-OHT) for 6 days to induce Cre activity. In the presence of 4-OHT, recombination was detected at the *Cxcr2* locus in *Cxcr2* $^{fl/fl}$ mice while vehicle treated cultures showed no background recombination **(A)**.

Following 4-OHT treatment, nearly all O1+ mature oligodendrocytes expressed Tdtomato red **(B)**. Two weeks following tamoxifen treatment in *Cxcr2* $^{fl/fl}$ mice, Cre-mediated recombination at the *Cxcr2* locus was detected within the brain and spinal cord **(C)**. A large percentage of GST-π-positive oligodendrocytes expressed Tdtomato following tamoxifen treatment **(D)**. Panel ***A*** is a representative image from 4 independent *Cxcr2* $^{fl/fl}$ OPC cultures. Quantification of Tdtomato red-positive O1+ oligodendrocytes in panel ***B*** represents 4 independent *Cxcr2* $^{fl/fl}$ OPC cultures; Quantification performed in Panel ***D*** is from 8 separate coronal spinal cord sections from 4 mice. Data in panels ***B*** and ***D*** are presented as average±SEM; ***p<0.001, *****p<0.00001

Reduced susceptibility to EAE in animals lacking CXCR2 in oligodendroglia.

To determine if CXCR2 signaling on oligodendroglia modulates an autoimmune-mediated neuroinflammatory disease, we induced EAE in *Cxcr2* $^{fl/fl}$ mice. Four-week old *Cxcr2* $^{fl/fl}$ mice were treated with tamoxifen for 5 days, rested two weeks and subsequently immunized with MOG_{35-55} in CFA to induce autoimmune EAE. Tamoxifen-treated *Cxcr2* $^{fl/fl}$ mice showed a significant delay in disease onset as well as an overall reduction ($p<0.0001$) in clinical disease severity compared to control mice as assessed by linear regression analysis (**Figure 2A**). Tamoxifen-treated *Cxcr2* $^{fl/fl}$ mice had a significantly reduced average peak clinical score (2.32 ± 0.285) compared to controls mice (3.54 ± 0.144) (**Figure 2B**) and overall weight loss was significantly less than control animals (**Figure 2C**). To confirm that loss of *Cxcr2* was responsible for a dampened EAE disease and not the result of immunomodulation by tamoxifen alone, 4-week old wildtype C57BL/6 mice were pretreated with tamoxifen and subsequently immunized with MOG_{35-55} peptide two weeks later. Tamoxifen-treated mice displayed a slightly reduced clinical disease course compared to control mice, but was not statistically significant. These data indicate that the dampened EAE-disease severity in *Cxcr2* $^{fl/fl}$ mice is not due to off-target effects of tamoxifen (**Figure 2D**).

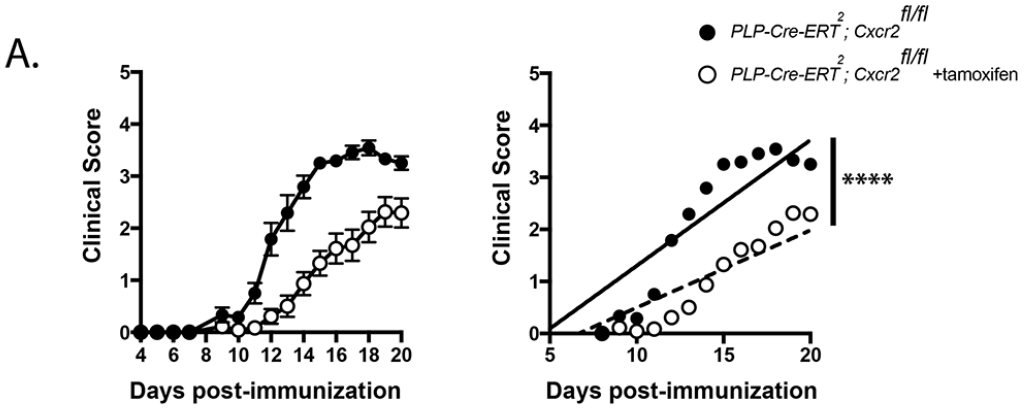

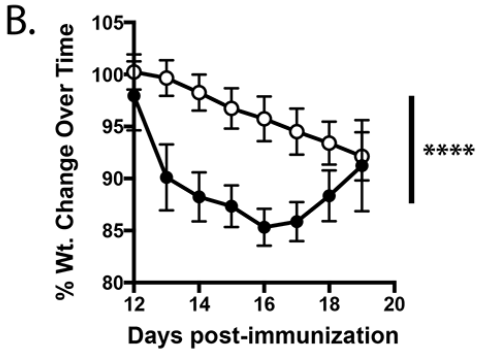

C.

Group	Incidence	Maximum clinical score	Day of maximum clinical score
Cxcr2$^{fl/fl}$	12/12 (100%)	3.54 ± 0.144	18
Cxcr2$^{fl/fl}$ +tamoxifen	19/23 (82.6%)	2.32 ± 0.285	19

Cumulative data from 3 experiments. All mice were scored to at least day 20 post-immunization

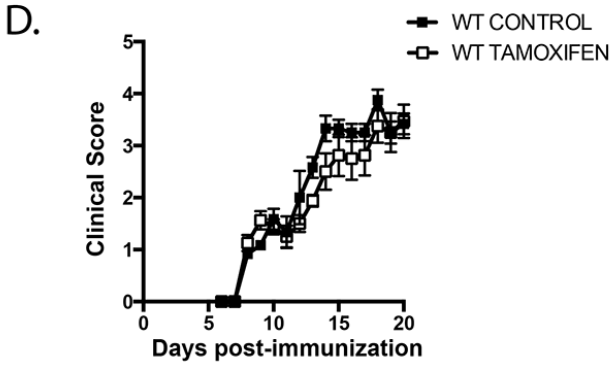

Figure 4.2. Tamoxifen-treated *Cxcr2* $^{fl/fl}$ mice display reduced susceptibility to EAE. Tamoxifen-treated and control *Cxcr2* $^{fl/fl}$ mice were induced with EAE and clinical disease and weights were recorded. Tamoxifen-treated mice displayed a reduced disease severity and delayed disease onset compared to control mice **(A)** as well as slower weight loss progression **(B)**. Raw clinical scoring data is represented in panel ***C***. To determine if

tamoxifen had any immunomodulatory properties, C57BL/6 mice were pre-treated with tamoxifen and immunized with MOG_{35-55} peptide to induce EAE. No statistical difference was observed between groups **(C)**. For clinical scoring data, n=12 for control *Cxcr2* $^{fl/fl}$ mice and n=23 for tamoxifen-treated *Cxcr2* $^{fl/fl}$ mice. Two-way ANOVA analysis was used to discover significance within clinical scoring data and weight change. *p<0.05, **p<0.01, ***p<0.001, ****p<0.0001

Dampened disease severity in tamoxifen-treated MOG_{35-55} immunized *Cxcr2* $^{fl/fl}$ mice correlates with reduced neuroinflammation and demyelination.

Flow cytometric analysis of the brains and spinal cords indicated that dampened disease severity in tamoxifen-treated MOG_{35-55} immunized *Cxcr2* $^{fl/fl}$ mice correlated with diminished neuroinflammation ($p<0.01$) as measured by the frequency of $CD45^{hi}$ infiltrating cells in both brain (**Figure 3A**) and spinal cord (**Figure 3B**) at day 11 post-immunization. Further analysis revealed a significant reduction in the total numbers of neutrophils, macrophages and T cells at day 11 p.i within the brains and spinal cords of tamoxifen-treated mice compared to control mice (**Figures 3A and B**). By day 20 p.i., total numbers of neutrophils, macrophages and T cells was similar between groups within the brain, whereas CD4+ T cells and CD8+ T cells remained significantly ($p<0.05$) reduced within the spinal cord. Immunophenotyping CNS infiltrating CD4+ T cells through cytokine secretion profiles following MOG_{35-55} stimulation showed no differences in the frequency of IFN- γ(+)IL-17(+) CD4+ T cells or IFN- γ(-) IL-17(+) CD4+ T cells within the brains of tamoxifen-treated mice compared to control mice yet there was a significant ($p<0.05$) reduction in CNS infiltrating IFN-γ(+) IL-17(-) CD4+ T cells in tamoxifen-treated *Cxcr2* $^{fl/fl}$ compared to control-treated mice (**Figure 3C**). These findings indicate that disruption of CXCR2 signaling only on oligodendroglia impedes disease onset and this correlates with an overall reduction in infiltration of MOG_{35-55}-specific CD4+ T cells. Further, these data argue for a prominent role for IFN-γ secretion by inflammatory MOG_{35-55}-specific CD4+ T cells in early disease induction.

Luxol fast blue (LFB) of the spinal cords at day 12 p.i. revealed an overall reduction in meningeal inflammation in tamoxifen-treated mice compared to controls (**Figure 3D**).

In contrast to control-treated mice in which inflammatory cells were entering white matter tracts, very few mononuclear cells from tamoxifen-treated *Cxcr2* $^{fl/fl}$ mice were exiting from either the meninges or the vasculature and entering the parenchyma (**Figure 3D, insets**). By day 22 p.i., leukocyte entry into the white matter tracts from tamoxifen-treated *Cxcr2* $^{fl/fl}$ mice were similar to control animals yet the severity of demyelination remained significantly ($p<0.01$) reduced (**Figure 3D, insets**). Correlating with reduced demyelination into the spinal cords of tamoxifen-treated *Cxcr2* $^{fl/fl}$ mice there was a pronounced reduction in reactive astrocytes as defined by GFAP staining as compared to control mice (**Figures 2E).**

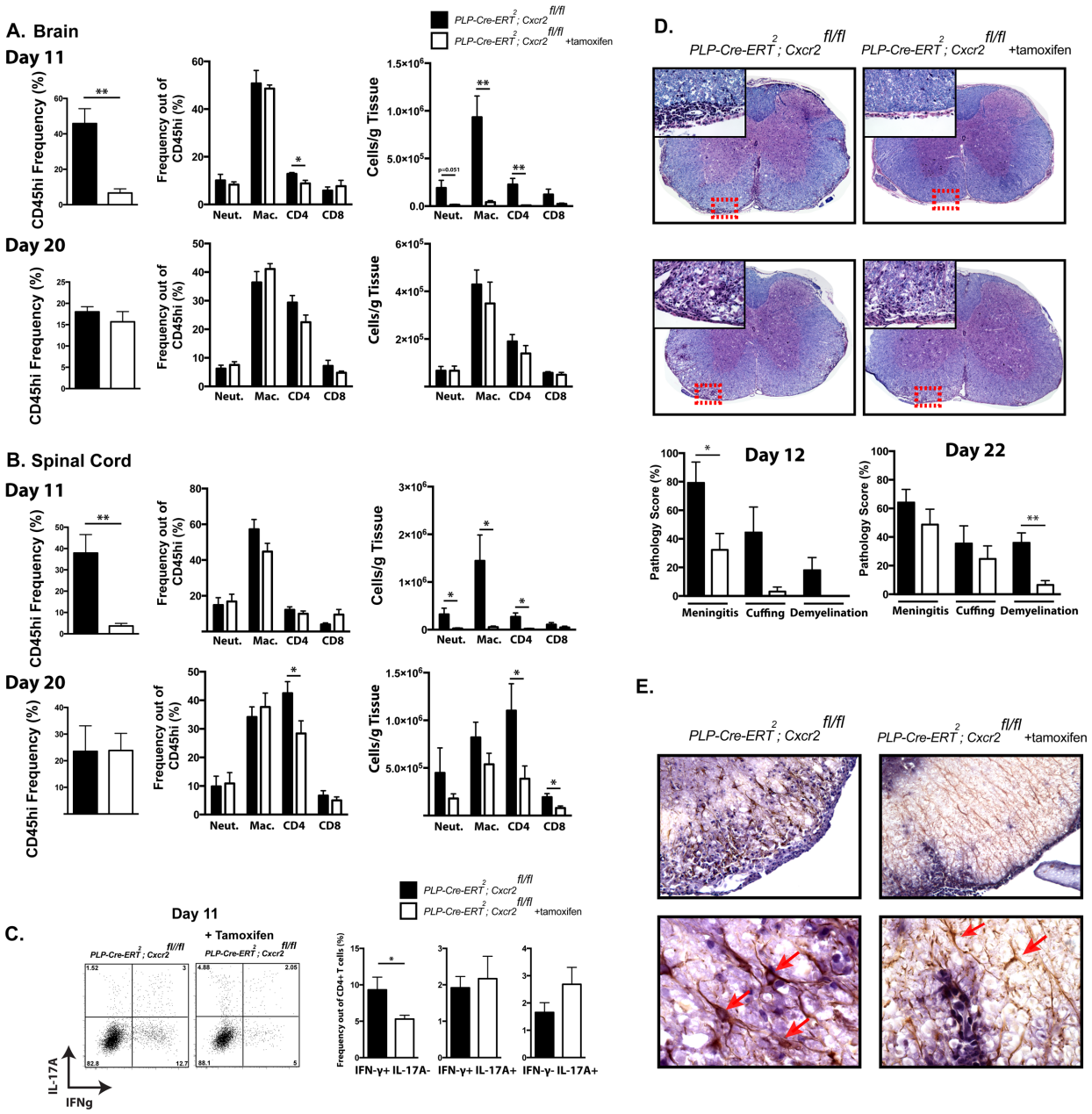

Figure 4.3. Reduced neuroinflammation and tissue pathology in tamoxifen-treated *Cxcr2* $^{fl/fl}$ mice. Immune cell infiltration was assessed at day 11 and day 20 post-immunization (p.i.) within CNS of *Cxcr2* $^{fl/fl}$ mice. The frequency of CD45hi cells was significantly reduced within the brain (**A**) and spinal cord (**B**) at day 11 p.i. in tamoxifen-treated mice. Immunophenotyping the immune cells within the brain revealed significantly lower numbers of macrophages (CD45^{hi}F4/80^{high}), CD4+ T cells and CD8+ T cells within the brain and spinal cords while neutrophils (Ly6g+CD11b+) showed significantly reduced numbers within the spinal cords but not the brain **(A-B)**. By day 20 p.i., the frequency and numbers neutrophils, macrophages and CD4+ and CD8+ T cells were similar within the brain, but reduced CD4+ and CD8+ T cell infiltration was observed within the spinal cord

(A-B). Cells isolated from the brains of MOG_{35-55} immunized *Cxcr2* $^{fl/fl}$ mice at day 11 p.i. were stimulated *ex vivo* with MOG_{35-55} peptide for 6 hours and revealed a reduction in the frequency of CD4+ IFN-γ+IL-17- T cells in tamoxifen-treated mice compared to controls **(C)**. Representative luxol fast blue (LFB) staining of spinal cords of experimental mice indicate significantly reduced meningeal inflammation at day 12 p.i. compared to controls and reduced demyelination at day 22 p.i. in tamoxifen-treated *Cxcr2* $^{fl/fl}$ mice compared to controls **(D)**. GFAP-staining revealed reduced astrogliosis within the white matter tracts of the spinal cords of tamoxifen-treated animals **(E)**. Flow cytometric data from panels **A-C** represents 2 independent experiments with a minimum of 4 mice per group per experiment. Data is presented as average±SEM; *$p<0.05$, **$p<0.01$

Tamoxifen-treated *Cxcr2* $^{fl/fl}$ mice display reduced proinflammatory gene expression in the CNS at onset of EAE disease.

The overall reduction in immune cell infiltration into the CNS of tamoxifen-treated *Cxcr2* $^{fl/fl}$ following MOG_{35-55} immunization suggests selective ablation of *Cxcr2* on oligodendroglia affects CNS proinflammatory gene expression. RNA array analysis revealed a dramatic reduction of several proinflammatory genes within the CNS in tamoxifen-treated *Cxcr2* $^{fl/fl}$ mice compared to control animals **(Figure 4A)**. RT-qPCR analysis confirmed that expression of CXCL1, CXCL2, CCL2, CCL5, CXCL10, IFN-γ and IL-17A were all dramatically reduced within tamoxifen-treated mice at disease onset (day 11 post MOG_{35-55} immunization) whereas there was elevated expression of these genes within the CNS of control animals and correlated with the appearance of immune cell infiltration into the CNS and clinical disease symptoms (**Figure 4B**). These findings support the concept that early signaling by CXCR2 in oligodendroglia amplifies proinflammatory gene expression within the CNS that subsequently attracts targeted leukocyte populations into the CNS.

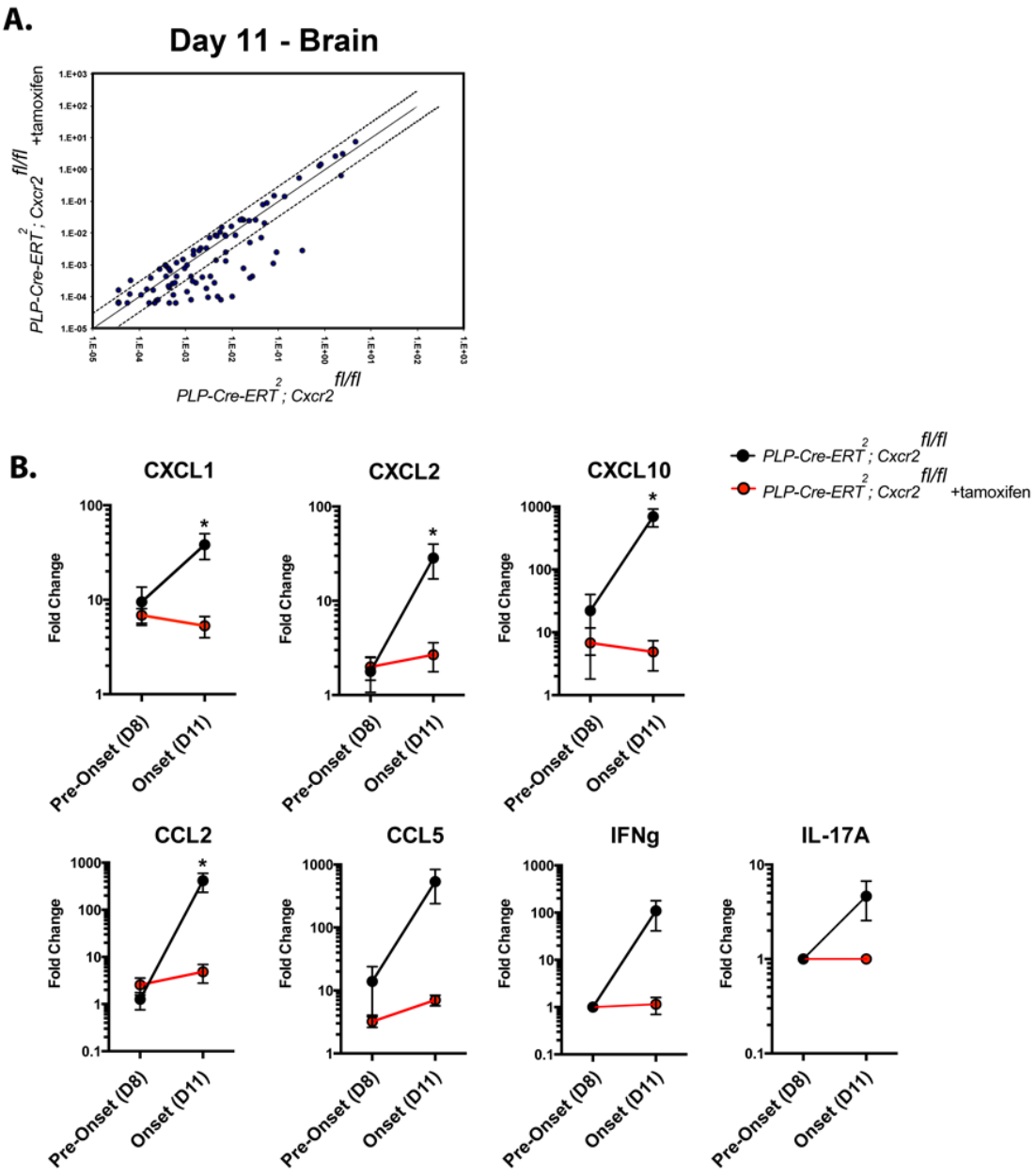

Figure 4.4. Proinflammatory gene expression is reduced in tamoxifen-treated *Cxcr2* $^{fl/fl}$ mice. At day 11 post-immunization, brains were removed from tamoxifen-treated or control *Cxcr2* $^{fl/fl}$ animals to assess proinflammatory genes using a PCR array. Scatter plot analysis revealed highly up-regulated genes within the control group compared to tamoxifen-treated mice **(A)**. Fold change in expression was measured by RT-qPCR for several genes important in leukocyte trafficking to the CNS **(B)**. Dashed lines within the PCR array scatter plot shown in panel **A** represents more than a 3-fold change in gene expression. Panel **B** represents 2 independent experiments with a minimum of 4 mice per experiment. RT-qPCR data is presented as the average fold change ±SEM; *p<0.05

Peripheral immune responses are intact in *Cxcr2 $^{fl/fl}$* mice.

To determine if the reduced trafficking of inflammatory cells to the CNS was a result of an altered generation of MOG_{35-55} -specific T cells following immunization, draining inguinal lymph nodes (ILN) and spleens were removed 8 days following immunization from tamoxifen-treated *Cxcr2 $^{fl/fl}$* mice and controls and subsequently characterized. Overall numbers of cells within the ILN and spleen were similar between groups and no differences were observed in the total numbers of neutrophils, macrophages, T cells and B cells from the spleen (**Figure 5A**). Further, we observed no differences in the frequency of CD4+ T cells with the $CD44^{hi}$ effector phenotype (**Figure 5B**). MOG_{35-55} peptide recall responses revealed no statistically difference in the frequency of MOG-specific CD4+ T cells expressing IFN-γ, IL-17A or co-expressing both cytokines (**Figure 5C**). Interestingly, IL-17A expressing CD4+ T cells were significantly increased in tamoxifen-treated mice within the ILN and spleen following PMA/ionomycin treatment, indicating that the CD4+ T cells displayed a more Th17-like phenotype within the tamoxifen-treated *Cxcr2 $^{fl/fl}$* mice (**Figure 5C**). We next examined the possibility that resistance to MOG_{35-55}-induced EAE in *Cxcr2 $^{fl/fl}$* mice was the result of reduced expression/deletion of CXCR2 expressed on peripheral immune cells as a result of leakiness in the genetic model system employed for these studies. Specifically, we examined CXCR2 expression on neutrophils as previous experiments have shown that neutrophils utilize CXCR2 to traffic and accumulate within the CNS and this is required for successful EAE induction [16]. We found no differences in levels of CXCR2 expression in neutrophils within the spleen between tamoxifen-treated *Cxcr2 $^{fl/fl}$* mice and controls (**Figure 5D**). Moreover, neutrophils from tamoxifen-treated mice did not display Tdtomato expression, suggesting Cre is not active within these cells

(**Data not shown**). Together, these data suggest that the generation of MOG-specific CD4+ T cells is unchanged within tamoxifen-treated mice and controls.

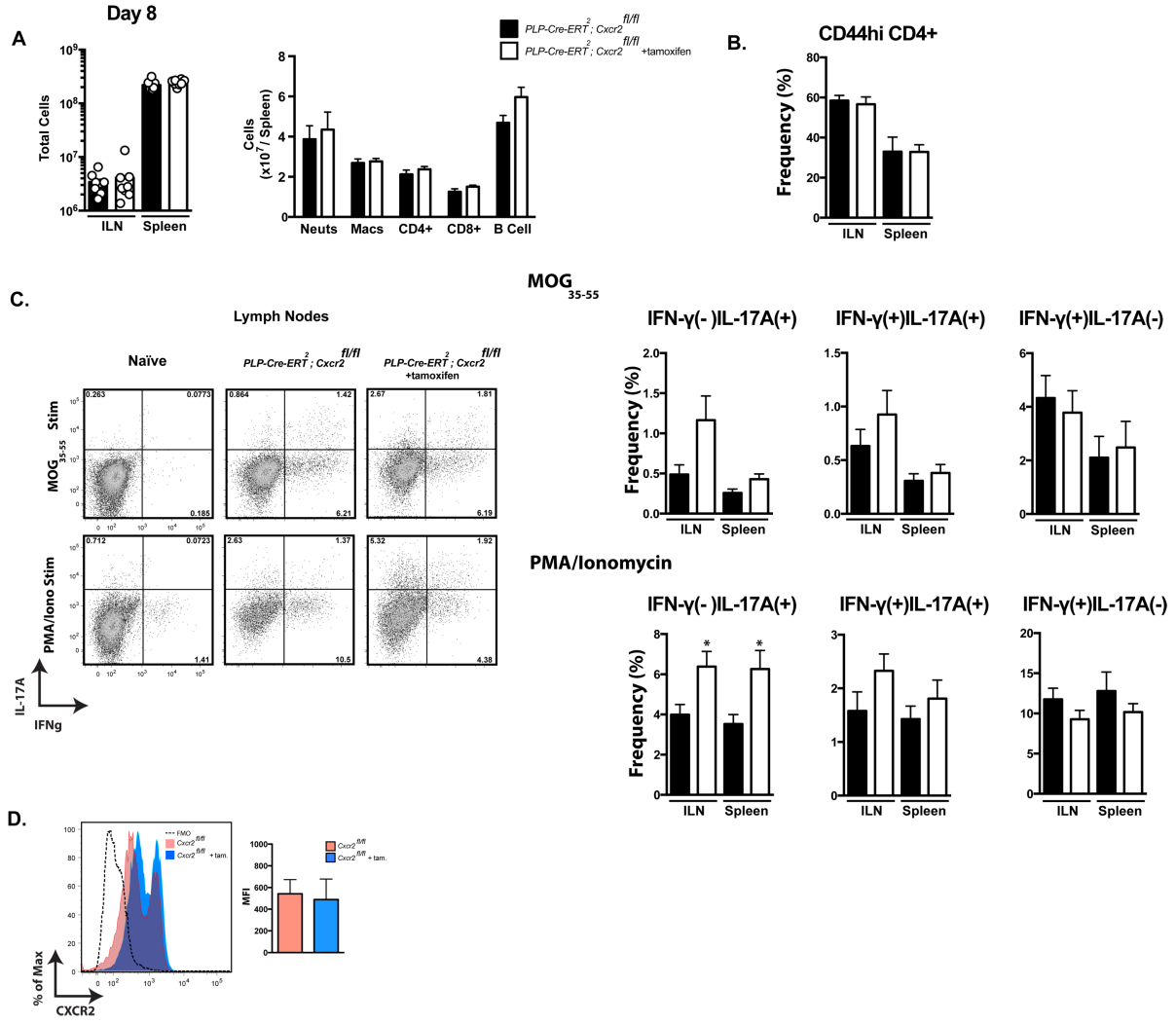

Figure 4.5. Peripheral expansion of MOG-reactive cells are intact in *Cxcr2* $^{fl/fl}$ mice. Inguinal lymph nodes (ILN) and spleens were removed at D8 from tamoxifen-treated and control *Cxcr2* $^{fl/fl}$ mice induced with EAE. The total numbers of cells in both tissues were indistinguishable between the groups, suggesting that the cells are expanding normally **(A)**. No significant difference was detected in the frequencies of neutrophils (CD45^{hi}Ly6g+), macrophages (CD45^{hi}F4/80+), CD4+ T cells, CD8+ T cells and B cells (CD19+) **(A)**. The frequency of CD44^{hi} CD4+ effector T cells were unchanged in tamoxifen-treated mice compared to controls **(B)**. Cells from the ILN and spleen were stimulated with MOG_{35-55} peptide (6hrs) or PMA/Ionomycin (5hrs) to assess IFN-γ and IL-17A expression. No significant differences were observed in the frequency of IFN-γ(+) IL-17A(-), IFN-γ(-) IL-17A(+) or IFN-γ(-) IL-17A(+) MOG-specific CD4+ T cells **(C)** while the frequency of IFN-γ(-) IL-17A(+) secreting CD4+ T cells was significantly higher within tamoxifen-treated animals following PMA/Ionomycin stimulation **(C)**. No differences were observed in the expression of CXCR2 on neutrophils in the spleen of tamoxifen-treated mice,

indicating that tamoxifen is not disrupting CXCR2 expression on these cells **(D)**. Data represents 2 independent experiments with a minimum of 4 mice per experiment. Data is presented as average±SEM; *$p<0.05$

Viral model of neuroinflammatory-mediated demyelination.

Intracranial infection of the neuroadapted JHM strain of mouse hepatitis virus (JHMV) results in acute encephalomyelitis, followed by an immune-mediated chronic demyelinating disease that is promoted by viral persistence within the white matter tracts of the spinal cord [52]. The JHMV model differs from MOG_{35-55}-induced EAE as it is characterized by transient neutrophil accumulation within the CNS early following infection and a Th1-mediated pathology whereby virus-specific IFN-γ - expressing CD4+ T cells and inflammatory macrophages contribute to white matter pathology. During chronic JHMV disease, ELR-chemokine signaling and the appearance of IL-17A - secreting Th17+ T cells remains minimal and are not considered important in contributing to either clinical disease or white matter damage [53,54]. Therefore, tamoxifen-treated *Cxcr2* $^{fl/fl}$ mice and controls were infected with 250 PFU of the neurotropic J2.2v-1 JHM strain of MHV (JHMV) in order to determine if lack of CXCR2 signaling in oligodendroglia impacts disease progression. As shown in **Figure 6A**, there was no difference in either morbidity or mortality between tamoxifen and control mice following JHMV infection of the CNS. *Cxcr2* ablation did not dampen early immune cell infiltration of neutrophils and macrophages at day 3 post-infection (**Figure 6B**) nor were there any observable differences in the frequency and total numbers of macrophages, neutrophils and T cells at day 6 post-infection (**Figure 6C**). The comparable acute inflammatory response to JHMV was further supported by the observation that there were no significant differences in the expression of pro-inflammatory genes within the brain at day 6 p.i. between both groups (**Figure 6D**). In addition, there was no difference in the infiltration of virus-specific CD4+ and CD8+ T cells into the CNS of tamoxifen-treated JHMV-infected mice compared to controls (**Figure 6E**).

Correspondingly, tamoxifen-treated mice were able to control viral infection within the CNS when compared to control mice (**data not shown**). Finally, assessment of demyelination in JHMV-infected mice either treated with tamoxifen or vehicle revealed no differences in white matter damage. Collectively, these data argue that CXCR2 signaling in oligodendrocytes does not alter host-defense or disease progression following JHMV infection.

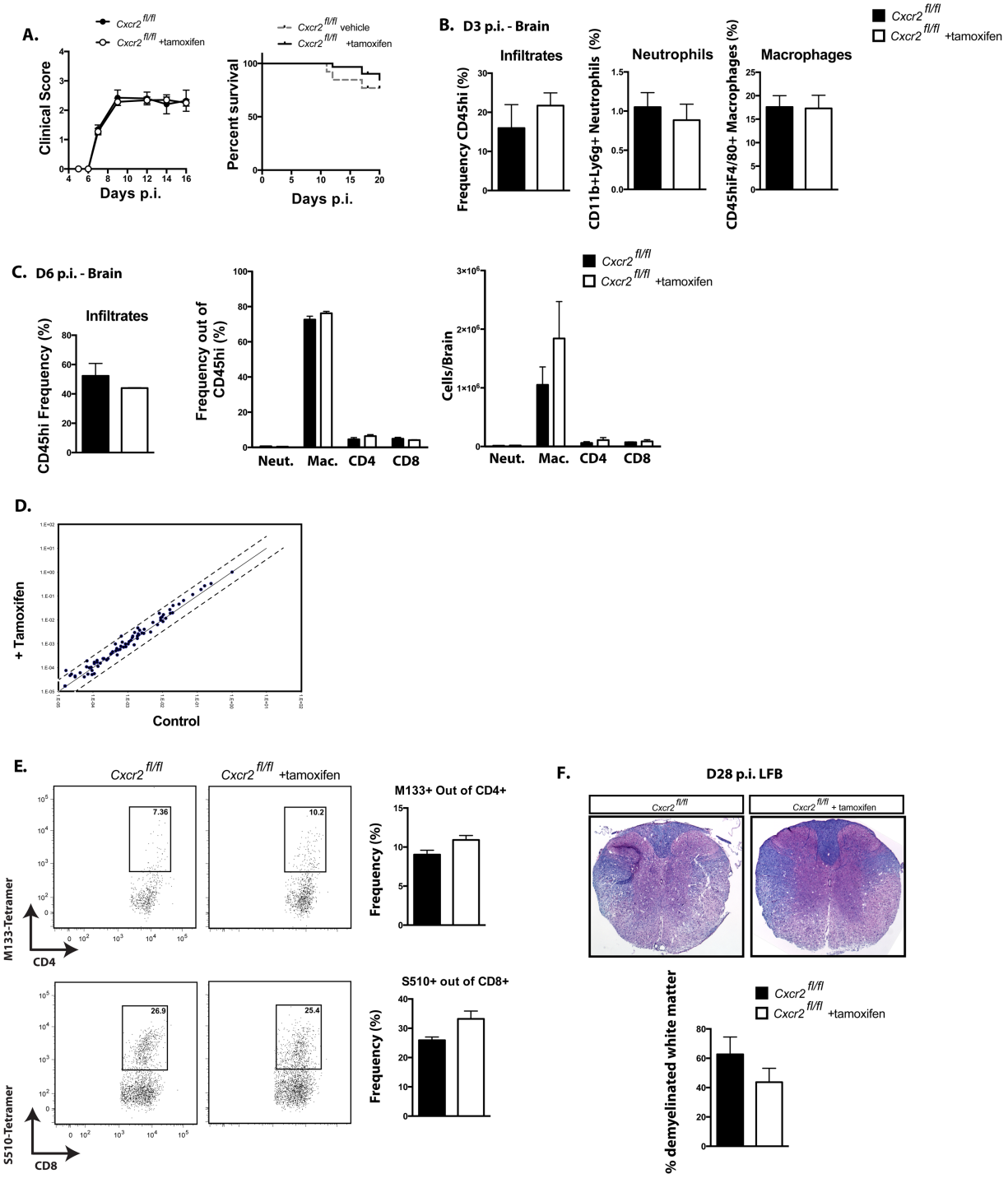

Figure 4.6. Tamoxifen-treated *Cxcr2 fl/fl* mice are susceptible a viral-induced chronic neurologic disease. To determine if *Cxcr2 fl/fl* mice display a dampened inflammatory response within a viral-model of demyelination, tamoxifen-treated *Cxcr2 fl/fl* mice or control animals were intracranially (i.c.) infected with the neurotropic J.2.2v-1 strain of mouse

hepatitis virus (JHMV). Clinical disease developed in both groups and no statistical difference was observed in disease severity or mortablity **(A)**. Assessment of the innate response to infection revealed similar numbers of neutrophils and macrophages infiltrating into the CNS at day 3 p.i. **(B)**. By day 6, similar frequencies and total numbers of neutrophils, macrophages and T cells were observed **(C)**. RNA array analysis demonstrated no changes in pro-inflammatory gene expression **(D)**. Comparable frequencies of virus-specific CD4+ and CD8+ T cells were observed within the CNS **(E)**. Assessment of demyelination revealed similar overall demyelination at day 28 p.i. **(F)**. Morbidity and mortality data is representative of 3 experiments with an n value of 22 for tamoxifen-treated *Cxcr2* $^{fl/fl}$ mice and n value of 10 for *Cxcr2* $^{fl/fl}$ controls. Day 3 and day 6 flow cytometric data is derived from 2 experiments with a minimum of 3 mice per group per experiment. RNA expression is the average of 2 mice per group. Demyelination quantification is from a minimum of 4 mice per group. Data is presented as average±SEM

4.4 Discussion

Chemokine signaling networks that are associated with chronic central nervous system (CNS) diseases such as MS or persistent viral infections are thought to amplify disease severity by attracted targeted populations of leukocytes into the CNS [55]. One chemokine signaling pathway that is emerging as an important in chronic CNS disease involves the CXCR2 receptor and its cognate ELR-positive chemokine ligands CXCL1 -2 -3 and CXCL5 -6 -7 -8. CXCR2 is highly expressed on circulating neutrophils, enabling these cells to rapidly migrate to the blood-brain-barrier (BBB) in response to CNS-derived ELR-ligand expression whereby these cells participate in degrading components of the BBB. Evidence for a pro-inflammatory role of neutrophils in chronic neurologic disease is supported by Segal and colleagues [16] who have shown that genetic silencing or antibody-mediated blockade of CXCR2 following PLP-induced EAE resulted in reduced clinical disease severity and disease relapses as a result of limited BBB permeability. Within the context of acute viral infection of the CNS, we have previously reported that antibody mediated neutralization of CXCR2 during JHMV-infection of the CNS enhanced disease severity [56]. This outcome was a result of reduced neutrophil and monocyte trafficking, as these cells are critical in permeabilizing the BBB that subsequently allows access of virus-specific T cells in the parenchyma to combat viral replication.

In addition to being expressed on circulating myeloid cells, CXCR2 is also expressed on neurons as well as resident glial cells including oligodendroglia [33]. With regards to a putative functional role for CXCR2 signaling during chronic JHMV-induced neuroinflammation and demyelination, administration of a CXCR2-specific blocking antibody increased clinical disease severity, and that this correlated with a significant

increase in oligodendrocyte apoptosis and demyelination [40]. In addition, JHMV infection or the addition of IFN-γ to cultured OPCs derived from mouse neural progenitor cells results in apoptosis, while inclusion of CXCL1 protein blocks OPC death [29].

Additional studies have revealed that signaling through CXCR2 is believed to influence OPC proliferation and differentiation [34], control the positional alignment of migrating OPCs during the development of the mouse spinal cord [35] as well as regulating the numbers of OPCs to insure structural integrity within the white matter of the spinal cord [35]. Global genetic ablation of *Cxcr2* results in a paucity of OPC numbers and structural misalignments that persist into adulthood of the mouse, resulting in reduced numbers of mature oligodendrocytes and total myelin within the white matter [36]. Within the context of mouse models of demyelination, the functional role of CXCR2 signaling within the CNS is enigmatic. Some findings suggest that the CXCR2 signaling axis downregulates myelin production by oligodendrocytes [37,38], while others have indicated that CXCR2 signaling is a survival mechanism for OPCs to halt apoptosis induced by cytotoxic factors secreted during an inflammatory response [29,39-41]. Liu and colleagues [57] used bone marrow chimeric mice to partition the contribution of CXCR2 expression on either hematopoietic or CNS derived cells. Transfer of hematopoietic cells derived from the bone-marrow of *Cxcr2* $^{+/+}$ mice into *Cxcr2* $^{-/-}$ mice lead to greater oligodendrocyte differentiation in both EAE and cuprizone models of demyelination suggesting that CXCR2 may be an inhibitory signaling cue for myelin repair [57]. Using CXCR2 antagonism via a neutralizing antibody resulted in enhanced oligodendrocyte differentiation and recovery during EAE, further supporting a detrimental role for CXCR2 signaling within the CNS in mouse models of chronic neurologic disease [37]. Conversely, inducible overproduction of

CXCL1 from astrocytes reduced EAE disease severity; although it is unclear whether increased levels of CXCL1 directly impacted oligodendrocyte biology or modulated immune cell recruitment to the CNS [39].

To better understand the importance of CXCR2 signaling in oligodendroglia lineage cells in terms of neuroinflammatory demyelinating disease, we employed an inducible Cre system to ablate *Cxcr2* in oligodendrocytes within adult mice. Surprisingly, tamoxifen-treated *Cxcr2* $^{fl/fl}$ mice immunized with MOG_{35-55} peptide in CFA displayed a diminished disease severity that was associated with reduced pro-inflammatory gene expression, diminished leukocyte infiltration into the CNS, and a marked reduction in the severity of demyelination. However, we did not observe any significant differences in the generation of MOG_{35-55} - specific CD4+ T cells within the draining lymph nodes or spleen, suggesting that peripheral expansion of these cells remains unaltered. Importantly, these findings further emphasize that the improved clinical/histologic outcome of restricted ablation of *Cxcr2* in oligodendroglia is derived from CNS-localized effects. In addition, these findings support the possibility that oligodendrocytes do not exhibit a passive role in neuorinflammation but are active participants in this process. Indeed, recent studies have demonstrated that oligodendrocytes are capable of eliciting pro-inflammatory gene expression. Addition of IL-17A to cultured OPCs upregulates several chemokines and cytokines including CXCL1, CCL5, IL-1α and TNF α [58] while addition of IFN-γ to OPC cultures can induce robust CXCL10 expression [29,41]. Moreover, *in vivo* disruption of IL-17A signaling specifically on NG2+ oligodendroglia before MOG-EAE induction resulted in dampened neuroinflammation that correlated with reduced disease severity [59].

Intriguingly, infection of tamoxifen-treated *Cxcr2* $^{fl/fl}$ mice with the neuroadapted JHM-strain of MHV elicited a prototypic immune response that resulted in a chronic disease that was comparable to control animals. These results highlight the differences in the EAE model compared to the JHMV model of demyelination. More specifically, one key difference that may be related to the dramatic differences in disease outcome is that CXCL1 (as well as other CXCR2 ligands) are only expressed for a transient period early following JHMV infection whereas following MOG_{35-55} immunization is elevated within the pre-clinical stage and expression is sustained during chronic disease [60]. Therefore, the overall increase in duration of CXCL1 signaling through CXCR2 in oligodendroglia during EAE disease may amplify neuroinflammation by allowing oligodendroglia to secrete proinflammatory cytokines/chemokines that subsequently induce additional proinflammatory gene expression by astrocytes, microglia and/or inflammatory leukocytes. Our previous results indicate that anti-CXCR2 treatment of mice persistently infected with JHMV increases demyelination most likely represents off-target effects of anti-CXCR2 binding to other resident CNS cells and/or inflammatory cells expressing this receptor.

In terms of a mechanism by which CXCR2 signaling on oligodendroglia amplifies disease, Segal and colleagues [60] have shown that MOG_{35-55} immunization results in a rapid elevation of CXCL1 protein within the CNS by 1 day. Astrocytes have been presumed to be the source of this chemokine, but it is possible that local production by glial-derived cells can signal through the CXCR2 receptor on oligodendrocytes, leading to either amplification of the ELR-signaling axis or expression of other proinflammatory factors. We have shown that addition of CXCL1 to OPC-enriched cultures leads to increased expression of CXCL1, acting as a feed-forward loop for this chemokine [29]. Alternatively, loss of

CXCR2 on oligodendrocytes could result in elevated CXCL1 expression, and together with IL-17A, delay Th1-mediated tissue damage. Indeed, we observed a dramatic reduction in several Th1 associated chemokines and cytokines within the brain of tamoxifen-treated mice. Remaining questions that will need to be addressed include determining if loss of *Cxcr2* in cultured oligodendrocytes results in altered expression of cytokines and chemokines that are important for establishing EAE disease. Furthermore, temporal analysis of the expression of ELR-chemokines following MOG_{35-55} immunization remains to be determined, and it will also be important to see how these chemokines impact the expansion of neutrophils and monocytes within tamoxifen-treated *Cxcr2* $^{fl/fl}$ mice shortly following EAE induction.

4.5 References

1. Steinman L. Immunology of relapse and remission in multiple sclerosis. *Annu Rev Immunol*, 32, 257-281 (2014).
2. Robinson AP, Harp CT, Noronha A, Miller SD. The experimental autoimmune encephalomyelitis (EAE) model of MS: utility for understanding disease pathophysiology and treatment. *Handbook of clinical neurology*, 122, 173-189 (2014).
3. Hosking MP, Lane TE. The Biology of Persistent Infection: Inflammation and Demyelination following Murine Coronavirus Infection of the Central Nervous System. *Curr Immunol Rev*, 5(4), 267-276 (2009).
4. Miller DH, Khan OA, Sheremata WA *et al.* A controlled trial of natalizumab for relapsing multiple sclerosis. *N Engl J Med*, 348(1), 15-23 (2003).
5. Kappos L, Radue EW, O'Connor P *et al.* A placebo-controlled trial of oral fingolimod in relapsing multiple sclerosis. *N Engl J Med*, 362(5), 387-401 (2010).
6. Liu MT, Chen BP, Oertel P *et al.* The T cell chemoattractant IFN-inducible protein 10 is essential in host defense against viral-induced neurologic disease. *J Immunol*, 165(5), 2327-2330 (2000).
7. Yednock TA, Cannon C, Fritz LC, Sanchez-Madrid F, Steinman L, Karin N. Prevention of experimental autoimmune encephalomyelitis by antibodies against alpha 4 beta 1 integrin. *Nature*, 356(6364), 63-66 (1992).
8. Webb M, Tham CS, Lin FF *et al.* Sphingosine 1-phosphate receptor agonists attenuate relapsing-remitting experimental autoimmune encephalitis in SJL mice. *J Neuroimmunol*, 153(1-2), 108-121 (2004).
9. Fujino M, Funeshima N, Kitazawa Y *et al.* Amelioration of experimental autoimmune encephalomyelitis in Lewis rats by FTY720 treatment. *J Pharmacol Exp Ther*, 305(1), 70-77 (2003).
10. Holman DW, Klein RS, Ransohoff RM. The blood-brain barrier, chemokines and multiple sclerosis. *Biochim Biophys Acta*, 1812(2), 220-230 (2011).
11. Engelhardt B, Ransohoff RM. Capture, crawl, cross: the T cell code to breach the blood-brain barriers. *Trends Immunol*, 33(12), 579-589 (2012).
12. Izikson L, Klein RS, Charo IF, Weiner HL, Luster AD. Resistance to experimental autoimmune encephalomyelitis in mice lacking the CC chemokine receptor (CCR)2. *J Exp Med*, 192(7), 1075-1080 (2000).
13. Ransohoff RM, Hamilton TA, Tani M *et al.* Astrocyte expression of mRNA encoding cytokines IP-10 and JE/MCP-1 in experimental autoimmune encephalomyelitis. *FASEB J*, 7(6), 592-600 (1993).
14. Karpus WJ, Lukacs NW, McRae BL, Strieter RM, Kunkel SL, Miller SD. An important role for the chemokine macrophage inflammatory protein-1 alpha in the pathogenesis of the T cell-mediated autoimmune disease, experimental autoimmune encephalomyelitis. *J Immunol*, 155(10), 5003-5010 (1995).
15. Fife BT, Huffnagle GB, Kuziel WA, Karpus WJ. CC chemokine receptor 2 is critical for induction of experimental autoimmune encephalomyelitis. *J Exp Med*, 192(6), 899-905 (2000).

16. Carlson T, Kroenke M, Rao P, Lane TE, Segal B. The Th17-ELR+ CXC chemokine pathway is essential for the development of central nervous system autoimmune disease. *J Exp Med*, 205(4), 811-823 (2008).
17. Kleinewietfeld M, Puentes F, Borsellino G, Battistini L, Rotzschke O, Falk K. CCR6 expression defines regulatory effector/memory-like cells within the CD25(+)CD4+ T-cell subset. *Blood*, 105(7), 2877-2886 (2005).
18. Reboldi A, Coisne C, Baumjohann D *et al.* C-C chemokine receptor 6-regulated entry of TH-17 cells into the CNS through the choroid plexus is required for the initiation of EAE. *Nat Immunol*, 10(5), 514-523 (2009).
19. Horuk R. Chemokine receptor antagonists: overcoming developmental hurdles. *Nat Rev Drug Discov*, 8(1), 23-33 (2009).
20. Liu MT, Keirstead HS, Lane TE. Neutralization of the chemokine CXCL10 reduces inflammatory cell invasion and demyelination and improves neurological function in a viral model of multiple sclerosis. *J Immunol*, 167(7), 4091-4097 (2001).
21. Stiles LN, Liu MT, Kane JA, Lane TE. CXCL10 and trafficking of virus-specific T cells during coronavirus-induced demyelination. *Autoimmunity*, 42(6), 484-491 (2009).
22. Stiles LN, Hosking MP, Edwards RA, Strieter RM, Lane TE. Differential roles for CXCR3 in CD4+ and CD8+ T cell trafficking following viral infection of the CNS. *Eur J Immunol*, 36(3), 613-622 (2006).
23. Phares TW, Stohlman SA, Hinton DR, Bergmann CC. Astrocyte-derived CXCL10 drives accumulation of antibody-secreting cells in the central nervous system during viral encephalomyelitis. *J Virol*, 87(6), 3382-3392 (2013).
24. Fife BT, Kennedy KJ, Paniagua MC *et al.* CXCL10 (IFN-gamma-inducible protein-10) control of encephalitogenic CD4+ T cell accumulation in the central nervous system during experimental autoimmune encephalomyelitis. *J Immunol*, 166(12), 7617-7624 (2001).
25. Byrne FR, Winters A, Brankow D *et al.* An antibody to IP-10 is a potent antagonist of cell migration in vitro and in vivo and does not affect disease in several animal models of inflammation. *Autoimmunity*, 42(3), 171-182 (2009).
26. Narumi S, Kaburaki T, Yoneyama H, Iwamura H, Kobayashi Y, Matsushima K. Neutralization of IFN-inducible protein 10/CXCL10 exacerbates experimental autoimmune encephalomyelitis. *Eur J Immunol*, 32(6), 1784-1791 (2002).
27. Witko-Sarsat V, Rieu P, Descamps-Latscha B, Lesavre P, Halbwachs-Mecarelli L. Neutrophils: molecules, functions and pathophysiological aspects. *Lab Invest*, 80(5), 617-653 (2000).
28. Omari KM, John G, Lango R, Raine CS. Role for CXCR2 and CXCL1 on glia in multiple sclerosis. *Glia*, 53(1), 24-31 (2006).
29. Tirotta E, Ransohoff RM, Lane TE. CXCR2 signaling protects oligodendrocyte progenitor cells from IFN-gamma/CXCL10-mediated apoptosis. *Glia*, (2011).
30. Horuk R, Martin AW, Wang Z *et al.* Expression of chemokine receptors by subsets of neurons in the central nervous system. *J Immunol*, 158(6), 2882-2890 (1997).
31. Flynn G, Maru S, Loughlin J, Romero IA, Male D. Regulation of chemokine receptor expression in human microglia and astrocytes. *J Neuroimmunol*, 136(1-2), 84-93 (2003).
32. Liu L, Li M, Spangler LC *et al.* Functional defect of peripheral neutrophils in mice with induced deletion of CXCR2. *Genesis*, (2013).

33. Robinson S, Tani M, Strieter RM, Ransohoff RN, Miller RH. The chemokine growth-regulated oncogene-alpha promotes spinal cord oligodendrocyte precursor proliferation. *Journal of Neuroscience*, 18(24), 10457-10463 (1998).
34. Filipovic R, Zecevic N. The effect of CXCL1 on human fetal oligodendrocyte progenitor cells. *Glia*, 56(1), 1-15 (2008).
35. Tsai HH, Frost E, To V *et al.* The chemokine receptor CXCR2 controls positioning of oligodendrocyte precursors in developing spinal cord by arresting their migration. *Cell*, 110(3), 373-383 (2002).
36. Padovani-Claudio DA, Liu LP, Ransohoff RM, Miller RH. Alterations in the oligodendrocyte lineage, myelin, and white matter in adult mice lacking the chemokine receptor CXCR2. *Glia*, 54(5), 471-483 (2006).
37. Kerstetter AE, Padovani-Claudio DA, Bai L, Miller RH. Inhibition of CXCR2 signaling promotes recovery in models of multiple sclerosis. *Experimental Neurology*, 220(1), 44-56 (2009).
38. Liu L, Belkadi A, Darnall L *et al.* CXCR2-positive neutrophils are essential for cuprizone-induced demyelination: relevance to multiple sclerosis. *Nat Neurosci*, 13(3), 319-326 (2010).
39. Omari KM, Lutz SE, Santambrogio L, Lira SA, Raine CS. Neuroprotection and remyelination after autoimmune demyelination in mice that inducibly overexpress CXCL1. *Am J Pathol*, 174(1), 164-176 (2009).
40. Hosking MP, Tirotta E, Ransohoff RM, Lane TE. CXCR2 signaling protects oligodendrocytes and restricts demyelination in a mouse model of viral-induced demyelination. *PLoS One*, 5(6), e11340 (2010).
41. Tirotta E, Kirby LA, Hatch MN, Lane TE. IFN-gamma-induced apoptosis of human embryonic stem cell derived oligodendrocyte progenitor cells is restricted by CXCR2 signaling. *Stem Cell Res*, 9(3), 208-217 (2012).
42. O'Meara RW, Ryan SD, Colognato H, Kothary R. Derivation of enriched oligodendrocyte cultures and oligodendrocyte/neuron myelinating co-cultures from post-natal murine tissues. *J Vis Exp*, (54) (2011).
43. Tsunoda I, Tanaka T, Terry EJ, Fujinami RS. Contrasting roles for axonal degeneration in an autoimmune versus viral model of multiple sclerosis: When can axonal injury be beneficial? *Am J Pathol*, 170(1), 214-226 (2007).
44. Lane TE, Liu MT, Chen BP *et al.* A central role for CD4(+) T cells and RANTES in virus-induced central nervous system inflammation and demyelination. *J Virol*, 74(3), 1415-1424 (2000).
45. Blanc CA, Rosen H, Lane TE. FTY720 (fingolimod) modulates the severity of viral-induced encephalomyelitis and demyelination. *Journal of neuroinflammation*, 11, 138 (2014).
46. Tsunoda I, Tanaka T, Fujinami RS. Regulatory role of CD1d in neurotropic virus infection. *J Virol*, 82(20), 10279-10289 (2008).
47. Feil R, Brocard J, Mascrez B, LeMeur M, Metzger D, Chambon P. Ligand-activated site-specific recombination in mice. *Proceedings of the National Academy of Sciences of the United States of America*, 93(20), 10887-10890 (1996).
48. Feil R, Wagner J, Metzger D, Chambon P. Regulation of Cre recombinase activity by mutated estrogen receptor ligand-binding domains. *Biochem Biophys Res Commun*, 237(3), 752-757 (1997).

49. Metzger D, Clifford J, Chiba H, Chambon P. Conditional site-specific recombination in mammalian cells using a ligand-dependent chimeric Cre recombinase. *Proc Natl Acad Sci U S A*, 92(15), 6991-6995 (1995).
50. Zhang Y, Riesterer C, Ayrall AM, Sablitzky F, Littlewood TD, Reth M. Inducible site-directed recombination in mouse embryonic stem cells. *Nucleic Acids Res*, 24(4), 543-548 (1996).
51. Mallon BS, Shick HE, Kidd GJ, Macklin WB. Proteolipid promoter activity distinguishes two populations of NG2-positive cells throughout neonatal cortical development. *J Neurosci*, 22(3), 876-885 (2002).
52. Bergmann CC, Lane TE, Stohlman SA. Coronavirus infection of the central nervous system: host-virus stand-off. *Nat Rev Microbiol*, 4(2), 121-132 (2006).
53. Kapil P, Atkinson R, Ramakrishna C, Cua DJ, Bergmann CC, Stohlman SA. Interleukin-12 (IL-12), but Not IL-23, Deficiency Ameliorates Viral Encephalitis without Affecting Viral Control. *Journal of Virology*, 83(12), 5978-5986 (2009).
54. Held KS, Glass WG, Orlovsky YI *et al.* Generation of a protective T-cell response following coronavirus infection of the central nervous system is not dependent on IL-12/23 signaling. *Viral Immunol*, 21(2), 173-188 (2008).
55. Charo IF, Ransohoff RM. The many roles of chemokines and chemokine receptors in inflammation. *N Engl J Med*, 354(6), 610-621 (2006).
56. Hosking MP, Liu L, Ransohoff RM, Lane TE. A protective role for ELR+ chemokines during acute viral encephalomyelitis. *PLoS Pathog*, 5(11), e1000648 (2009).
57. Liu L, Darnall L, Hu T, Choi K, Lane TE, Ransohoff RM. Myelin repair is accelerated by inactivating CXCR2 on nonhematopoietic cells. *J Neurosci*, 30(27), 9074-9083 (2010).
58. Rodgers JM, Robinson AP, Rosler ES *et al.* IL-17A activates ERK1/2 and enhances differentiation of oligodendrocyte progenitor cells. *Glia*, (2014).
59. Kang Z, Wang C, Zepp J *et al.* Act1 mediates IL-17-induced EAE pathogenesis selectively in NG2+ glial cells. *Nat Neurosci*, 16(10), 1401-1408 (2013).
60. Rumble JM, Huber AK, Krishnamoorthy G *et al.* Neutrophil-related factors as biomarkers in EAE and MS. *J Exp Med*, 212(1), 23-35 (2015).

CHAPTER FIVE

SUMMARY AND SIGNIFICANCE

5.1 Summary and Significance

CXCR2 expressing neutrophils rapidly migrate to the CNS in response to JHMV-induced expression of the ELR-chemokines CXCL1 and CXCL2 where they act in concert with macrophages and resident glial cells in breaking down components of the BBB [1,2]. The importance of neutrophils in shaping host-defense responses was previously demonstrated by antibody-mediated blockade of CXCR2 following JHMV infection, resulting in abrogated neutrophil recruitment to the CNS [1]. As a result of halting neutrophil chemotaxis, BBB permeability decreased and this was associated with higher viral titers and increased mortality. These results demonstrated a protective role for CXCR2-bearing neutrophils in combating JHMV infection of the CNS. The generation of an astroglial-specific CXCL1 overexpressing mouse line has allowed us to further explore mechanisms by which neutrophils shape host-defense responses. We found that CXCL1 overexpression from the CNS resulted in rapid and sustained neutrophil migration to the CNS that was associated with an increase in mortality and morbidity. One explanation for the amplified disease severity in double tg mice is that CXCL1 is having a direct toxic effect on oligodendroglia lineage cells by signaling through CXCR2. However, we have previously demonstrated that addition of CXCL1 to OPC cultures reduces their susceptibility to IFN-γ – induced apoptosis, indicating that CXCL1 is more protective than toxic to these cells [3,4]. This is further supported by our observation that JHMV-infected mice that have *Cxcr2* deleted from oligodendrocytes did not display any differences in demyelination within the spinal cords, suggesting that ELR-chemokines are not contributing to oligodendrocyte destruction during JHMV-induced disease (**Figure 4.6**).

We observed no differences in the infiltration of T cells and inflammatory macrophages in double tg mice, suggesting that the augmented clinical disease was not a result of neutrophils promoting the migration of other myelin-damaging cells into the white matter of the spinal cord. One important finding was that neutrophils were primarily localized to parenchymal regions within the spinal cord that had significant demyelination. This suggests that neutrophils may have a role in contributing to white matter damage via non-selective bystander toxicity, as neutrophils contain a variety of toxic-factors that have been shown to impact the survival of CNS-derived cells [5]. To determine if neutrophils were involved in amplifying demyelination within double tg mice, neutrophils were depleted starting at day 5 p.i. with anti-Ly-6g. This resulted in a modest decrease in clinical disease severity that reached significance at day 12 p.i. and this was congruent with a modest diminishment in demyelination. These data suggest that neutrophils are, in part, responsible for the increased disease severity in double tg mice. To further explore the consequences of chronic neutrophil accumulation within the CNS following JHMV infection, it will be important to extend anti-Ly-6g treatment within double tg mice to determine if neutrophil depletion accelerates recovery and reduces white matter damage. Moreover, it will also be critical to determine if neutrophils are releasing toxic mediators within the parenchyma by staining for factors such as neutrophil elastase, myeloperoxidase and nitric oxide. The pBI-CXCL1-rtTA transgenic mouse line will undoubtedly serve as an excellent tool for future experiments assessing the role of CXCL1 in neuroinflammation. Our future goals will be to utilize these mice within the autoimmune EAE model of demyelination where ELR-chemokines are highly expressed and modulate neutrophil levels following EAE induction [6]. Moreover, in the autoimmune disorder neuromyelitis optica (NMO), newly

formed lesions within the white matter of the spinal cord often show a large parenchymal presence of neutrophils, and these cells have been implicated in directly contributing to the pathology [7-9]. Defining the functional role of neutrophils in pre-clinical models of human neurologic diseases will potentially lead to the development of interventional therapies designed to impede trafficking and infiltration of neutrophils into the CNS.

CXCR2 is a unique chemokine receptors as it is expressed by oligodendroglia lineage cells and it's signaling has been demonstrated to have pronounced effects on oligodendrocyte biology [3,4]. Within the context of JHMV-infection, we have previously shown that administration of CXCR2 anti-sera into mice persistently infected with JHMV results in improved clinical disease and this was associated with reduced overall demyelination and apoptosis within the spinal white matter [10]. Paradoxically, CXCR2 neutralization in mice induced with autoimmune EAE showed enhanced recovery that was associated with accelerated myelin repair, implicating CXCR2 as an inhibitory cue for OPC differentiation [11]. However, these approaches often include off-target effects induced by the use of blocking reagents and lack of specificity in terms of confirming the importance of CXCR2 signaling on specific cell types. Therefore, we bypassed potential obstacles associated with the use of neutralizing antibodies and generated a tamoxifen-inducible *Cxcr2* conditional knockout mouse line. We found that *Cxcr2* ablation within oligodendrocytes in mice immunized with MOG_{35-55} induced EAE resulted in a dramatic decrease in disease severity and this was associated with reduced entry of inflammatory leukocytes into the CNS. Conversely, we observed no difference in host-defense or development of neurologic disease following infection with the neurotropic JHM virus. These findings highlight the disparity in the pathogenesis within these models and suggests

a detrimental role for CXCR2 signaling in oligodendrocytes within the context of auto-immune mediated demyelination.

ELR-chemokine expression following MOG_{35-55} peptide immunization appears to be essential to induce disease, as CXCR2 neutralization or global genetic deletion of *Cxcr2* results in EAE resistance that is associated with a lack of neutrophil migration to the CNS [12]. Curiously, JHMV-infected CXCR2-deficient mice develop a similar host-defense response to wildtype mice that results in normal viral clearance and the development of a chronic demyelinating disease [1]. These results are supported by another study demonstrating that neutropenic mice have a comparable response to JHMV infection compared to control animals, indicating that the CXCR2-signaling network following JHMV infection may not have a critical role in establishing an antiviral response that leads to disease, and may partially explain why tamoxifen-treated *CXCR2* $^{fl/fl}$ mice do not display a dampened neuroinflammatory response to JHMV infection [13]. One possibility for the dramatic reduction in EAE-induced neuroinflammation in CXCR2-deficient oligodendrocytes is that CXCL1 and CXCL2 may signal through CXCR2-expressing oligodendrocytes that can further amplify expression of CXCL1, CXCL2 as well as additional proinflammatory molecules that enhance leukocyte infiltration into the CNS. Therefore, loss of CXCR2 would lead to reduced ELR-chemokine expression, thus impacting neutrophil mobilization and function. However, preliminary data from our lab suggests that CXCL1 protein levels within the CNS at day 1 and day 8 post-immunization are unperturbed in tamoxifen-treated *Cxcr2* $^{fl/fl}$ mice, suggesting an alternative mechanism may modulate disease outcome. CXCR2 has also been shown to be an effective scavenger receptor for ELR-chemokines within various tissues, thus regulating the local concentrations of ELR

chemokines. Ransohoff and colleagues [14] demonstrated that *Cxcr2* knockout mice display elevated CXCL1 and CXCL2 protein levels within the CNS and blood compared to naïve wildtype mice, while transfer of *Cxcr2 +/+* hematopoetic cells into *Cxcr2 -/-* lowered ELR-chemokine levels, indicating that CXCR2-expressing cells can regulate the local concentrations of chemokines by binding through CXCR2. These findings are further supported by another study demonstrating that *Cxcr2 -/-* mice display elevated levels of IL-17A within the brain [15]. IL-17A is a known inducer of ELR-chemokines and may further amplify their expression when there is a paucity of CXCR2 expression within the CNS. One potential scenario would be that loss of CXCR2 signaling in oligodendroglia elevates the local concentrations of both CXCL1 and IL-17A within the blood, thus redirecting the cytokine/chemokine signature within the CNS that favors a Th17 mediated CD4+ T cell response rather than Th1. This would explain the reduced infiltration of CD4+ T cells as well as Th1-associated cytokines and chemokines that act to attract monocytes and T cells such as CCL2, CCL5 and CXCL10. Moreover, we have observed statistically significant increases in CXCL1 serum levels within tamoxifen-treated mice (**unpublished observations**), while we are currently investigating the concentrations of IL-17A within the serum and various tissues. Furthermore, we will gain important insights from primary oligodendrocyte cultures derived from *Cxcr2* $^{fl/fl}$ mice, as we can induce Cre-mediated *Cxcr2* deletion in vitro to determine how loss of CXCR2 impact proinflammatory gene expression.

5.2 References

1. Hosking MP, Liu L, Ransohoff RM, Lane TE. A protective role for ELR+ chemokines during acute viral encephalomyelitis. *PLoS Pathog*, 5(11), e1000648 (2009).
2. Savarin C, Stohlman SA, Atkinson R, Ransohoff RM, Bergmann CC. Monocytes regulate T cell migration through the glia limitans during acute viral encephalitis. *J Virol*, 84(10), 4878-4888 (2010).
3. Tirotta E, Kirby LA, Hatch MN, Lane TE. IFN-gamma-induced apoptosis of human embryonic stem cell derived oligodendrocyte progenitor cells is restricted by CXCR2 signaling. *Stem Cell Res*, 9(3), 208-217 (2012).
4. Tirotta E, Ransohoff RM, Lane TE. CXCR2 signaling protects oligodendrocyte progenitor cells from IFN-gamma/CXCL10-mediated apoptosis. *Glia*, (2011).
5. Chen H, Song YS, Chan PH. Inhibition of NADPH oxidase is neuroprotective after ischemia-reperfusion. *Journal of cerebral blood flow and metabolism : official journal of the International Society of Cerebral Blood Flow and Metabolism*, 29(7), 1262-1272 (2009).
6. Rumble JM, Huber AK, Krishnamoorthy G *et al.* Neutrophil-related factors as biomarkers in EAE and MS. *J Exp Med*, 212(1), 23-35 (2015).
7. Saadoun S, Waters P, MacDonald C *et al.* Neutrophil protease inhibition reduces neuromyelitis optica-immunoglobulin G-induced damage in mouse brain. *Ann Neurol*, 71(3), 323-333 (2012).
8. Zhang H, Bennett JL, Verkman AS. Ex vivo spinal cord slice model of neuromyelitis optica reveals novel immunopathogenic mechanisms. *Ann Neurol*, 70(6), 943-954 (2011).
9. Lucchinetti CF, Mandler RN, McGavern D *et al.* A role for humoral mechanisms in the pathogenesis of Devic's neuromyelitis optica. *Brain*, 125(Pt 7), 1450-1461 (2002).
10. Hosking MP, Tirotta E, Ransohoff RM, Lane TE. CXCR2 Signaling Protects Oligodendrocytes and Restricts Demyelination in a Mouse Model of Viral-Induced Demyelination. *PLoS One*, 5(6), 12 (2010).
11. Kerstetter AE, Padovani-Claudio DA, Bai L, Miller RH. Inhibition of CXCR2 signaling promotes recovery in models of multiple sclerosis. *Experimental Neurology*, 220(1), 44-56 (2009).
12. Carlson T, Kroenke M, Rao P, Lane TE, Segal B. The Th17-ELR+ CXC chemokine pathway is essential for the development of central nervous system autoimmune disease. *J Exp Med*, 205(4), 811-823 (2008).
13. Savarin C, Stohlman SA, Rietsch AM, Butchi N, Ransohoff RM, Bergmann CC. MMP9 deficiency does not decrease blood–brain barrier disruption, but increases astrocyte MMP3 expression during viral encephalomyelitis. *Glia*, 59(11), 1770-1781 (2011).
14. Cardona AE, Sasse ME, Liu L *et al.* Scavenging roles of chemokine receptors: chemokine receptor deficiency is associated with increased levels of ligand in circulation and tissues. *Blood*, 112(2), 256-263 (2008).
15. Mei J, Liu Y, Dai N *et al.* Cxcr2 and Cxcl5 regulate the IL-17/G-CSF axis and neutrophil homeostasis in mice. *J Clin Invest*, 122(3), 974-986 (2012).